

## SMALL- $x$ BEHAVIOUR OF INITIAL STATE RADIATION IN PERTURBATIVE QCD\*

S. CATANI

*Dipartimento di Fisica, Università di Firenze, INFN, Sezione di Firenze, Italy*

F. FIORANI and G. MARCHESINI

*Dipartimento di Fisica, Università di Parma, INFN, Gruppo Collegato di Parma, Italy*

Received 17 July 1989

We analyze in perturbative QCD the asymptotic behaviour of deep inelastic processes in the semi-hard region  $x \rightarrow 0$ . The study is done by extending the soft gluon insertion techniques. We confirm and extend the analysis recently performed by Ciafaloni. The main results are the following: (i) Soft gluon emission from the incoming parton takes place in a region where the angles between incoming and outgoing partons are ordered. This is due to coherent effects similar to the ones in the  $x \rightarrow 1$  region. (ii) Virtual corrections involving an internal line with energy fraction  $x$  give rise, for  $x \rightarrow 0$ , to a new form factor of non-Sudakov type. This regularizes collinear singularities when an emitted gluon is parallel to the incoming parton. (iii) At the complete inclusive level, the new form factor plays the same role as the virtual corrections in the Lipatov equation for the Regge regime. We show that, in the semi-hard regime, the gluon anomalous dimension coincides with the Lipatov ansatz. (iv) We identify the branching structure of initial-state radiation including the semi-hard regime. The branching is formulated as a probability process given in terms of Sudakov and non-Sudakov form factors. This process, in principle, can be used to extend the existing simulations of QCD cascades to the semi-hard regime.

### 1. Introduction

One of the most arduous problems in perturbative QCD is the analysis of processes involving incoming hadrons in the regime

$$\Lambda \ll Q \ll \sqrt{s}, \quad (1.1)$$

where  $\sqrt{s}$  is the energy,  $Q$  is the hard scale of the process and  $\Lambda$  the QCD scale. This regime has been the subject of intensive studies in perturbative QCD [1–6] but a general theoretical understanding is still lacking.

\*Research supported in part by the Italian Ministero della Pubblica Istruzione.

The extension of the QCD analysis to the semi-hard regime (1.1) is becoming crucial for the interpretation of a large set of high energy data from hadron–hadron and hadron–lepton collisions.

At the inclusive level we have, for instance, the cross sections and the distributions of semi-hard jets with  $E_T \ll \sqrt{s}$  (mini-jets), and the emission of heavy particles with mass  $M \ll \sqrt{s}$ . Such quantities crucially depend on the behaviour of the quark and gluon structure functions for small  $x \sim Q/\sqrt{s}$ . In perturbative QCD these functions grow rapidly for  $x \rightarrow 0$  (see refs. [1–3,6]) so that semi-hard jet events provide a large contribution to the total cross section.

At the semi-inclusive level the structure of the emitted radiation is characterized by the soft gluon interference effect (coherence). In the hard regime  $x \rightarrow 1$  or in the timelike processes of final state emission (e.g. in  $e^+e^-$  annihilation) we have a quite satisfactory understanding of this phenomenon, at least to leading order (see refs. [1, 2, 6, 7]). In the regime  $x \rightarrow 0$ , instead, the QCD coherence of the radiation emitted by the incoming parton is not completely known.

Monte Carlo simulations of hard events are important tools both for theoretical and phenomenological study of QCD. At least to leading order, coherence of the soft gluon radiation in hard processes can be described by a Markov process. A reliable description of coherence in the initial state radiation is already implemented in one of the existing Monte Carlo program [7]. However in regime (1.1), a satisfactory description is still lacking.

On the theoretical point of view, the analysis of the phase space region (1.1) is quite interesting. Let us recall some of the known results.

(i) On the basis of the analysis of soft emission amplitudes at tree level, it has been suggested [6] that the initial state soft gluon radiation is emitted within an angular ordered region. Outside this region, destructive interference takes place and the distribution vanishes to leading order. In this spacelike process for  $x \rightarrow 0$ , the structure of soft gluon coherence is the same for  $x \rightarrow 1$  or in the timelike processes (e.g. in  $e^+e^-$  annihilation).

(ii) On the contrary, virtual corrections to the initial state radiation in the semi-hard regime (1.1) are expected to be quite different from virtual corrections to the final state radiation of a soft gluon. Consider for instance the timelike and spacelike gluon anomalous dimension  $\gamma_N$  for  $N \rightarrow 1$ , with  $N$  the energy–moment index. In the timelike case we have the known result [8]

$$\begin{aligned} \gamma_N^T(\alpha_s) &\simeq -\frac{N-1}{4} + \sqrt{\left(\frac{N-1}{4}\right)^2 + \frac{1}{2}\bar{\alpha}_s} \\ &= \left(\frac{\bar{\alpha}_s}{N-1}\right) - 2\frac{\bar{\alpha}_s^2}{(N-1)^3} + \dots, \quad \bar{\alpha}_s = \frac{\alpha_s C_A}{\pi}, \end{aligned} \quad (1.2)$$

which shows that, at the perturbative order  $\alpha_s^n$ , the leading singularity as  $N \rightarrow 1$  is  $\alpha_s^n(N-1)^{1-2n}$ .

The structure of the spacelike anomalous dimension for  $N \rightarrow 1$  is quite different. From two-loop calculations [14] it is known that

$$\gamma_N^S(\alpha_s) = \frac{\bar{\alpha}_s}{N-1} + a \frac{\bar{\alpha}_s^2}{N-1} + \dots, \quad (1.3)$$

with  $a$  a known number. In contrast with the timelike case the leading  $\alpha_s^2/(N-1)^3$  and the next to leading  $\alpha_s^2/(N-1)^2$  singularities are absent.

(iii) From the analysis of the complete two-loop calculation it has been shown [2, 4, 6] that the absence of the leading  $\alpha_s^2/(N-1)^3$  singularity of  $\gamma_N$  is the result of a cancellation between real emission contributions and virtual corrections of non-Sudakov type. The virtual correction of Sudakov type regularizes the soft emission singularity  $1/(1-z)$  in the Altarelli–Parisi splitting function, while this non-Sudakov virtual correction regularizes the collinear singularity present when an additional emitted gluon becomes parallel to the incoming parton. Such a cancellation of collinear singularities is also present in the equation which Lipatov [3] obtained long time ago in his investigation of Regge behaviour in gauge theories. Although the semi-hard regime is different from the Regge regime, one may try to translate the Lipatov equation in terms of a gluon anomalous dimension ansatz and obtain the following equation involving the Euler function (see e.g. ref. [2])

$$\frac{\bar{\alpha}_s}{N-1} = [2\psi(1) - \psi(\gamma_N) - \psi(1-\gamma_N)]^{-1} = \frac{1}{f(\gamma_N)}. \quad (1.4)$$

According to this ansatz,  $\gamma_N(\alpha_s)$  is a function of  $\alpha_s/(N-1)$  with perturbative expansion

$$\gamma_N(\alpha_s) = \sum_{j=1}^{\infty} g_j \left( \frac{\bar{\alpha}_s}{N-1} \right)^j = \frac{\bar{\alpha}_s}{N-1} + \mathcal{O}\left( \left( \frac{\bar{\alpha}_s}{N-1} \right)^4 \right), \quad (1.5)$$

which is consistent with the two-loop result in eq. (1.3).

(iv) According to this ansatz, the first correction to the one-loop result is of order  $\alpha_s^4$  and therefore one could think that the one-loop anomalous dimension could provide a reliable approximation to the structure function for small  $x$ . However this is not the case since expansion (1.5) generates a square-root singularity in the moment index  $N$  for  $N = N^*$  given by

$$N^* = 1 + \bar{\alpha}_s f\left(\frac{1}{2}\right) = 1 + \bar{\alpha}_s 4 \ln 2. \quad (1.6)$$

The presence of this singularity at  $N^* > 1$  implies that the actual behaviour of the structure function is much more singular than the one-loop expression: the structure function diverges as  $x^{-N^*}$  for  $x \rightarrow 0$ , thus yielding a violation of the Froissart

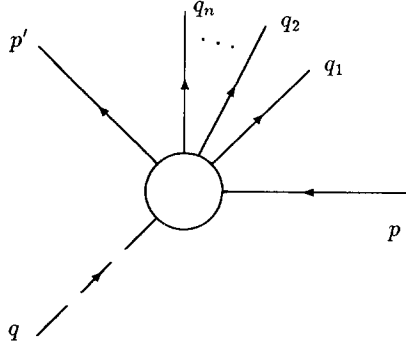


Fig. 1. The deep inelastic parton scattering. Here and in the following figures all solid lines indicate gluons.

bound. In refs. [1, 5] it has been shown that such a violation could be overcome by a consistent unitarization procedure.

(v) No real proof of the Lipatov ansatz (1.4) still exists. A sizable step in this direction has been made in ref. [6] in which a method is suggested to factorize and resum higher order QCD corrections. Here a new form factor of non-Sudakov type is introduced to regularize to all orders the real emission collinear singularities and the Lipatov ansatz is obtained. However, in that paper there is not a real proof of factorization, especially at the virtual level, or of exponentiation of loop corrections. One of the aims of the present paper is to obtain such a proof.

In this paper we study the process of parton deep inelastic scattering (see fig. 1)

$$p + q \rightarrow p' + q_1 + q_2 + \cdots + q_n, \quad (1.7)$$

where  $q$  is the hard probe

$$q^2 = -Q^2 < 0 \quad \text{and} \quad x = Q^2/2pq, \quad (1.8)$$

and  $p'$  represents the recoiling parton. Since gluons provide the most singular contributions for  $x \rightarrow 0$ , we focus our attention on deep inelastic scattering in pure Yang–Mills theory. We consider a hard probe generated by the gauge-invariant colour-singlet source current  $(F_{\mu\nu}^a)^2$ . However we will point out the generalization when quarks are also included (see appendix B).

We study this process in the phase space region

$$q_{it} < Q, \quad (1.9)$$

with  $q_{it}$  the transverse momentum of gluon  $i$ . It is only within this region that the cross section for the process (1.7) admits a parton interpretation in terms of a single

incoming parton structure function. Note that for  $x \rightarrow 0$  values of  $q_{it} \gg Q$  are allowed, since the kinematical boundary is  $q_{it}^2 < Q^2/x$ . Processes with  $q_{it}^2 \gg Q^2$  correspond to the Drell–Yan emission of jets which are harder than the probe  $Q$ . These processes have two hard scales and have to be analyzed independently. Our analysis in the region (1.9) provides, via the factorization theorem, a complete description of jet emission in  $p\bar{p}$  collisions with  $E_t \approx Q \ll \sqrt{s}$ .

Before explaining the results of this paper we describe the method we use.

To compute the multi-gluon amplitudes in fig. 1, we follow the method of ref. [6] which consists in generalizing to semi-hard processes the soft gluon insertion technique which has been extensively used [2, 11–13] for the study of infrared singularities in hard processes.

The leading infrared singularities in hard processes are obtained by studying the process of fig. 1 in the energy ordered region

$$y_n \ll \dots \ll y_2 \ll y_1 \ll x \sim 1, \quad (1.10)$$

where  $y_k$  is the energy fraction of the emitted gluon  $k$ . The soft gluon insertion technique [2] consists in factorizing the emission of the softest gluon  $n$  in terms of a soft current. In the region (1.10) this is given by the eikonal current of all external harder gluons

$$\mathbf{J}_{\text{eik}}^{(n-1)}(q_n) = -\mathbf{T}_p \frac{p}{pq_n} + \mathbf{T}_{p'} \frac{p'}{p'q_n} + \sum_{l=1}^{n-1} \mathbf{T}_l \frac{q_l}{q_l q_n}, \quad (1.11)$$

where the  $\mathbf{T}$ 's are the colour charges of emitting partons. Virtual corrections are treated in a similar way [11, 12] by factorizing the contributions with the softest gluon in the loop. This technique allows one to obtain a recurrence relation which enables one to compute the leading infrared contributions to the multi-gluon amplitudes and to exponentiate the virtual corrections giving the proper Sudakov form factors.

The  $x \rightarrow 0$  leading contributions of the multi-gluon amplitudes of fig. 1 are obtained by studying the energy region

$$x \ll y_n \ll \dots \ll y_2 \ll y_1 \sim 1. \quad (1.12)$$

The main difficulty in the study of this region is the presence of an internal line with energy fraction  $x$ , which for  $x \rightarrow 0$  may be less energetic than the softest emitted gluon. This implies that insertions on this internal line cannot be described by eq. (1.11) and one has to generalize the form of the soft current. A similar difficulty appears in the evaluation of virtual corrections involving this less energetic internal line. We shall show that all these complications can be overcome by appealing to the properties of soft gluon coherence.

Our calculations are done in the axial gauge with the gauge vector essentially parallel to the recoiling gluon  $p'$ . We check the gauge invariance of final results to the extent of current conservation. Let us list the results obtained in this paper.

(i) We show that, in the semi-hard regime (1.12), the emission of the softest gluon  $n$  can be factorized in terms of the total current (see eqs. (3.4) and (3.5))

$$\mathbf{J}_{\text{tot}}^{(n-1)}(q_n) = \mathbf{J}_{\text{eik}}^{(n-1)}(q_n) + \mathbf{J}_{\text{nc}}(Q_n, q_n), \quad (1.13)$$

where the additional current  $\mathbf{J}_{\text{nc}}$  is a non-eikonal current which corresponds to the soft gluon emission from the softest internal line with momentum  $Q_n = p - q_1 - \dots - q_n$ . This factorization gives a recurrence relation (see eq. (3.3)) which allows us to compute the multi-gluon amplitude at tree level in the phase space region (1.12).

(ii) We solve the recurrence relation and compute the leading contribution to the multi-gluon distributions at tree level (see eq. (4.16)). Mass singularities related to spacelike internal lines are present in individual graphs but they are cancelled in the final result due to a coherence effect (see eq. (4.2)). We confirm that there are leading collinear singularities only for  $\theta_{pq_i} \rightarrow 0$ ,  $\theta_{q_i q_j} \rightarrow 0$  and  $\theta_{p' q_i} \rightarrow 0$ , where  $\theta_{kk'}$  are the angles between parton  $k$  and  $k'$ . As a consequence one obtains that the soft gluon emission from the incoming parton  $p$  takes place within the angular ordered region

$$\theta_{p\bar{p}} > \theta_{pq_n} > \dots > \theta_{pq_2} > \theta_{pq_1}. \quad (1.14)$$

(iii) We show that the softest virtual correction to the multi-gluon amplitudes factorizes and gives two contributions of different origin (see eq. (5.29)). The first is the usual one of eikonal type and the second one is of non-eikonal type and related to the non-eikonal current in eq. (1.13), (see eq. (3.5)). This factorization provides a way to exponentiate both types of virtual corrections (see eq. (5.2)). The complete form factor is given by the usual Sudakov one (see eq. (5.3)) and by a non-Sudakov form factor (see eq. (5.4)) which is similar to the one suggested in ref. [6]. This last one is relevant only for  $x \rightarrow 0$ .

(iv) We write a recurrence relation for the complete multi-gluon amplitudes (see eqs. (5.2) and (5.5)). By solving this recurrence relation (see eq. (6.14)) and integrating over final state emission we compute the initial state multi-gluon distribution (see eq. (6.25)). This distribution takes into account only the contributions with collinear singularities for  $\theta_{pq_i} \rightarrow 0$  and includes the corresponding virtual corrections. The structure function is obtained by integrating this initial state distribution (see eq. (6.26)).

(v) If we extrapolate the multi-gluon distributions, computed for  $x \rightarrow 0$ , into the complementary region  $x \rightarrow 1$  we find that, apart from contributions which are subleading, they match with those already known in the latter region (see ref. [2]).

Therefore we can assume the distribution (6.25) to be valid for any values of  $x$ . In this way we neglect only subleading singularities for finite  $x$  which contribute in the intermediate regions  $y_i \ll x \ll y_j$  and give the finite terms for  $z \rightarrow 0, 1$  of the Altarelli–Parisi splitting functions.

(vi) For  $x \rightarrow 0$  we obtain an equation for the structure function at fixed total transverse momentum similar to the one in refs. [2, 6] (see eq. (7.28)). This can be solved by the diagonalization of the energy  $N$  moments (see eq. (7.31)). We confirm the Lipatov ansatz (1.4) for the  $N \rightarrow 1$  anomalous dimension.

(vii) We cast the initial state multi-gluon distribution in terms of a spacelike branching process and give the branching distribution (see eqs. (7.54) and (7.55)). The branching takes place within the angular ordered region (1.14), and the branching probability contains two form factors: the usual Sudakov one (see eq. (7.48)) and a non-Sudakov form factor (see eq. (7.17)). The last form factor is relevant only when the emitted gluon is fast and therefore it is important only in presence of the  $1/z$  term in the Altarelli–Parisi splitting function.

The paper is organized as follows. In sect. 2 we set the notations and recall some of the general results on the soft gluon insertion techniques which are needed in the following. In sect. 3 we analyze the factorization of softest gluon emission for  $x \rightarrow 0$  and we give the general recurrence relation at tree level for the multi-gluon amplitudes. In sect. 4 we solve the previous recurrence relation and compute the general multi-gluon distributions at tree level. We discuss also the structure of soft gluon interference (coherence). In sect. 5 we perform a detailed analysis of virtual corrections at the same level of accuracy as in the calculation of real emission and we prove the exponentiation of these virtual corrections. We deduce also the recurrence relation for the multi-gluon amplitude including the appropriate form factor. In sect. 6 we solve the above relation and compute the initial state multi-gluon distributions. In sect. 7 we discuss the coherence of multi-gluon emission, we compute the anomalous dimension for  $N \rightarrow 1$  and we deduce the branching structure of initial state emission. The paper is completed by two appendices. In appendix A the two-gluon emission amplitude is evaluated in a general axial gauge and we check the gauge invariance of the total soft gluon emission current. In appendix B we discuss deep inelastic scattering with incoming quarks. By using coherent state techniques we extend the results obtained in the pure Yang–Mills theory.

## 2. General features

For the kinematics of the process in fig. 1 we introduce two lightlike vectors

$$p = E(1, 0, 0, 1), \quad \bar{p} = E(1, 0, 0, -1), \quad 2p\bar{p} = 4E^2. \quad (2.1)$$

The other momenta in eq. (1.7) can be written as

$$q = -xp + \frac{Q^2}{x} \frac{\bar{p}}{2p\bar{p}}, \quad q_i = y_i p + (pq_i) \frac{\bar{p}}{p\bar{p}} + q_{it}, \quad (2.2)$$

where  $2pq_i = q_{it}^2/y_i$  for  $q_i$  massless and  $x = Q^2/2pq$ . For large  $Q^2$  we have

$$x \simeq x_n \equiv (1 - y_1 - \dots - y_n), \quad p' \sim \bar{p}, \quad (2.3)$$

where  $y_i$  is essentially the energy fraction of  $q_i$  and  $\sim$  stands for almost parallel. In the deep inelastic process of fig. 1 the kinematical boundary for the total squared transverse momentum  $Q_{nt}^2 = (\sum_{i=1}^n \mathbf{q}_{it})^2$  is of order  $2pp'$  and for small  $x$  we have  $Q_{nt}^2 \leq Q^2/x$ . As already mentioned, in this paper we limit our analysis to simple deep inelastic process in which the only hard scale is  $Q$  and we consider the phase space region  $Q_t \ll Q$ .

As mentioned in the introduction, since only gluons are relevant for  $x \rightarrow 0$ , we focus our attention on deep inelastic scattering in Yang–Mills theory. The case with a quark in the initial state will be discussed in appendix B. For the hard probe we take the simple gauge invariant current  $(F_{\mu\nu}^a)^2$ . To first order it gives rise to the two-gluon vertex

$$V^{\mu\mu'}(p, p') = -g^{\mu\mu'}(pp') + (p'^\mu p^{\mu'}), \quad (2.4)$$

with  $\mu$  and  $\mu'$  the Lorentz indices of gluons  $p$  and  $p'$  respectively. In addition to this we have a contribution of order  $g_s$  with three-gluon vertex. The four-gluon coupling can be neglected in our approximation.

For  $x \rightarrow 0$  the dominant part of the multi-gluon amplitude is obtained by studying the process of fig. 1 in the phase space with strongly ordered energies. For the emitted gluons which are softer than  $x$  the soft emission factorization works as in the case of  $x \rightarrow 1$ . We then focus our attention on the phase space in which  $x$  is softer than the emitted gluons

$$x \ll y_n \ll y_{n-1} \ll \dots \ll y_1 \simeq 1. \quad (2.5)$$

## 2.1. GAUGE FRAME AND STRUCTURE OF LEADING DIAGRAMS

We work in axial gauge and introduce the polarization projection vector

$$\epsilon_\mu^{(\lambda)}(q) = g_\mu^\lambda - q_\mu \eta^\lambda / (q\eta), \quad (2.6)$$

so that

$$k \cdot \epsilon^{(\lambda)}(q) = k^\lambda - \frac{kq}{q\eta} \eta^\lambda, \quad \epsilon^{(\lambda)}(q) q_\lambda = \eta \cdot \epsilon^{(\lambda)}(q) = 0, \quad (2.7)$$

and the gluon polarization sum is

$$d_\mu{}^\nu(q) = -\epsilon_\mu^{(\lambda)}(q) \epsilon_{(\lambda)}{}^\nu(q), \quad \eta^\mu d_{\mu\nu}(q) = 0. \quad (2.8)$$

We choose the gauge

$$\eta = \bar{p} \sim p', \quad (2.9)$$

in which the gauge vector  $\eta$  is essentially parallel to the recoiling momentum  $p'$ . The topological and Lorentz structure of the dominant Feynman diagrams for  $x \rightarrow 0$  greatly simplify in this gauge. Let us list the main simplifications:

(i) First we can neglect the Feynman diagrams in which the gluons  $q_1, \dots, q_n$  are emitted by the recoiling parton  $p'$ . This is due to the fact that in the phase space (2.5) soft gluon emission from  $p'$  can be approximated by the eikonal vertex  $2p'_\mu \sim 2\bar{p}_\mu$  which is orthogonal to the polarization vector in our gauge  $\eta = \bar{p}$ .

In our gauge we need to consider only the contributions of the hard current  $(F_{\mu\nu}^a)^2$  coming from the two-gluon coupling in eq. (2.4). This is due to the same reason described above. The contribution from this current with three-gluon coupling gives rise to two terms. The first is of order  $y_i \bar{p}_\mu$  with respect to the one corresponding to eq. (2.4) and gives a nonleading infrared contribution. The second is proportional to  $p'_\mu \sim \bar{p}_\mu$  and does not contribute in our gauge. As a result we limit our analysis to the diagrams with the structure in fig. 2. For the analysis in a general gauge we refer to appendix A.

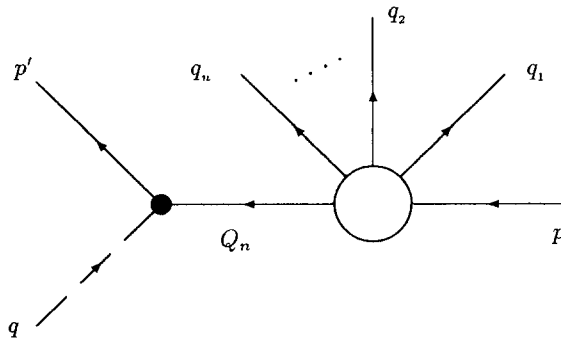


Fig. 2. Structure of diagrams for the leading infrared contribution in the gauge (2.9). The full circle corresponds to the effective vertex in eq. (2.11).

(ii) A further important simplification comes from the structure of the following effective hard vertex

$$V_{\text{eff}\mu}^{(\lambda)}(Q_n, p') \equiv \frac{1}{Q_n^2} d_{\mu\nu}(Q_n) \left( \frac{V^{\nu\nu'}(Q_n, p')}{p'Q_n} \right) \epsilon_{\nu'}^{(\lambda)}(p'), \quad (2.10)$$

where  $V^{\nu\nu'}(Q_n, p')$  is given by eq. (2.4) and corresponds to the vertex  $Q_n + q \rightarrow p'$  in fig. 2. Eq. (2.10) can be rewritten as

$$V_{\text{eff}\mu}^{(\lambda)}(Q_n, p') = \Gamma^{(\lambda)}(Q_n, p') - \frac{1}{p'Q_n} \left( \frac{d(Q_n) \cdot p'}{Q_n^2} \right) (Q_n \cdot \epsilon^{(\lambda)}(p')), \quad (2.11)$$

where 
$$\Gamma_{\mu}^{(\lambda)}(Q_n, p') = (1/Q_n^2) d_{\mu}^{\nu}(Q_n) \epsilon_{\nu}^{(\lambda)}(p'). \quad (2.12)$$

In our gauge  $\eta \sim p'$ , the second term can be neglected and the effective hard vertex is just given by  $\Gamma(Q_n, p')$  which for  $x \simeq x_n \rightarrow 0$  is essentially parallel to the gauge vector  $\eta$

$$\begin{aligned} \Gamma_{\mu}^{(\lambda)}(Q_n, p') &= \frac{1}{x_n Q_n^2} \left\{ \frac{\bar{p}_{\mu}}{\bar{p}p} (Q_n - x_n p) \cdot \epsilon^{(\lambda)}(p') - x_n \left[ \epsilon_{\mu}^{(\lambda)}(p') - \frac{\bar{p}_{\mu}}{\bar{p}p} p \cdot \epsilon^{(\lambda)}(p') \right] \right\} \\ &\simeq \frac{2(Q_n - x_n p) \cdot \epsilon^{(\lambda)}(p')}{x_n Q_n^2} \left( \frac{\bar{p}_{\mu}}{2\bar{p}p} \right). \end{aligned} \quad (2.13)$$

The neglected term of order  $x_n$  is a purely transverse vector.

(iii) The fact that for  $x \rightarrow 0$  the effective hard vertex  $V_{\text{eff}}(Q_n, p')$  becomes proportional to the gauge vector  $\bar{p}$  provides a further simplification in the relevant Lorentz index flow in the Feynman diagrams. Let us illustrate this for the case of fig. 3 in which we represent the three polarization flow contributions to the

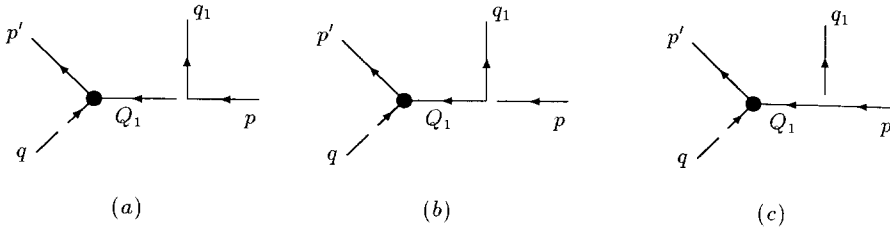


Fig. 3. The three polarization flow contributions in the three-gluon vertex. In our gauge, the leading contribution is given only by the diagram (a).

three-gluon vertex  $\Gamma(-p, q_1, Q_1)$  as

$$\begin{aligned} \epsilon_v^{(\lambda)}(p) \epsilon_{v_1}^{(\lambda_1)}(q_1) \Gamma^{vv_1\rho}(-p, q_1, Q_1) &= \epsilon^{(\lambda)}(p) \cdot \epsilon^{(\lambda_1)}(q_1) (2p - Q_1)^\rho \\ &+ (p - 2q_1) \cdot \epsilon^{(\lambda)}(p) \epsilon^{(\lambda_1)\rho}(q_1) \\ &- (2p - q_1) \cdot \epsilon^{(\lambda_1)}(q_1) \epsilon^{(\lambda)\rho}(p), \end{aligned} \quad (2.14)$$

where  $\rho$  is the Lorentz index of the virtual gluon  $Q_1$ . Since the dominant contribution to the effective hard vertex in eq. (2.13) is proportional to the gauge vector, only the first term in eq. (2.14) (fig. 3a) contributes to the dominant part of the amplitude ( $\eta \cdot \epsilon(p) = \eta \cdot \epsilon(q_1) = 0$ ) and one finds ( $x \simeq x_1 \rightarrow 0$ )

$$\begin{aligned} M_1(pp'q_1, \lambda\lambda'\lambda_1, acb_1) &= (\epsilon^{(\lambda)}(p) \cdot \epsilon^{(\lambda_1)}(q_1)) (2p - Q_1) \cdot V_{\text{eff}}^{(N)}(Q_n, p') ig_s f_{acb_1} \\ &\simeq (\epsilon^{(\lambda)}(p) \cdot \epsilon^{(\lambda_1)}(q_1)) \frac{2(Q_1 - x_1 p) \cdot \epsilon^{(N)}(p')}{x_1 Q_1^2} ig_s f_{acb_1}, \end{aligned} \quad (2.15)$$

with  $\bar{p} \cdot (2p - Q_1) \simeq 2\bar{p}p$  for  $x_1 = 1 - y_1 \rightarrow 0$ .

Such a feature of our gauge frame can be generalized. The leading contributions come from diagrams in which the Lorentz index of the recoiling gluon  $p'$  is saturated by the index of a three-gluon vertex within the diagram and not with the Lorentz index of any of the other external gluons  $p q_1 \dots q_n$ .

(iv) In general, the leading contributions in region (2.5) come from diagrams with the topological and polarization structure of fig. 4 in which the Lorentz index of the recoiling gluon  $p'$  is saturated before the emission of any soft gluon; thus the hard vertex factorizes giving

$$(2k - Q_n) \cdot V_{\text{eff}}^{(N)}(Q_n, p') \simeq \left[ \frac{(2k - Q_n) \cdot \eta}{\eta p} \right] \frac{(Q_n - x_n p) \cdot \epsilon^{(N)}(p')}{x_n Q_n^2}. \quad (2.16)$$

To show the dominance of the diagrams in fig. 4, consider for instance fig. 5 in which a gluon  $q_j$  is emitted before the saturation of the Lorentz index of  $p'$ . In our gauge, the effective vertex gives

$$\begin{aligned} (2k - Q'_n) \cdot \frac{d(Q'_n)}{Q_n'^2} V_{\text{eff}}^{(N)}(Q_n, p') \\ \simeq \frac{1}{Q_n'^2} (2k - Q'_n) \cdot V_{\text{eff}}^{(N)}(Q'_n, p') \\ \simeq \left[ \frac{(2k - Q'_n) \cdot \eta}{\eta p} \right] \frac{1}{Q_n'^2} \frac{(Q'_n - (x_n + y_j) p) \cdot \epsilon^{(N)}(p')}{Q_n'^2 (x_n + y_j)}, \end{aligned} \quad (2.17)$$

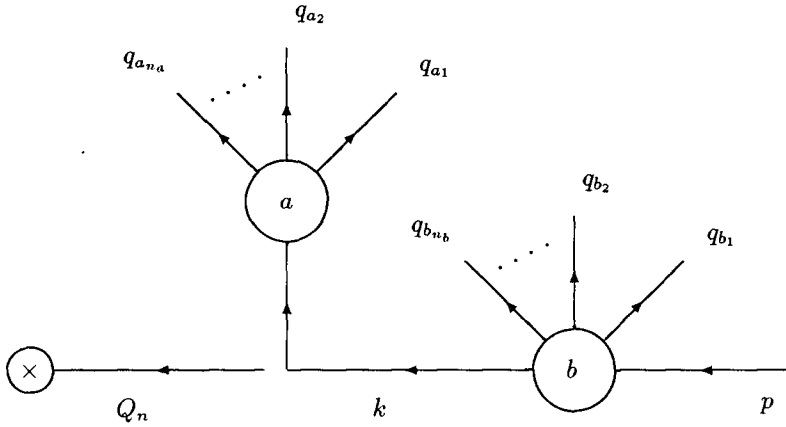


Fig. 4. Structure of diagrams giving, in our gauge, the dominant contribution in the region (2.5). The polarization flow is also indicated.

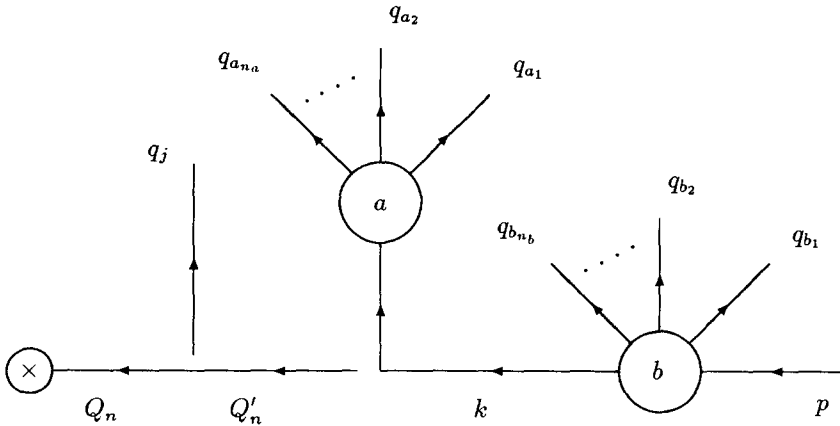


Fig. 5. Emission of soft gluon  $q_j$  gives a subleading contribution in the region (2.5).

with  $Q'_n = Q_n + q_j$ . The  $1/x_n$  singularity in eq. (2.16) is replaced in eq. (2.17) by  $1/(x_n + y_j)$ . The singularity is then screened by  $y_j$  and one obtains a nonleading contribution.

## 2.2. COLOUR NOTATIONS

The  $n$ -gluon emission amplitude  $M_n$  for process (1.7) is a function of the external momenta  $p, p', q_1, \dots, q_n$ , the corresponding Lorentz indices  $\lambda, \lambda', \lambda_1, \dots, \lambda_n$  and the colour indices  $a, c, b_1, \dots, b_n$  (see fig. 2). For each process with a given number of emitted gluons we introduce a space of colour indices  $\{|acb_1 \dots b_n\rangle\}$  and write

the amplitude as a representative state in this space

$$M_n = \langle acb_1 \dots b_n | \mathbf{M}_n(pp'q_1 \dots q_n; \lambda\lambda'\lambda_1 \dots \lambda_n) \rangle. \quad (2.18)$$

As shown in a previous analysis [13] of the infrared structure of deep inelastic scattering for  $x \rightarrow 1$  or of final state emission processes as  $e^+e^-$  annihilation, this notation not only simplifies the Feynman diagram calculations but also helps in grasping the consequences of colour conservation and the physical properties of coherence of QCD radiation.

In the colour space for  $n$  emitted gluons we introduce  $SU(N)$  colour charge matrices  $\mathbf{T}_p, \mathbf{T}_{p'}, \mathbf{T}_1, \dots, \mathbf{T}_n$  for each external gluon  $p, p', q_1, \dots, q_n$  acting as follows

$$\mathbf{T}_i^b |acb_1 \dots b_n\rangle = if_{bb'b'_i} |acb_1 \dots b'_i \dots b_n\rangle, \quad (2.19)$$

and similarly for  $\mathbf{T}_p$  and  $\mathbf{T}_{p'}$ . The charge conservation condition is

$$\left( -\mathbf{T}_p + \mathbf{T}_{p'} + \sum_{l=1}^n \mathbf{T}_l \right) |M_n\rangle = 0. \quad (2.20)$$

This condition is satisfied by  $M_0$  and  $M_1$  (see eq. (2.15)).

### 2.3. SOFT GLUON EMISSION FOR $x \rightarrow 1$

Before analyzing the  $x \rightarrow 0$  case we recall here the results of soft gluon factorization in the case  $x \rightarrow 1$ . This will help in describing the general method and in understanding the physical differences between  $x \rightarrow 1$  and  $x \rightarrow 0$  cases.

For  $x \rightarrow 1$  the leading infrared structure of  $M_n$  is obtained by studying the process of fig. 1 in the strongly ordered energy region for the emitted gluons

$$y_n \ll y_{n-1} \ll \dots \ll y_1 \ll x \sim 1. \quad (2.21)$$

As well known [2], the emission of the softest gluon  $q_n$  can be factorized in terms of the eikonal current and, in the colour notations of the previous subsections, one has

$$\langle acb_1 \dots b_n | M_n \rangle \simeq \langle acb_1 \dots b_{n-1} | \mathbf{J}_{\text{eik}}^{(n-1)b_n}(q_n) | M_{n-1} \rangle, \quad (2.22)$$

where

$$\mathbf{J}_{\text{eik}}^{(n-1)}(q) = -\mathbf{T}_p \frac{p}{pq} + \mathbf{T}_{p'} \frac{p'}{p'q} + \sum_{l=1}^{n-1} \mathbf{T}_l \frac{q_l}{q_l q}, \quad (2.23)$$

is the classical current for the emission of the soft gluon by the other harder charges. This current is conserved due to the vanishing of the total charge (see eq. (2.20)).

The fact that, after the factorization of  $q_n$  emission, one is able to reconstruct the amplitude  $M_{n-1}$ , is crucial in order to provide a recurrence relation which allows one to construct the dominant part of  $M_n$  in the phase space (2.21).

### 3. Factorization of soft emission current for $x \rightarrow 0$

For  $x \rightarrow 0$  the dominant part of  $M_n$  is obtained by studying the process of fig. 1 in the phase space region (2.5). In this section we extend the method of soft gluon factorization extensively used [2] in the region  $x \rightarrow 1$ . We prove that this factorization is possible in general and we construct the corresponding soft current. We are able to obtain a recurrence relation which allows one to evaluate the leading  $x \rightarrow 0$  contributions to all amplitudes  $M_n$  at tree level.

Due to the form (2.13) of the effective hard vertex  $V_{\text{eff}}(Q_n, p')$  in our gauge, we factorize in all  $M_n$  the following subamplitude

$$M_n \simeq \frac{2(Q_n - x_n p) \cdot \epsilon^{(\lambda')}(p')}{x Q_n^2} \langle acb_1 \dots b_n | \mathbf{h}_n(pp'q_1 \dots q_n) \rangle, \quad (3.1)$$

where  $\mathbf{h}_n$  corresponds to the diagram in fig. 4 in which the hard vertex  $Q_n + q \rightarrow p'$  is replaced by  $\eta/2\eta p$  (see eq. (2.13)). We have already found this structure in the case of  $n = 1$  (see eq. (2.15)) in which the subamplitude  $\mathbf{h}_1$  is

$$\langle acb_1 | \mathbf{h}_1(pp'q_1) \rangle = \epsilon^{(\lambda)}(p) \cdot \epsilon^{(\lambda_1)}(q_1) i g_s f_{acb_1}. \quad (3.2)$$

In the following we show that the soft gluon factorization and the corresponding recurrence relation hold not for the full amplitude  $M_n$  but for the subamplitude  $\mathbf{h}_n$  in the form

$$\langle acb_1 \dots b_n | \mathbf{h}_n(pp'q_1 \dots q_n) \rangle \simeq g_s \langle acb_1 \dots b_{n-1} | \mathbf{J}_{\text{tot}}^{(n-1)b_n}(q_n) | \mathbf{h}_{n-1}(pp'q_1 \dots q_{n-1}) \rangle. \quad (3.3)$$

We show also that the soft emission current  $\mathbf{J}_{\text{tot}}^{(n-1)}(q_n)$  is given by the following two contributions

$$\mathbf{J}_{\text{tot}}^{(n-1)}(q_n) = \mathbf{J}_{\text{eik}}^{(n-1)}(q_n) + \mathbf{J}_{\text{ne}}(Q_n, q_n), \quad (3.4)$$

where  $\mathbf{J}_{\text{eik}}^{(n-1)}(q_n)$  is the eikonal current in eq. (2.22) and  $\mathbf{J}_{\text{ne}}(Q_n, q_n)$  is a non-eikonal current given by

$$\mathbf{J}_{\text{ne}}(Q_n, q_n) = \frac{2(Q_{n-1} - x_{n-1} p) \cdot \epsilon(q_n)}{Q_{n-1}^2} \mathbf{T}_{p'}, \quad (3.5)$$

with  $Q_{n-1} = Q_n + q_n$ ,  $x_{n-1} = x_n + y_n$ .

This result is obtained as follows. The emission of the softest gluon  $n$  from the harder external and internal lines can be factorized as usual [2] and is described by the eikonal part of the current. In the phase space (2.5) only the internal line  $Q_n$  is softer than the emitted gluon. In this case the emission of the softest gluon  $n$  from  $Q_n$  cannot be evaluated by the eikonal approximation. However we are able to factorize also this contribution by taking into account the property of coherence of the radiation and obtain the non-eikonal current  $\mathbf{J}_{ne}$ .

This additional non-eikonal contribution to the total soft current for  $x \rightarrow 0$  has been introduced also in ref. [6] in a one-loop calculation. In this section we present the generalization to all loops.

We shall present in subsect. 3.3 the general proof by induction of eqs. (3.3) and (3.4). To this purpose we first analyze in detail the case with  $n = 2$  and some general features of the case  $n = 3$ .

### 3.1. SOFT EMISSION FOR $n = 2$

The leading contributions to  $M_2$  in the phase space

$$x \ll y_2 \ll y_1 \approx 1, \quad (3.6)$$

come, in our gauge, from the diagrams in fig. 6 (see sect. 2).

Consider first the two diagrams (figs. 6a, b) which correspond to the usual eikonal emission of the softest gluon  $q_2$  from the hard external gluons  $p$  and  $q_1$ . In these two diagrams the soft emission can be factorized giving the usual result [2]

$$\langle acb_1 b_2 | \mathbf{h}_2^{(a+b)} \rangle \approx g_s \langle acb_1 | \mathbf{J}_{\text{eik}}^{(1)}(q_2) | \mathbf{h}_1 \rangle, \quad (3.7)$$

with

$$\mathbf{J}_{\text{eik}}^{(1)}(q_2) = \left( \frac{p}{-pq_2} \mathbf{T}_p + \frac{q_1}{q_1 q_2} \mathbf{T}_1 \right) \cdot \epsilon(q_2). \quad (3.8)$$

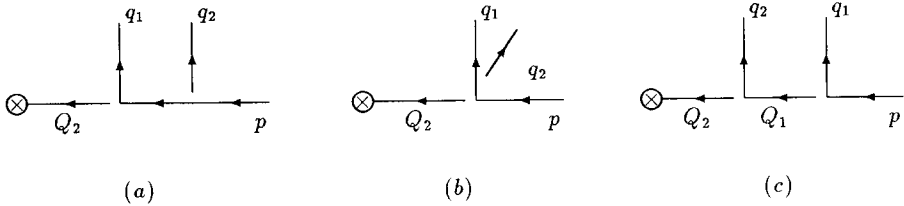


Fig. 6. Diagrams for  $n = 2$  giving the leading contribution in (3.6).

Since in this gauge  $\eta \sim p'$  we have

$$\frac{p}{pq_2} \cdot \epsilon(q_2) \simeq \frac{p}{pq_2} - \frac{p'}{p'q_2}, \quad \frac{q_1}{q_1q_2} \cdot \epsilon(q_2) \simeq \frac{q_1}{q_1q_2} - \frac{p'}{p'q_2}, \quad (3.9)$$

and the hard probe is a colour singlet

$$(-\mathbf{T}_p + \mathbf{T}_1 + \mathbf{T}_{p'})|\mathbf{h}_1\rangle = 0, \quad (3.10)$$

and the eikonal current can be written as follows

$$\mathbf{J}_{\text{eik}}^{(1)}(q_2) = \frac{p}{-pq_2} \mathbf{T}_p + \frac{p'}{p'q_2} \mathbf{T}_{p'} + \frac{q_1}{q_1q_2} \mathbf{T}_1. \quad (3.11)$$

We consider now the last graph of fig. 6 and show that also in this case the soft gluon  $q_2$  can be factorized. Notice that in diagram of fig. 6c, the gluon  $q_2$  is emitted with the same effective vertex  $\Gamma(Q_1, q_2)$  we have introduced in the previous section (eq. (2.13))

$$\Gamma_\mu^{(\lambda_2)}(Q_1, q_2) = \frac{1}{Q_1^2} d(Q_1) \cdot \epsilon_\mu^{(\lambda_2)}(q_2) \simeq \frac{2(Q_1 - x_1 p) \cdot \epsilon^{(\lambda_2)}(q_2)}{x_1 Q_1^2} \frac{\eta_\mu}{2\eta p}. \quad (3.12)$$

We have neglected a contribution regular as  $x \simeq x_1 = 1 - y_1 \rightarrow 0$  and purely transverse.

As in the case of the hard vertex, in this gauge the saturation of the Lorentz index with external gluon polarizations gives only a nonleading contribution of order  $x_1$ . By using the approximation in eq. (2.13), the diagram of fig. 6c gives

$$\begin{aligned} \langle acb_1 b_2 | \mathbf{h}_2^{(c)} \rangle &\simeq g_s \frac{\eta \cdot (2Q_1 - Q_2)}{2\eta p} [(2p - Q_1) \cdot \Gamma^{(\lambda_2)}(Q_1, q_2)] \langle acb_1 | \mathbf{T}_{p'}^{b_2} | \mathbf{h}_1 \rangle \\ &\simeq g_s \langle acb_1 | \frac{2(Q_1 - x_1 p) \cdot \epsilon^{(\lambda_2)}(q_2)}{Q_1^2} \mathbf{T}_{p'}^{b_2} | \mathbf{h}_1 \rangle \\ &= g_s \langle acb_1 | \mathbf{J}_{\text{nc}}^{(\lambda_2)}(Q_2, q_2) | \mathbf{h}_1 \rangle, \end{aligned} \quad (3.13)$$

where the factor  $(2Q_1 - Q_2) \cdot (\eta/2\eta p) = x_1 - \frac{1}{2}x_2 \simeq x_1$  has canceled the  $1/x_1$  singular factor in the effective vertex  $\Gamma(Q_1, q_2)$ .

### 3.2. CASE $n = 3$ AND THE STRUCTURE OF GENERAL SOFT INSERTIONS

The features of the calculations for  $n = 2$  can be generalized to higher  $n$ . However the generalization requires some new features which we want to illustrate by



Fig. 7. Example of diagrams for  $n = 3$ . (a) Diagram with a leading contribution. (b) Diagram with a nonleading contribution.

analyzing the case  $n = 3$  in the region

$$x \ll y_3 \ll y_2 \ll y_1 \simeq 1. \quad (3.14)$$

In our gauge the subamplitude  $\mathbf{h}_3$  can be obtained by considering all possible insertions of the softest gluon  $q_3$  on the diagrams of fig. 6. These insertions can be divided into four general categories:

- (i) non-eikonal insertion on the softest internal line  $Q_2$ ,
- (ii) non-eikonal insertion on harder lines,
- (iii) eikonal insertion on harder lines emitted from eikonal vertices,
- (iv) eikonal insertion on harder lines emitted from non-eikonal vertices

(i) *Non-eikonal insertion on the softest internal line  $Q_2$ .* This gives a new vertex  $Q_2 \rightarrow Q_3 + q_3$ , with the Lorentz index structure of fig. 4. For example, in the case of fig. 6a this type of insertion gives the diagram of fig. 7a. For all diagrams of fig. 6 this will contribute to the subamplitude  $\mathbf{h}_3$  with the momentum factor

$$\frac{\eta}{2\eta p} \cdot (2Q_2 - Q_3) \Gamma_\mu^{(\lambda_3)}(Q_2, q_3) \simeq \frac{2(Q_2 - x_2 p) \cdot \epsilon^{(\lambda_3)}(q_3)}{Q_2^2} \frac{\eta_\mu}{2\eta p}, \quad (3.15)$$

where we have replaced the effective hard vertex  $V_{\text{eff}}^{(\lambda)}(Q_3, p')$  by  $\eta/2\eta p$  and approximated the effective vertex  $\Gamma^{(\lambda_3)}(Q_2, q_3)$  for the emission of  $q_3$  according to eq. (2.13).

From eq. (3.15) we have the following factorized contribution to the soft gluon emission

$$\langle acb_1 b_2 b_3 | \mathbf{h}_3 \rangle \simeq g_s \langle acb_1 b_2 | \frac{2(Q_2 - x_2 p) \cdot \epsilon^{(\lambda_3)}(q_3)}{Q_2^2} \mathbf{T}_{p'}^{b_3} | \mathbf{h}_2 \rangle + \dots \quad (3.16)$$

(ii) *Non-eikonal insertion on hard lines.* An example is given in fig. 7b. All insertions of this type give nonleading contributions.

(iii) *Eikonal insertion on harder lines emitted from eikonal vertices.* This refers to the insertions into figs. 6a, b in which  $q_2$  is emitted from an eikonal vertex. Let us

consider for instance the diagram of fig. 6a, in which this type of insertion can be factored out and gives the following soft emission current ( $k_2 = p - q_2$ ,  $k'_2 = k_2 - q_3$ )

$$\mathbf{J}^{(a)}(q_3) \equiv \left\{ \frac{q_1}{q_1 q_3} \mathbf{T}_1 + \frac{k_2^2}{k_2'^2} \left[ -\frac{p}{p q_3} \mathbf{T}_p + \frac{q_2}{q_2 q_3} \mathbf{T}_2 \right] + \left( 1 - \frac{k_2^2}{k_2'^2} \right) \frac{k_2}{k_2 q_3} (-\mathbf{T}_p + \mathbf{T}_2) \right\} \cdot \epsilon(q_3). \quad (3.17)$$

The first term is the eikonal emission from  $q_1$ . The second term with the brackets corresponds to the emission from external gluons  $p, q_2$  and the factor  $k_2^2/k_2'^2$  is needed in order to reconstruct the original subamplitude  $\mathbf{h}_2^{(a)}$  in fig. 6a. The third term corresponds to insertion of  $q_3$  on the internal line  $k_2$  which, according to charge conservation, has the colour charge  $\mathbf{T}_{k_2} = -\mathbf{T}_p + \mathbf{T}_2$ . As shown in ref. [13], at the leading collinear level, the last two contributions can be replaced just by the sum of the eikonal currents for the emission of  $q_3$  from external gluons  $p$  and  $q_2$  with no rescaling of internal momenta. We have then

$$\mathbf{J}^{(a)}(q_2) \simeq \mathbf{J}_{\text{eik}}^{(3)}(q_3) \equiv \left\{ -\frac{p}{p q_3} \mathbf{T}_p + \frac{q_1}{q_1 q_3} \mathbf{T}_1 + \frac{q_2}{q_2 q_3} \mathbf{T}_2 \right\} \cdot \epsilon(q_3). \quad (3.18)$$

The reason for the above approximation is a coherent effect. When  $q_3$  is parallel to  $k_2$  we have  $k_2'^2 \simeq k_2^2$  since  $q_3$  is the softest gluon. In this case the last term in eq. (3.17) can be neglected, the factor of momentum rescaling in the second term is 1 and we obtain eq. (3.18). In the opposite case  $p$  and  $q_2$  can be considered nearly parallel at the leading collinear level and we have  $|k_2'^2| \gg |k_2^2| \simeq 0$ . It follows that the second term in eq. (3.17) can be neglected and the last one becomes

$$\frac{k_2}{k_2 q_3} (-\mathbf{T}_p + \mathbf{T}_2) \simeq \left[ -\frac{p}{p q_3} \mathbf{T}_p + \frac{q_2}{q_2 q_3} \mathbf{T}_2 \right], \quad (3.19)$$

thus leading again to eq. (3.18). A similar result holds also for fig. 6b.

(iv) *Eikonal insertions on harder lines emitted from non-eikonal vertices.* This refers to insertions on fig. 6c in which  $q_2$  is emitted from non-eikonal vertex. Considering the soft emission of  $q_3$  from all harder lines in fig. 6c we can factorize the following expression ( $Q'_1 = Q_1 - q_3$ )

$$\begin{aligned} \mathbf{F}^{(c)} \equiv & \left\{ \frac{q_2 \cdot \epsilon(q_3)}{q_2 q_3} \mathbf{T}_2 \right\} d(Q_1) \cdot \epsilon(q_2) \\ & + \left\{ \frac{Q_1^2}{Q_1'^2} \left[ -\frac{p}{p q_3} \mathbf{T}_p + \frac{q_1}{q_1 q_3} \mathbf{T}_1 \right] \cdot \epsilon(q_3) \right\} d(Q'_1) \cdot \epsilon(q_2) \\ & + \left\{ \left( 1 - \frac{Q_1^2}{Q_1'^2} \right) \frac{Q_1 \cdot \epsilon(q_3)}{-Q_1 q_3} (-\mathbf{T}_p + \mathbf{T}_1) \right\} d(Q'_1) \cdot \epsilon(q_2). \end{aligned} \quad (3.20)$$

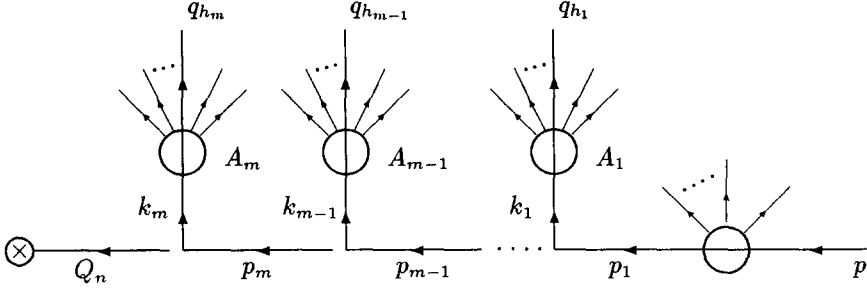


Fig. 8. Structure of diagrams giving the leading contributions to the general amplitude.

The first term corresponds to the emission from  $q_2$ ; the second one to the emission from  $p$  and  $q_1$  and the last one corresponds to the emission from the internal hard line  $Q_1$  with colour charge  $\mathbf{T}_{Q_1} = -\mathbf{T}_p + \mathbf{T}_1$ . The expression in eq. (3.20) is similar to the one in eq. (3.17). We can apply the same analysis and by coherence we obtain

$$\mathbf{F}^{(c)} \simeq \mathbf{J}_{\text{eik}}^{(2)}(q_3) d(Q_1) \cdot \epsilon(q_2), \quad (3.21)$$

where the quantity  $d(Q_1) \cdot \epsilon(q_2)$  is needed to reconstruct the original subamplitude  $\mathbf{h}_2^{(c)}$  of fig. 6c.

Combining all these contributions we obtain the soft emission formulae (3.3) and (3.4) for the  $n = 3$  case.

### 3.3. GENERAL LEADING AMPLITUDES

Here we give the general proof by iteration of eqs. (3.3) and (3.4). First we show that in the phase space region (2.5) the leading diagrams have the structure in fig. 8. In this figure we denote by  $q_{h_j}$  the hardest gluon emitted within the subgraph  $A_j$ . Other specific features are the following:

- (i) As indicated, the Lorentz index of  $q_{h_1}$  is saturated by the Lorentz index of  $p$ .
- (ii) The Lorentz index of the gluon  $q_{h_j}$  is saturated within the vertex  $p_{j-1} \rightarrow p_j + k_{j-1}$ .
- (iii) The soft emission from the various subamplitudes  $A_0 \dots A_m$  is of eikonal type only.

The above helicity structure can be proved by an iterative method. We suppose that this structure holds for a graph with a given number  $(n - 1)$  of emitted gluons and then we analyze all possible insertions of a softer gluon  $q_n$  ( $x_n \ll y_n \ll y_i$ ).

Due to the simplifications discussed in the  $n = 2, 3$  cases, we have to consider only the following categories of insertions:

- (i) *Non-eikonal insertions on the softest internal line  $Q_{n-1}$ .* In this case we can follow the calculation for  $n = 3$  in eq. (3.15) and reconstruct the original subampli-

tude  $\mathbf{h}_{n-1}$  by factorizing the soft current contribution of non-eikonal type  $\mathbf{J}_{\text{nc}}(Q_n, q_n)$  given in eq. (3.5).

(ii) *Non-eikonal insertions on harder lines.* These are of the type of fig. 7b and can be neglected in general.

(iii) *Eikonal insertion on harder lines.* Consider first the eikonal insertions of the softest gluon  $n$  on the last subgraph  $A_m$ . It is known [13] that all these insertions can be factorized in terms of eikonal current emission

$$\mathbf{J}^{(A_m)}(q_n) \simeq \mathbf{J}_{\text{eik}}^{(A_m)}(q_n) \equiv \sum_{i \in A_m} \frac{q_i \cdot \epsilon^{(\lambda_n)}(q_n)}{q_i q_n} \mathbf{T}_i. \quad (3.22)$$

Consider now the sum of the insertions on the line  $p_m, p_{m-1}, k_{m-1}$  and on the next eikonal subgraph  $A_{m-1}$ . For insertions on  $A_{m-1}$  and  $k_{m-1}$  we can use the approximations in the previous subsection. As in eq. (3.20) we can factorize the expression

$$\begin{aligned} \mathbf{F}^{(A_{m-1})} \equiv & \left\{ \left( 1 - \frac{p_m^2}{p_m'^2} \right) \frac{p_m \cdot \epsilon(q_n)}{-p_m q_n} \mathbf{T}_{p_m} \right\} (d(p_m) \cdot \epsilon(q_{h_m})) \\ & - \left\{ \frac{p_m^2}{p_m'^2} \left[ \left( 1 - \frac{p_{m-1}^2}{p_{m-1}'^2} \right) \frac{p_{m-1} \cdot \epsilon(q_n)}{p_{m-1} q_n} \mathbf{T}_{p_{m-1}} - \mathbf{J}_{\text{eik}}^{(A_{m-1})}(q_n) \right] \right\} \\ & \times (d(p'_m) \cdot \epsilon(q_{h_m})), \end{aligned} \quad (3.23)$$

where  $\mathbf{T}_{p_{m-1}}$  and  $\mathbf{T}_{p_m}$  are the colour charges of lines  $p_{m-1}$  and  $p_m$ , and  $p'_m = p_m - q_n$ ,  $p'_{m-1} = p_{m-1} - q_n$ . Using colour conservation we have

$$\mathbf{T}_{p_{m-1}} = \mathbf{T}_{p_m} + \sum_{i \in A_{m-1}} \mathbf{T}_i. \quad (3.24)$$

The factors  $p_m^2/p_m'^2$  and  $(1 - p_m^2/p_m'^2)$ , etc. are set in order to reconstruct the full subamplitude  $\mathbf{h}_{n-1}$  (apart from the factor  $d(p_m) \cdot \epsilon(q_{h_m})$  which is included in eq. (3.23)).

Eq. (3.23) has the same structure of eq. (3.20) and as in the previous case, we have

$$\begin{aligned} \mathbf{F}^{(A_{m-1})} \simeq & (d(p_m) \cdot \epsilon(q_{h_m})) \\ & \times \left\{ \mathbf{J}_{\text{eik}}^{(A_{m-1})}(q_n) - \left( 1 - \frac{p_{m-1}^2}{p_{m-1}'^2} \right) \frac{p_{m-1} \cdot \epsilon(q_n)}{p_{m-1} q_n} \mathbf{T}_{p_{m-1}} \right\}, \end{aligned} \quad (3.25)$$

where the factor  $d(p_m) \cdot \epsilon(q_{h_m})$  allows one to complete the reconstruction of the full

original subamplitude  $\mathbf{h}_{n-1}$ . The current  $\mathbf{J}_{\text{eik}}^{(A_{m-1})}(q_n)$  contributes to the eikonal part of the total current. The remaining soft current contribution,

$$\left(1 - \frac{p_{m-1}^2}{p_{m-1}'^2}\right) \frac{p_{m-1} \cdot \epsilon(q_n)}{p_{m-1} q_n} \mathbf{T}_{p_{m-1}}, \quad (3.26)$$

can be added to the insertion of gluon  $n$  on  $p_{m-2}$ ,  $k_{m-2}$  and  $A_{m-2}$  to obtain  $F^{(A_{m-2})}$  given by eq. (3.25) with  $m \rightarrow m-1$ . Continuing this procedure down the ladder of fig. 8 we always reconstruct the original amplitude  $\mathbf{h}_{n-1}$  and factor out the eikonal emission current  $\mathbf{J}_{\text{eik}}^{(A_j)}(q_n)$  from all eikonal subgraphs  $A_m, A_{m-1}, \dots, A_0$ . The remaining term in eq. (3.26) for  $m=0$  is now the contribution from the insertion of gluon  $n$  on the incoming gluon  $p$ .

In conclusion from the iterative analysis of all these insertions we have shown that (i) the structure of the dominant diagrams (in our gauge) is given in fig. 8, (ii) the factorization of soft emission gives the recurrence relation (3.3), (iii) the soft current has the form (3.4).

As shown in ref. [13] one can explicitly check that, in our approximation, charge and current are conserved.

#### 4. Soft gluon coherence for $x \rightarrow 0$ : tree level distributions

In this section we solve the recurrence relation as in eqs. (3.1) and (3.3) and compute the leading contribution of  $|M_n^{(\text{tree})}|^2$ , the spin and colour average square amplitude at tree level. We then analyze the structure of coherence of soft gluon radiation emitted in initial jets for small  $x$  and compute the gluon structure function at tree level.

Let us recall the main differences between the two cases  $x \rightarrow 0$  and  $x \rightarrow 1$ . First we have that in the case  $x \rightarrow 0$  the total soft current (3.4) contains an additional contribution of non-eikonal type. The second difference is in the recurrence relation: for  $x \rightarrow 1$ , it holds directly for the full amplitude  $\mathbf{M}_n$  (see eq. (2.22)); while for  $x \rightarrow 0$  it holds for the subamplitude  $\mathbf{h}_n$  (see (3.3)). This subamplitude is obtained by factorizing the effective hard vertex in eq. (2.10) and therefore the multi-gluon distribution for  $x \rightarrow 0$  is given by

$$\begin{aligned} |M_n^{(\text{tree})}|^2 &\simeq \frac{1}{x^2} \frac{4}{Q_n^2} \langle \mathbf{h}_n(pp'q_1 \dots q_n) | \mathbf{h}_n(pp'q_1 \dots q_n) \rangle \\ &\simeq \frac{1}{x^2} \frac{4g_s^2}{Q_n^2} \langle \mathbf{h}_{n-1} | (\mathbf{J}_{\text{tot}}^{(n-1)}(q_n))^2 | \mathbf{h}_{n-1} \rangle. \end{aligned} \quad (4.1)$$

We shall show that the role of these differences is the following:

- (i) The factor  $1/x^2$  from the hard vertex gives rise to the contribution in the Altarelli–Parisi splitting function which becomes singular as a fast gluon is emitted.
- (ii) The non-eikonal term in the total soft current has the role of compensating the singular factor  $1/Q_n^2$  from the effective vertex. In general we find that there are no leading mass singularities in spacelike momenta. This fact, as pointed out in ref. [2, 6] from a one-loop analysis, is an important consequence of coherence in the region  $x \rightarrow 0$ . As we shall see, this cancellation is based on the remarkable result

$$(\mathbf{J}_{\text{tot}}^{(n-1)}(q_n))^2 \simeq \frac{Q_n^2}{Q_{n-1}^2} (\mathbf{J}_{\text{eik}}^{(n-1)}(q_n))^2, \quad (4.2)$$

valid in the energy ordered region (2.5).

By iterating eq. (4.2), all mass singularities of spacelike legs  $Q_k = p - q_1 - \dots - q_k$ ,  $k \geq 2$  are cancelled and the recurrence relation for the squared amplitudes (4.1) involves only the eikonal currents. Therefore we find the important result that, to leading order, the structure of coherence in initial jets for the two regions  $x \rightarrow 0$  and  $x \rightarrow 1$  is similar. In particular, as we shall explicitly show, the soft gluon emission takes place in the angular ordered region

$$\theta_{pq_n} \gg \dots \gg \theta_{pq_2} \gg \theta_{pq_1}, \quad (4.3)$$

where  $\theta_{pq_i}$  is the angle between  $p$  and  $q_i$ .

The disappearance of all  $1/Q_j^2$  ( $j \geq 2$ ) pole contributions in  $|M_n|^2$  has been observed [15] in the exact calculations up to  $n = 3$ . Beside extending this feature for any values of  $n$  to leading order, our analysis provides an insight into the physical origin of this cancellation: soft gluon coherence.

#### 4.1. SQUARED AMPLITUDES

Because of eq. (4.2), the multi-gluon distribution for the  $x \rightarrow 0$  case can be computed by the same techniques used for the  $x \rightarrow 1$  case.

We start by proving eq. (4.2). The total soft current in eq. (3.4) can be written as

$$\mathbf{J}_{\text{tot}}^{(n-1)}(q_n) = -(j_p(q_n) - j_{Q_n}(q_n))\mathbf{T}_p + \sum_{l=1}^{n-1} (j_l(q_n) - j_{Q_n}(q_n))\mathbf{T}_l, \quad (4.4)$$

with

$$j_p(q_n) = \frac{p}{pq_n}, \quad j_l(q_n) = \frac{q_l}{q_l q_n}, \quad j_{p'}(q_n) = \frac{p'}{p' q_n}, \quad (4.5)$$

$$j_{Q_n}(q_n) = \frac{1}{Q_{n-1}^2} \left\{ \frac{p'}{p' q_n} (Q_n^2 + 2pq_n x_{n-1}) + 2(Q_{n-1} - x_{n-1}p) \right\}. \quad (4.6)$$

The current  $j_{Q_n}(q_n)$  is obtained from

$$\mathbf{J}_{\text{ne}}(Q_n, q_n) + j_{p'}(q_n) \mathbf{T}_{p'} = j_{Q_n}(q_n) \mathbf{T}_{p'}, \quad (4.7)$$

with  $Q_n = Q_{n-1} - q_n$ ,  $x_n = x_{n-1} - y_n$  and we used the charge conservation in eq. (2.20).

Eq. (4.2) can be obtained by using the following two results:

(i) In the semi-hard phase space region (2.5), the first term of the quantity

$$\begin{aligned} & (j_l(q_n) - j_{Q_n}(q_n))^2 \\ &= -\frac{1}{Q_{n-1}^2} \frac{2}{y_n q_l q_n} \left\{ y_l Q_n^2 + 2 y_n q_l (Q_{n-1} - x_{n-1} p) + 2 p q_n x_{n-1} y_l - 2 q_l q_n y_n \right\}, \end{aligned} \quad (4.8)$$

dominates and we obtain

$$(j_l - j_{Q_n})^2 \simeq -\frac{Q_n^2}{Q_{n-1}^2} \frac{2 y_l}{y_n q_l q_n} = \frac{Q_n^2}{Q_{n-1}^2} (j_l - j_{p'})^2, \quad (4.9)$$

where, in the currents, the  $q_n$  dependence is understood.

(ii) Moreover for  $x \rightarrow 0$  we have

$$\frac{1}{Q_n^2} (j_l - j_{p'})^2 \simeq \frac{1}{Q_{n-1}^2} (j_l - j_{p'})^2. \quad (4.10)$$

This is due to the fact that in the region (2.5) the coefficient of the  $Q_n^2 \rightarrow 0$  singularity vanishes for  $q_n \sim p$  or  $q_n \sim q_i$  and one has  $Q_n \sim Q_{n-1}$ .

By using eqs. (4.9) and (4.10) we get

$$\begin{aligned} (j_l - j_{Q_n})(j_{l'} - j_{Q_n}) &= \frac{1}{2} \left\{ (j_l - j_{Q_n})^2 + (j_{l'} - j_{Q_n})^2 - (j_l - j_{l'})^2 \right\} \\ &\simeq (Q_n^2 / Q_{n-1}^2) (j_l - j_{p'})(j_{l'} - j_{p'}). \end{aligned} \quad (4.11)$$

At this point we insert eqs. (4.9), (4.10) and (4.11) into the square of  $\mathbf{J}_{\text{tot}}^{(n-1)}(q_n)$  given in eq. (4.4) and obtain the result in eq. (4.2).

In view of the discussion in sect. 6 it is useful to recall here the main points needed to obtain the multi-gluon distributions and to prove the coherence property leading to eq. (4.3). We follow the method of ref. [13]. In general the colour

amplitudes can be written as follows (see also ref. [15])

$$\langle acb_1 \dots b_n | \mathbf{h}_n \rangle = \sum_{\pi_{n+1}} h_n(pq_{l_0} \dots q_{l_n}) 2 \text{Tr}(\lambda^a \lambda^{b_0} \dots \lambda^{b_n}), \quad (4.12)$$

where the sum is over permutations  $l_0, \dots, l_n$  with  $q_0 = p'$ ,  $b_0 = c$ . By performing the colour algebra one has ( $\sigma_0 = (N_c^2 - 1)$ )

$$\langle \mathbf{h}_n | \mathbf{h}_n \rangle \simeq \sigma_0 \left( \frac{C_A}{2} \right)^n \sum_{\pi_{n+1}} |h_n(pq_{l_0} \dots q_{l_n})|^2, \quad C_A = N_c. \quad (4.13)$$

Here we have neglected terms which are doubly suppressed (see ref. [13]) since they are nonleading collinear and nonplanar (suppressed by  $1/N_c^2$ ). These terms are absent up to  $n = 3$ . One uses eqs. (3.3) and (4.2) to obtain a recurrence relation for the colour component in eq. (4.12)

$$\frac{1}{Q_n^2} |h_n(\dots q_l q_n q_{l'} \dots)|^2 \simeq -\frac{g_s^2}{Q_{n-1}^2} |h_{n-1}(\dots q_l q_{l'} \dots)|^2 (j_l(q_n) - j_{l'}(q_n))^2, \quad (4.14)$$

with the initial condition

$$\frac{1}{Q_1^2} |h_1(pp'q_1)|^2 = \frac{1}{Q_1^2} |h_1(pq_1p')|^2 = \frac{g_s^2}{4} (j_p(q_1) - j_{p'}(q_1))^2. \quad (4.15)$$

The solution of this equation is obtained in ref. [13]. We find

$$|M_n^{(\text{tree})}|^2 \simeq \sigma_0 \frac{(g_s^2 C_A)^n}{x_n^2} \sum_{\pi_{n+1}} W_n(pq_{l_0} \dots q_{l_n}), \quad (4.16)$$

where  $W_n$  is the multi-eikonal distribution

$$W_n(pq_{l_0} \dots q_{l_n}) = \frac{(pp')^2}{(pq_{l_0}) \dots (q_{l_n}p)}, \quad (4.17)$$

introduced in ref. [2].

The multi-gluon distribution (4.16) although computed for  $x \rightarrow 0$ , can be assumed to be valid also for  $x \rightarrow 1$ . As previously mentioned, this is due to the observation that if we extrapolate (4.16) into the region  $x \rightarrow 1$ , the resulting distributions match the ones obtained here (see ref. [2]). We then assume eq. (4.16) to be valid for any value of  $x$ . In the resulting multi-gluon distributions we do not take into account in a reliable way the intermediate regions  $y_i \ll x \ll y_{i-1}$  which, however, are nonleading both for  $x \rightarrow 0$  and  $x \rightarrow 1$ .

The expression in eq. (4.16) has been obtained in the  $y$ -ordered region  $y_i \ll y_{i-1}$ . Notice however that  $|M_n^{(\text{tree})}|^2$  is symmetric with respect to the emitted gluons. Therefore, eq. (4.16) is valid in any  $y$ -ordered region and, as in the  $x \rightarrow 1$  case, the spacelike branching takes place in the ordered angular region (4.3). To show this one has to discuss the structure of collinear singularities of  $|M_n^{(\text{tree})}|^2$ . The collinear singularities in  $\theta_{p'q_k} = 0$  and  $\theta_{q_k q_{k'}} = 0$  are relevant for the analysis of final state branching. Since we are interested in the initial state branching, we limit our following analysis to the  $\theta_{pq_k} = 0$  singular terms.

It is convenient to express the multi-eikonal distribution in the following form

$$W_n(p l_1 \dots l_k p' l_{k+1} \dots l_n) = W_{pp'}(q_{l_k}) W_{pp'}(q_{l_{k+1}}) \prod_{i=1}^{k-1} W_{pq_{i+1}}(q_{l_i}) \prod_{i=k+2}^n W_{pq_{i-1}}(q_{l_i}), \quad (4.18)$$

where  $W_{pq_i}(q_{l'})$  is the usual eikonal distribution for the emission of  $q_{l'}$  from the two charges  $p$  and  $q_i$

$$W_{pq_i}(q_{l'}) = (pq_{l'}) / (pq_i)(q_{l'} q_i). \quad (4.19)$$

By introducing the angular variables

$$\begin{aligned} \xi_{ij} &= \frac{q_i q_j}{\omega_i \omega_j} = (1 - \cos \theta_{q_i q_j}) \simeq \frac{1}{2} \theta_{q_i q_j}^2, \\ \xi_i &= \frac{pq_i}{E \omega_i} = (1 - \cos \theta_{pq_i}) \simeq \frac{1}{2} \theta_{pq_i}^2, \quad q_{it}^2 \simeq 2 \omega_i^2 \xi_i, \end{aligned} \quad (4.20)$$

we can write

$$\omega_{p'}^2 W_{pq_i}(q_{l'}) = \frac{\xi_{l'}}{\xi_{l'} \xi_{l'l}} \rightarrow \frac{1}{\xi_{l'}} \Theta(\xi_l - \xi_{l'}) + \frac{1}{\xi_{l'l}} \Theta(\xi_l - \xi_{l'l}), \quad (4.21)$$

where the last expression is obtained by performing the azimuthal integrations (see refs. [8, 10]). The initial state singularities are then given by

$$W_n(p l_1 \dots l_k p' l_{k+1} \dots l_n) = \left( \prod_1^n \frac{1}{\omega_i^2 \xi_i} \right) \Theta_{l_k \dots l_1}^{\xi} \Theta_{l_{k+1} \dots l_n}^{\xi} + \dots, \quad (4.22)$$

where  $\Theta^{\xi}$  are angular ordering theta-functions

$$\Theta_{l_k \dots l_1}^{\xi} = \prod_1^{k-1} \Theta(\xi_{l_{i+1}} - \xi_{l_i}), \quad (4.23)$$

and the dots in eq. (4.22) correspond to collinear singular terms for  $\theta_{p'q_i} \rightarrow 0$  and  $\theta_{q_i q_j} \rightarrow 0$ .

Finally, summing over all permutations in eq. (4.16), we obtain the initial state radiation distribution

$$|M_n^{(\text{tree})}|^2 \simeq \sigma_0 \frac{(2g_s^2 C_A)^n}{x_n^2} \sum_{\pi_n} \prod_1^n \frac{1}{\omega_i^2 \xi_i} \Theta_{l_n \dots l_1}^\xi + \dots \quad (4.24)$$

#### 4.2. THE STRUCTURE FUNCTION (TREE LEVEL)

We compute here the contributions to the structure function obtained from eq. (4.24). For a given distribution  $|M_n|^2$  we have

$$\sigma_0 F(Q, x) = \sigma_0 \delta(1-x) + \sum_n \frac{1}{n!} \int \prod_{i=1}^n (dq_i) \Theta(Q - q_{it}) |M_n|^2 \delta\left(1 - \frac{x}{x_n}\right), \quad (4.25)$$

where

$$(dq_i) = \frac{d^3 q_i}{2\omega_i (2\pi)^3}, \quad (4.26)$$

and, as discussed in the introduction, we integrate over the region  $q_{it} < Q$  only. Taking into account only the initial state collinear singularities in eq. (4.24), we have

$$F^{(\text{tree})}(Q, x) \simeq \delta(1-x) + \sum_{n=1}^{\infty} \int \prod_{i=1}^n \frac{d\xi_i}{\xi_i} \frac{dy_i}{y_i} \bar{\alpha}_s \times \Theta(Q - q_{it}) \frac{1}{x_n^2} \delta\left(1 - \frac{x}{x_n}\right) \Theta_{n, \dots, 2, 1}^\xi, \quad (4.27)$$

where  $\bar{\alpha}_s = C_A \alpha_s / \pi$  and  $x_n = 1 - y_1 - \dots - y_n$ . Introducing the energy fractions

$$x_j = z_1 z_2 \dots z_j, \quad x_n = z_1 z_2 \dots z_n \quad y_l = x_{l-1} (1 - z_l), \quad (4.28)$$

we obtain

$$F^{(\text{tree})}(Q, x) \simeq \delta(1-x) + \sum_{n=1}^{\infty} \int \prod_{i=1}^n \frac{d\xi_i}{\xi_i} dz_i \frac{\alpha_s}{2\pi} P(z_i) \Theta(Q - q_{it}) \times \delta(x - z_1 \dots z_n) \Theta_{n, \dots, 2, 1}^\xi, \quad (4.29)$$

where

$$P(z) = \frac{2C_A}{z(1-z)} = 2C_A \left( \frac{1}{z} + \frac{1}{1-z} \right), \quad (4.30)$$

is the sum of the two singular contributions for  $z \rightarrow 0, 1$  of the Altarelli–Parisi

splitting function for gluon emission

$$P_g(z) = 2C_A \left( \frac{1}{z} + \frac{1}{1-z} - 2 + z(1-z) \right). \quad (4.31)$$

The finite terms in  $P_g$ , i.e.  $-2 + z(1-z)$ , are not obtained in our analysis. As noted before this is due to the fact that we do not take reliably into account the subleading energy regions with  $y_i \ll x \ll y_j$ .

The tree approximation (4.29) of the structure function contains infrared singularities for  $z \rightarrow 1$  which should be regularized by appropriate virtual corrections corresponding to the Sudakov form factor. Moreover, as recalled in the introduction, the anomalous dimension for  $N \rightarrow 1$  computed from this tree expression shows leading singularities of the type  $\alpha_s^n / (N-1)^{2n-1}$  which should be cancelled by virtual corrections. The virtual contributions are computed in the next section.

### 5. Virtual contributions and form factors

In the present section we show that, as in the soft emission current for  $x \rightarrow 0$ , in the virtual corrections there are two types of contributions as well, the eikonal and the non-eikonal one. The eikonal one leads to the Sudakov form factor which, as usual, regularizes the soft gluon emission singularities. The non-eikonal one leads to a non-Sudakov form factor which regularizes the collinear singularities when a relatively fast gluon is emitted parallel to the incoming parton.

We compute virtual corrections by using the method of refs. [11,12]. In each virtual loop one of the integrals is evaluated by the residue theorem, i.e. by putting on-shell a gluon in the loop. The complex plane contours can be selected in such a way that the on-shell gluon corresponds to the soft momentum in the loop. This method is equivalent to compute the virtual corrections by considering all possible diagrams in which an on-shell soft gluon is emitted and absorbed. In this way the virtual corrections are evaluated by a technique which is very similar to the one previously used to compute the real emission diagrams. We have the advantage that the approximations we use in the evaluation of real and virtual contributions are the same.

Before entering into technical details, it may be useful to summarize here the main points of the method and the main results. We consider the virtual corrections to the multi-gluon amplitude  $M_n^{(\text{tree})}$  obtained in sect. 3 in the semi-hard  $y$ -ordered region relevant for the  $x \rightarrow 0$  analysis

$$x \ll y_n \ll y_{n-1} \ll \dots \ll y_1 \simeq 1. \quad (5.1)$$

We divide the phase space of momenta  $\tilde{q}$  of the on-shell virtual gluons in two regions, of which (i)  $\tilde{q}$  is softer ( $0 < \tilde{y} \ll y_n$ ) or (ii)  $\tilde{q}$  is harder ( $y_n \ll \tilde{y}$ ) than the softest external gluon  $n$ . We consider separately these regions.

(i) *On-shell virtual gluons softer than all external gluons.* We show that all these corrections *factorize* and they can be summed by *exponentiation* as follows

$$|\mathbf{h}_n\rangle \approx \mathbf{S}_{\text{eik}}^{(n)}(y_n, 0) S_{\text{ne}}(y_n, x_n, Q_{nt}) |\tilde{\mathbf{h}}_n\rangle, \quad (5.2)$$

where  $\mathbf{h}_n$  is the subamplitude with all virtual corrections included to leading order. In the subamplitude  $\tilde{\mathbf{h}}_n$  we include all virtual corrections which are in region (ii). The two form factors are obtained from eikonal and non-eikonal virtual contributions.

The Sudakov form factor  $\mathbf{S}_{\text{eik}}^{(n)}(y_n, 0)$  is given by the following  $y$ -ordered colour matrix function

$$\begin{aligned} \mathbf{S}_{\text{eik}}^{(n)}(y_n, 0) &\equiv \bar{P}_y \left\{ \exp \frac{1}{2} g_s^2 \int_0^{y_n} (d\tilde{q}) \left( \mathbf{J}_{\text{eik}}^{(n)}(\tilde{q}) \right)^2 \right\} \\ &= 1 + \frac{1}{2} g_s^2 \int_0^{y_n} (d\tilde{q}) \left( \mathbf{J}_{\text{eik}}^{(n)}(\tilde{q}) \right)^2 \mathbf{S}_{\text{eik}}^{(n)}(\tilde{y}, 0). \end{aligned} \quad (5.3)$$

This form factor is well known from the analysis of the region  $x \rightarrow 1$  (see for instance refs. [11, 12]): it sums all virtual corrections in which gluons  $\tilde{q}$  are emitted and absorbed from harder external and internal lines with eikonal vertices. The  $\tilde{y}$ -range of integration implies that this form factor sums any number of virtual on-shell gluons in region (i).

The non-Sudakov form factor  $S_{\text{ne}}(y_n, x_n, Q_{nt})$  sums all virtual corrections in which the on-shell gluons  $\tilde{q}$  are emitted from the internal line  $Q_n$  which is softer than  $\tilde{q}$  for  $x_n < \tilde{y}$ . This contribution is analogous to the non-eikonal real emission described by the soft current  $\mathbf{J}_{\text{ne}}$ . Actually we find that this virtual correction can be expressed in terms of a product of  $\mathbf{J}_{\text{ne}}(Q_n, \tilde{q})$  (emission from  $Q_n$ ) and  $\mathbf{J}_{\text{eik}}^{(n)}(\tilde{q})$  (emission from harder external partons). Also these corrections factorize and can be summed by exponentiation. By using colour conservation we show that the corresponding non-Sudakov form factor is diagonal in colour and given by

$$S_{\text{ne}}(y_n, x_n, Q_{nt}) = \exp \left\{ \frac{1}{2} \bar{\alpha}_s \int_{x_n}^{y_n} \frac{d\tilde{y}}{\tilde{y}} \int \frac{d\tilde{q}_t^2}{\tilde{q}_t^2} \Theta(\tilde{q}_t - Q_{nt}) \right\}; \quad \bar{\alpha}_s = \frac{\alpha_s C_A}{\pi}, \quad (5.4)$$

where  $Q_{nt}$  is the total transverse momentum of emitted gluons.

(ii) *On-shell virtual gluons harder than the softest external gluon.* Since  $q_n$  is the softest momentum, before computing the virtual corrections to the subamplitude  $\tilde{\mathbf{h}}_n$  in eq. (5.2), we evaluate the contribution from the emission of the external gluon  $n$ . This is achieved by factorizing the total emission current  $\mathbf{J}_{\text{tot}}^{(n-1)}(q_n)$  as in sect. 3. After the emission of gluon  $n$  the virtual corrections due to gluons  $\tilde{q}$  with  $\tilde{y} \ll y_{n-1}$  can be computed as in the previous region (i) and one obtains the following

recurrence relation

$$\begin{aligned} & \langle acb_1 \dots b_n | \tilde{\mathbf{h}}_n \rangle \\ & \simeq g_s \langle acb_1 \dots b_{n-1} | \mathbf{J}_{\text{tot}}^{(n-1)b_n}(q_n) \mathbf{S}_{\text{eik}}^{(n-1)}(y_{n-1}, y_n) S_{\text{nc}}(y_{n-1}, y_n, Q_{n-1t}) | \tilde{\mathbf{h}}_{n-1} \rangle, \end{aligned} \quad (5.5)$$

where by definition  $\tilde{\mathbf{h}}_1 = \mathbf{h}_1^{(\text{tree})}$  as given in eq. (3.2). The Sudakov and non-Sudakov form factors in eq. (5.5) are defined as in eqs. (5.3) and (5.4).

Before proving the general results in eqs. (5.2) and (5.5) we describe the main features of the virtual corrections for  $n = 1, 2$ .

### 5.1. VIRTUAL CORRECTIONS IN $h_1$

We evaluate here the leading order virtual corrections to  $\mathbf{h}_1$  by starting with a detailed discussion of the one-loop contribution. Then the resummation of the virtual corrections for all loops will be performed by showing their exponentiation.

*5.1.1. One-loop corrections.* As previously discussed, the order  $\alpha_s$  virtual corrections to the diagram in fig. 3a are given by the insertion of an on-shell soft gluon of momentum  $q$ , with  $y = (q\bar{p})/(p\bar{p})$  and  $q_t^2 = 2pqy$ . The leading contribution is obtained for  $q$  soft ( $0 < y \ll y_1 \sim 1$ ) and we have to consider the diagrams of fig. 9. We divide them into two groups: diagrams in which the soft gluon  $q$  is emitted and absorbed from two eikonal vertices (figs. 9a–f) and diagrams with one eikonal and one non-eikonal vertex (figs. 9g–h). Notice that the non-eikonal soft energy diagram of fig. 9l is nonleading. Let us discuss them separately.

(a) *Eikonal–eikonal contributions.* The diagrams of figs. 9a–c, in which only harder lines are involved, give leading contributions in the full region  $0 < y \ll y_1 \simeq 1$ . The corresponding corrections to the tree subamplitude  $\mathbf{h}_1^{(\text{tree})}$  can be computed as in sect. 3 and they factorize in the form

$$|\mathbf{h}_1^{(1)}\rangle_{\text{eik}} \simeq \left\{ \frac{1}{2} g_s^2 \int_0^{y_1} (dq) \left( \mathbf{J}_{\text{eik}}^{(1)}(q) \right)^2 \right\} |\mathbf{h}_1^{(\text{tree})}(p, q_1)\rangle, \quad (dq) = \frac{d^3q}{2\omega(2\pi)^3}, \quad (5.6)$$

where  $\mathbf{J}_{\text{eik}}^{(1)}(q)$  is the eikonal current in eq. (3.8) for the emission of the soft gluon  $q$  from  $p$  and  $q_1$ .

Eikonal diagrams of fig. 9d–f, in which the soft gluon is emitted from the internal line  $Q_1$ , give a nonleading collinear contribution. This is due to coherence: as  $Q_1^2 \rightarrow 0$  the external gluons  $p$  and  $q_1$  become parallel and eikonal insertions on  $p$  and  $q_1$  become the same as the insertion on  $Q_1$ .

(b) *Non-eikonal–eikonal contributions.* The diagrams of figs. 9g–h, in which  $q$  is emitted from the internal line  $Q_1$  with non-eikonal vertex, give leading contributions only in the region  $x_1 \ll y \ll y_1 \sim 1$ . The virtual corrections to the subampli-

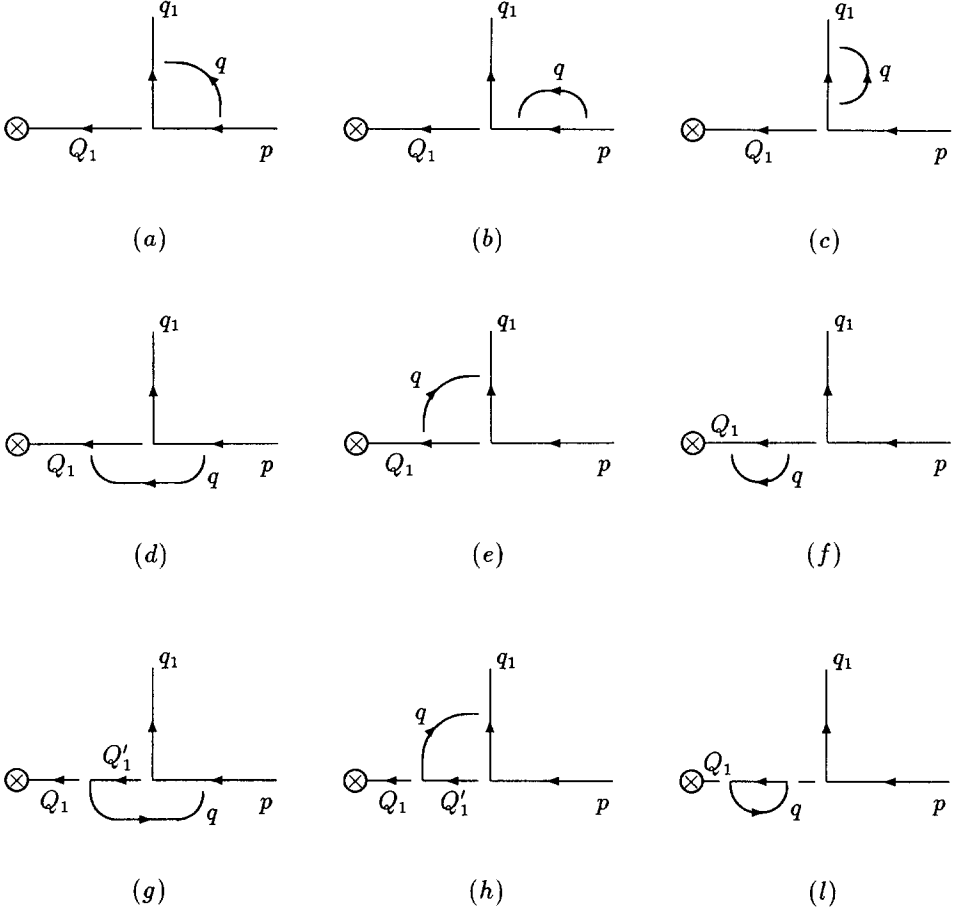


Fig. 9. Diagrams of one-loop virtual corrections to the diagram in fig. 3a. The gluon  $Q$  in the virtual loop is on-shell and soft. See discussion in the text and in refs. [11,12].

tude  $\mathbf{h}_1^{(\text{tree})}$  from figs. 9g,h can be computed as in sect. 3. They factorize in the form

$$\begin{aligned}
 |\mathbf{h}_1^{(1)}\rangle_{\text{ne}} \simeq & \left\{ g_s^2 \int_{x_1}^{y_1} (dq) \left( \frac{\eta(2q + Q_1)}{2\eta p} \right) \right. \\
 & \left. \times \left( \frac{2p - Q'_1}{Q_1'^2} \right) d(Q'_1) d(q) \left[ \frac{p}{-pq} \mathbf{T}_p^b + \frac{q_1}{q_1 q} \mathbf{T}_1^b \right] \cdot \mathbf{T}_{p'}^b \right\} |\mathbf{h}_1^{(\text{tree})}\rangle, \quad (5.7)
 \end{aligned}$$

where  $Q'_1 = Q_1 - q$  and we have substituted the effective hard vertex with  $\eta/(2\eta p)$ .

In order to find the way to generalize this result it is useful to notice that this expression can be written in terms of the effective vertex  $\Gamma(Q'_1, q)$ , hence in terms of

the soft non-eikonal current introduced in sect. 3. This is obtained by writing the gluon polarization  $d(q)$  as in eq. (2.8) and by taking the leading term of  $\Gamma(Q'_1, q)$  (see eq. (2.13)). We have then

$$|\mathbf{h}_1^{(1)}\rangle_{\text{ne}} \simeq \left\{ g_s^2 \int_{x_1}^{y_1} (dq) (\mathbf{J}_{\text{ne}}(Q_1, q) \mathbf{J}_{\text{eik}}^{(1)}(q)) \right\} |\mathbf{h}_1^{(\text{tree})}\rangle, \quad (5.8)$$

where

$$\mathbf{J}_{\text{ne}}(Q_1, q) = \frac{2(Q'_1 - x'_1 p) \epsilon(q)}{Q_1'^2} \mathbf{T}_{p'}, \quad (5.9)$$

is the non-eikonal soft current we have introduced in sect. 3 ( $Q'_1 = Q_1 - q$ ,  $x'_1 = x_1 - y$ ).

To evaluate eq. (5.8), notice that for  $x_1 \ll y \ll y_1 \sim 1$  we have

$$\begin{aligned} \frac{1}{Q_1'^2} (2p - Q'_1) d(Q'_1) d(q) \frac{p}{pq} &\simeq -\frac{4}{q_t'^2} \frac{(\mathbf{Q}_{1t} + \mathbf{q}_t) \cdot \mathbf{q}_t}{(\mathbf{Q}_{1t} + \mathbf{q}_t)^2 - q_t'^2}, \\ \frac{1}{Q_1'^2} (2p - Q'_1) d(Q'_1) d(q) \frac{q_1}{q_1 q} &\simeq -\frac{4}{q_t'^2} \frac{(\mathbf{Q}_{1t} + \mathbf{q}'_t) \cdot \mathbf{q}'_t}{(\mathbf{Q}_{1t} + \mathbf{q}'_t)^2 - q_t'^2}, \end{aligned} \quad (5.10)$$

where  $\mathbf{q}_t$  is the transverse momentum of  $q$  with respect to  $p$ , and  $\mathbf{q}'_t$  is the transverse momentum of  $q$  with respect to  $q_1$

$$\mathbf{q}'_t = \mathbf{q}_t - \frac{y}{y_1} \mathbf{q}_{1t}, \quad q_t^2 = 2pqy, \quad q_t'^2 = 2q_1 q \frac{y}{y_1}, \quad (5.11)$$

$$Q_1'^2 = (Q_1 + q)^2 \simeq -(\mathbf{Q}_{1t} + \mathbf{q}_t)^2 + q_t^2 \simeq -(\mathbf{Q}_{1t} - \mathbf{q}'_t)^2 + q_t'^2. \quad (5.12)$$

We find therefore that the two contributions of figs. 9g, h give approximately the same functions of  $q_t$  and  $q'_t$  respectively. We get

$$|\mathbf{h}_1^{(1)}\rangle_{\text{ne}} \simeq \left\{ \frac{\alpha_s}{\pi} \int_{x_1}^{y_1} \frac{dy}{y} \int \frac{d^2 q_t}{\pi q_t^2} \left[ \frac{(\mathbf{Q}_{1t} - \mathbf{q}_t) \cdot \mathbf{q}_t}{(\mathbf{Q}_{1t} - \mathbf{q}_t)^2 - q_t^2} \right] (\mathbf{T}_p + \mathbf{T}_1) \cdot \mathbf{T}_{p'} \right\} |\mathbf{h}_1^{(\text{tree})}\rangle. \quad (5.13)$$

By using the colour singlet condition  $\mathbf{T}_p = \mathbf{T}_1 - \mathbf{T}_{p'}$  this contribution is diagonal in colour ( $\mathbf{T}_p^2 = C_A$ ). Performing the angular integration we obtain

$$\int \frac{d^2 q_t}{\pi q_t^2} \left[ \frac{(\mathbf{Q}_{1t} - \mathbf{q}_t) \cdot \mathbf{q}_t}{(\mathbf{Q}_{1t} - \mathbf{q}_t)^2 - q_t^2} \right] = \frac{1}{2} \int \frac{dq_t^2}{q_t^2} \Theta(q_t - Q_{1t}). \quad (5.14)$$

Finally

$$|\mathbf{h}_1^{(1)}\rangle_{\text{ne}} \simeq \frac{1}{2} \bar{\alpha}_s \int_{x_1}^{y_1} \frac{dy}{y} \int \frac{dq_t^2}{q_t^2} \Theta(q_t - Q_{1t}) |\mathbf{h}_1^{(\text{tree})}\rangle, \quad \bar{\alpha}_s = \frac{\alpha_s C_A}{\pi}. \quad (5.15)$$

In conclusion the complete one-loop virtual correction to leading order is

$$|\mathbf{h}_1^{(1)}\rangle \simeq \left\{ \frac{1}{2} g_s^2 \int_0^{y_1} (dq) \left( \mathbf{J}_{\text{eik}}^{(1)}(q) \right)^2 + \frac{1}{2} \bar{\alpha}_s \int_{x_1}^{y_1} \frac{dy}{y} \int \frac{dq_t^2}{q_t^2} \Theta(q_t - Q_{1t}) \right\} |\mathbf{h}_1^{(\text{tree})}\rangle. \quad (5.16)$$

*5.1.2 Exponentiation.* In order to compute virtual corrections to order  $\alpha_s^n$  we have to consider the diagram of fig. 3a in which  $n$  on shell virtual gluons,  $\tilde{q}_1 \tilde{q}_2 \dots \tilde{q}_n$ , are emitted–absorbed in all possible ways. To evaluate the leading contributions of these we study the following strongly ordered integration region in the virtual loops

$$\tilde{y}_n \ll \tilde{y}_{n-1} \ll \dots \ll \tilde{y}_1 \ll y_1 \simeq 1, \quad (5.17)$$

where  $\tilde{y}_j = (\tilde{q}_j \bar{p}) / (p \bar{p})$  and  $\tilde{q}_{jt}^2 = 2(\tilde{q}_j \bar{p}) \tilde{y}_j$ . Note that for the case of  $\mathbf{h}_1$ , all virtual on-shell gluons are in region (i) previously introduced. In the ordered region (5.17) we can recursively apply the soft gluon technique [2, 13] to obtain the exponentiation of (5.16). We start from the softest gluon  $\tilde{q}_n$  and consider all possible diagrams in which  $\tilde{q}_n$  can be emitted and absorbed. As in the previous subsection, the leading diagrams can be divided into two groups: (a) Eikonal–eikonal diagrams in which  $\tilde{q}_n$  is emitted and absorbed with eikonal vertices only (see figs. 9a–f and 10a, b), (b) Non-eikonal–eikonal diagrams in which  $\tilde{q}_n$  is emitted from  $Q_1$  with non-eikonal vertex and absorbed from harder lines with eikonal vertices (see figs. 9g– $\ell$  and fig. 10c).

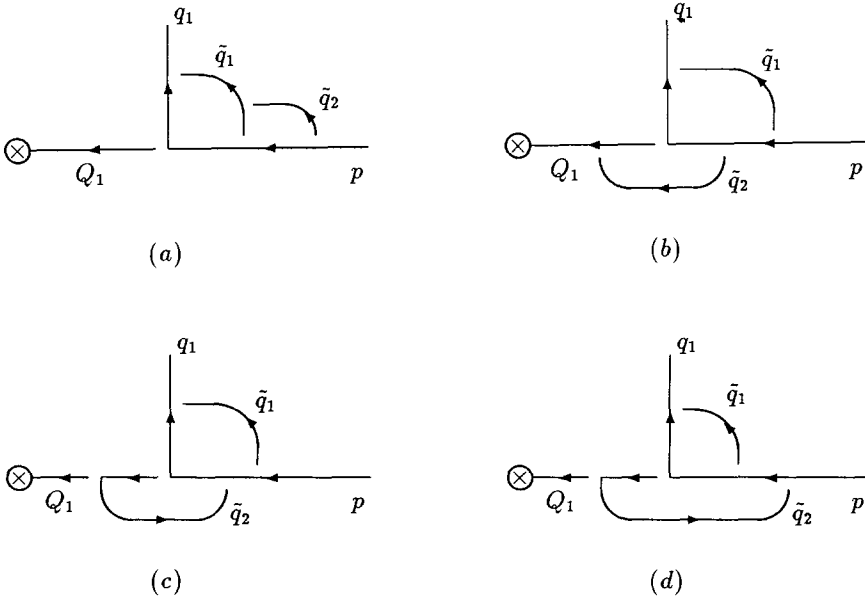


Fig. 10. Examples of two-loop virtual corrections to the diagram in fig. 3a. The on-shell gluons in the virtual loops are ordered in energy.

By using the soft gluon technique of sect. 3, we obtain that both virtual corrections *factorize* and, as in eqs. (5.6) and (5.8), we find

$$|\mathbf{h}_1^{(n)}\rangle \simeq \left\{ \frac{1}{2} g_s^2 \int_0^{\bar{y}_{n-1}} (d\tilde{q}_n) (\mathbf{J}_{\text{eik}}^{(1)}(\tilde{q}_n))^2 + \frac{1}{2} \bar{\alpha}_s \int_{x_1}^{\bar{y}_{n-1}} \frac{dy}{y} \int \frac{dq_t^2}{q_t^2} \Theta(q_t - Q_{1t}) \right\} |\mathbf{h}_1^{(n-1)}\rangle. \quad (5.18)$$

This equation has a recurrence structure which allows us to sum all leading virtual corrections by exponentiation of the one-loop result [11, 12]. The complete leading virtual contributions to  $\mathbf{h}_1$  are then given by

$$|\mathbf{h}_1\rangle \simeq \mathbf{S}_{\text{eik}}^{(1)}(y_1, 0) S_{\text{nc}}(y_1, x_1, Q_{1t}) |\mathbf{h}_1^{(\text{tree})}\rangle. \quad (5.19)$$

Here  $S_{\text{nc}}$  is the non-Sudakov form factor in eq. (5.4), which is obtained by exponentiation of one-loop correction in eq. (5.15) and  $\mathbf{S}_{\text{eik}}^{(1)}(y_1, 0)$  is Sudakov form factor given by the  $y$ -ordering colour matrix function in eq. (5.3).

At the end of this section we explicitly evaluate the full amplitude  $\tilde{\mathbf{h}}_1$  by diagonalizing the eikonal form factor.

## 5.2. VIRTUAL CORRECTIONS TO $h_2$

In order to develop the method to compute the complete leading virtual correction to the general amplitude  $\mathbf{h}_n$  we analyze here the case of  $\mathbf{h}_2$  which, in the ordered region

$$x \ll y_2 \ll y_1 \simeq 1, \quad (5.20)$$

is given, at tree level, by the diagrams in fig. 6.

As in the previous subsection we consider on-shell virtual gluons emitted and absorbed in all possible ways. In order to apply the soft gluon techniques for each virtual gluon  $q$ , we have to consider the following two regions

$$\mathbf{R}^{(2)}: \quad y \ll y_2, \quad \mathbf{R}^{(1)}: \quad y_2 \ll y \ll y_1 \simeq 1, \quad (5.21)$$

with  $y = (q\bar{p})/(p\bar{p})$  and  $q_t^2 = 2(pq)y$ .

*5.2.1. Region  $\mathbf{R}^{(2)}$ .* Let us consider first the one-loop corrections in which the on-shell virtual gluon  $q$  is softer than  $q_2$ . As before, we have diagrams with eikonal–eikonal or non-eikonal–eikonal types of vertices. Both contributions factorize giving

$$|\mathbf{h}_2^{(1)}\rangle = \left\{ \frac{1}{2} g_s^2 \int_0^{y_2} (dq) (\mathbf{J}_{\text{eik}}^{(2)}(q))^2 + g_s^2 \int_{x_2}^{y_2} (dq) (\mathbf{J}_{\text{eik}}^{(2)}(q) \mathbf{J}_{\text{nc}}(Q_2, q)) \right\} |\mathbf{h}_2^{(\text{tree})}\rangle. \quad (5.22)$$

The first term corresponds to the eikonal emission of soft gluon  $q$  from the harder external lines  $p$ ,  $q_1$  and  $q_2$ . The second term corresponds to the non-eikonal emission from the internal leg  $Q_2$  and takes contribution only for  $x_2 < y$ . It can be explicitly evaluated by using the approximation in eq. (5.11) and gives

$$\left\{ g_s^2 \int_{x_2}^{y_2} (dq) (\mathbf{J}_{\text{eik}}^{(2)}(q) \mathbf{J}_{\text{ne}}(Q_2, q)) \right\} |h_2^{(\text{tree})}\rangle \\ \simeq \left\{ \frac{\alpha_s}{\pi} \int_{x_2}^{y_2} \frac{dy}{y} \int \frac{d^2 q_t}{\pi q_t^2} \left[ \frac{(Q_{2t} + q_t) \cdot q_t}{(Q_{2t} + q_t)^2 - q_t^2} \right] (\mathbf{T}_p - \mathbf{T}_1 - \mathbf{T}_2) \cdot \mathbf{T}_{p'} \right\} |h_2^{(\text{tree})}\rangle, \quad (5.23)$$

where  $Q_{2t} = -q_{1t} - q_{2t}$ . As in the case of  $h_1$ , the eikonal emission of  $q$  from the external legs  $p$ ,  $q_1$  and  $q_2$  gives, after integration, the same momentum factor. By using the colour singlet condition  $\mathbf{T}_p = \mathbf{T}_{p'} + \mathbf{T}_1 + \mathbf{T}_2$ , (5.23) is diagonal in colour. The final one-loop result for the virtual correction in the region  $R^{(2)}$  is

$$|h_2^{(1)}\rangle \simeq \left\{ \frac{1}{2} g_s^2 \int_0^{y_2} (dq) (\mathbf{J}_{\text{eik}}^{(2)}(q))^2 + \frac{1}{2} \bar{\alpha}_s \int_{x_2}^{y_2} \frac{dy}{y} \int \frac{dq_t^2}{q_t^2} \Theta(q_t - Q_{2t}) \right\} |h_2^{(\text{tree})}\rangle. \quad (5.24)$$

Consider now the contributions with  $n$  on-shell virtual gluons  $\tilde{q}_1 \dots \tilde{q}_n$  all in the region  $R^{(2)}$  ( $\tilde{y}_i \ll y_2$ ). The leading terms can be summed by exponentiating the one-loop result in eq. (5.24) and the complete virtual corrections in region  $R^{(2)}$  are given by

$$|h_2\rangle = \mathbf{S}_{\text{eik}}^{(2)}(y_2, 0) S_{\text{ne}}(y_2, x_2, Q_{2t}) |\tilde{h}_2\rangle. \quad (5.25)$$

The form factors are given in eqs. (5.3) and (5.4). In eq. (5.25) the subamplitude  $\tilde{h}_2$  involves virtual corrections only in the harder region of phase space  $R^{(1)}$  we are now going to compute.

**5.2.2. Region  $R^{(1)}$ .** In order to evaluate the virtual corrections to  $\tilde{h}_2$  we consider the case in which the on-shell virtual gluons  $\tilde{q}_1 \dots \tilde{q}_n$  are all in region  $R^{(1)}$ , i.e.  $y_2 \ll \tilde{y}_i \ll y_1$ . In this case the emitted gluon  $q_2$  is the softest one and has to be factorized before computing the harder virtual corrections. This can be achieved by using the recurrence relation of sect. 3 which at tree level is

$$\langle acb_1 b_2 | h_2^{(\text{tree})}(pq_1 q_2) \rangle \simeq g_s \langle acb_1 | \mathbf{J}_{\text{tot}}^{(1)b_2}(q_2) | h_1^{(\text{tree})}(pq_1) \rangle. \quad (5.26)$$

The virtual corrections in the region  $y_2 \ll \tilde{y}_i \ll y_1$  affect only the subamplitude  $h_1^{(\text{tree})}$  and are given by eq. (5.19). In conclusion the complete virtual corrections in the region  $R^{(1)}$  are given by the recurrence relation

$$\langle acb_1 b_2 | \tilde{h}_2 \rangle \simeq g_s \langle acb_1 | \mathbf{J}_{\text{tot}}^{(1)b_2}(q_2) \mathbf{S}_{\text{eik}}^{(1)}(y_1, y_2) S_{\text{ne}}(y_1, y_2, Q_{1t}) | h_1^{(\text{tree})}(p, q_1) \rangle, \quad (5.27)$$

where  $Q_{1t}$  is the transverse momentum of  $Q_1 = p - q_1$ . Notice the arguments of the matrix eikonal form factor which implies that virtual corrections here take place only in the region  $y_2 \ll \tilde{y}_i \ll y_1$ . This form factor is then given by eq. (5.3) with  $\tilde{y}$  restricted to the interval  $(y_1, y_2)$ .

### 5.3. VIRTUAL CORRECTIONS TO THE GENERAL AMPLITUDE

By generalizing the analysis of the case  $\mathbf{h}_2$ , one can develop a method to compute the leading virtual corrections for the general case. The strategy is the one anticipated at the beginning of this section. We consider the multi-gluon amplitude  $\mathbf{h}_n$  in the energy ordered region (5.1). As in the case  $n = 2$  we consider the various phase space regions for on-shell gluons  $\tilde{q}$  in the virtual loops

$$\begin{aligned} \mathbf{R}^{(n)}: \quad & 0 < \tilde{y} \ll y_n, \\ \mathbf{R}^{(j)}: \quad & y_{j+1} \ll \tilde{y} \ll y_j, \quad j = 1, 2, \dots, n-1. \end{aligned} \quad (5.28)$$

Let us start from the one-loop virtual correction. When  $\tilde{q} \in \mathbf{R}^{(n)}$  all external gluons are harder than gluon  $\tilde{q}$ . The eikonal and non-eikonal contributions factorize as in the cases  $n = 1, 2$  and one obtains

$$|\mathbf{h}_n^{(1)}\rangle \simeq \left\{ \frac{1}{2} g_s^2 \int_0^{y_n} (d\tilde{q}) (\mathbf{J}_{\text{eik}}^{(n)}(\tilde{q}))^2 + g_s^2 \int_{x_n}^{y_n} (d\tilde{q}) (\mathbf{J}_{\text{eik}}^{(n)}(\tilde{q}) \mathbf{J}_{\text{nc}}(Q_n, \tilde{q})) \right\} |\mathbf{h}_n^{(\text{tree})}\rangle. \quad (5.29)$$

As before the non-eikonal contribution can be written in the form

$$\begin{aligned} |\mathbf{h}_n^{(1)}\rangle_{\text{nc}} &\simeq \left\{ \frac{\alpha_s}{\pi} \int_{x_n}^{y_n} \frac{dy}{y} \int \frac{d^2 q_t}{\pi q_t^2} \left[ \frac{(Q_{nt} + q_t) \cdot q_t}{(Q_{nt} + q_t)^2 - q_t^2} \right] (\mathbf{T}_p - \mathbf{T}_1 - \dots - \mathbf{T}_n) \cdot \mathbf{T}_{p'} \right\} |\mathbf{h}_n^{(\text{tree})}\rangle \\ &= \left\{ \frac{1}{2} \bar{\alpha}_s \int_{x_n}^{y_n} \frac{dy}{y} \int \frac{d^2 q_t}{q_t^2} \Theta(q_t - Q_{nt}) \right\} |\mathbf{h}_n^{(\text{tree})}\rangle, \quad \bar{\alpha}_s = \frac{\alpha_s C_A}{\pi}, \end{aligned} \quad (5.30)$$

where  $Q_{nt}$  is the transverse momentum of the spacelike gluon  $Q_n$ . Again the non-eikonal term is diagonal in colour due to charge conservation.

We then consider the contribution from any number of on-shell virtual gluons in region  $\mathbf{R}^{(n)}$ . All these contributions exponentiate as in the  $n = 1, 2$  cases and we obtain the general expression (5.2).

The virtual corrections to  $\tilde{\mathbf{h}}_n$  involve only on-shell virtual gluons which are harder than  $q_n$ . Therefore the real emission of gluon  $n$  can be factorized as in sect. 3 in terms of the total soft current  $\mathbf{J}_{\text{tot}}^{(n-1)}(q_n)$  in eq. (5.2).

The virtual corrections to  $\tilde{\mathbf{h}}_n$  are then obtained iteratively. We consider the on-shell virtual gluons in region  $\mathbf{R}^{(n-1)}$ . These contributions can be factorized and we find the general recurrence relation in eq. (5.5) which involves  $\tilde{\mathbf{h}}_{n-1}$ . To compute the virtual corrections in the subamplitude  $\tilde{\mathbf{h}}_{n-1}$  we iterate the previous procedure. This iteration stops at  $|\tilde{\mathbf{h}}_1\rangle = |\mathbf{h}_1^{(\text{tree})}\rangle$ .

In conclusion eqs. (5.2) and (5.5) are the recurrence relations for the complete multi-gluon amplitudes. Virtual corrections and real emission are computed at the same level of infrared and collinear accuracy. In the next section we perform the colour algebra and we evaluate the general multi-gluon distributions.

We conclude this section by explicitly evaluating the complete subamplitude  $\mathbf{h}_1$ . This requires the diagonalization of the colour matrix eikonal form factor.

#### 5.4. COLOUR DIAGONALIZATION OF $\mathbf{h}_1$

By using the fact that the hard probe is a colour singlet we can diagonalize the matrix  $\mathbf{S}_{\text{eik}}^{(1)}(y, 0)$ .

Let us start from the one-loop eikonal contribution in eq. (5.6). By introducing

$$\mathbf{J}_{\text{eik}}^{(1)}(q) = -j_p(q)\mathbf{T}_p + j_1(q)\mathbf{T}_1 + j_{p'}(q)\mathbf{T}_{p'}, \quad j_k(q) = k/kq, \quad (5.31)$$

and by using the colour singlet condition  $(\mathbf{T}_p - \mathbf{T}_1 - \mathbf{T}_{p'})|\mathbf{h}_1^{(\text{tree})}\rangle = 0$  we find

$$|\mathbf{h}_1^{(1)}\rangle_{\text{eik}} = \left\{ g_s^2 \frac{C_A}{4} \int_0^{y_1} (dq) \left[ (j_p(q) - j_1(q))^2 + (j_1(q) - j_{p'}(q))^2 + (j_{p'}(q) - j_p(q))^2 \right] \right\} |\mathbf{h}_1^{(\text{tree})}\rangle. \quad (5.32)$$

All virtual corrections to  $\mathbf{h}_1^{(\text{tree})}$  are diagonal and obtained by exponentiating (5.32). To evaluate this more explicitly we introduce the usual angular variables of sect. 4:  $\xi_1 \equiv \xi_{pq}$ ,  $\xi \equiv \xi_{p'q}$ ,  $\xi' \equiv \xi_{q_1q}$  and  $\bar{\xi} \equiv \xi_{pp'}$ . Neglecting contributions from collinear singularities when the soft gluon becomes parallel to the recoiling gluon  $p'$ , we obtain

$$|\mathbf{h}_1^{(1)}\rangle_{\text{eik}} \simeq - \left\{ g_s^2 \frac{C_A}{4} \int_0^{y_1} (dq) \frac{2}{\omega^2} \left[ \frac{1}{\xi} \Theta(\xi_1 - \xi) + \frac{1}{\xi'} \Theta(\xi_1 - \xi') + \frac{1}{\xi} + \frac{1}{\xi'} \right] \right\} |\mathbf{h}_1^{(\text{tree})}\rangle, \quad (5.33)$$

where we have taken into account that, after taking the average in the azimuthal

direction we have

$$\frac{\xi_1}{\xi\xi'} \rightarrow \frac{1}{\xi}\Theta(\xi_1 - \xi) + \frac{1}{\xi'}\Theta(\xi_1 - \xi'). \quad (5.34)$$

For the one-loop virtual corrections we then have

$$\begin{aligned} & \left\{ \frac{1}{2}g_s^2 \int_0^{y_1} (dq) (\mathbf{J}_{\text{eik}}^{(1)}(q))^2 \right\} |h_1^{(\text{tree})}\rangle \\ & \simeq \left\{ -\frac{1}{2}\bar{\alpha}_s \int_{0^+}^{y_1} \frac{dy}{y} \int_{0^+}^{\bar{\xi}} \frac{d\xi}{\xi} [1 + \Theta(\xi_1 - \xi)] \right\} |h_1^{(\text{tree})}\rangle, \end{aligned} \quad (5.35)$$

where  $0^+$  indicates the infrared and collinear cutoff.

In conclusion the full virtual correction to  $h_1^{(\text{tree})}$  is given by

$$|h_1\rangle \simeq S_{\text{eik}}(y_1, \bar{\xi}) S_{\text{eik}}(y_1, \xi_1) S_{\text{nc}}(y_1, x, Q_{1t}) |h_1^{(\text{tree})}(p, q_1)\rangle, \quad (5.36)$$

where the eikonal form factors are now diagonal in colour and obtained by exponentiating the result in eq. (5.35)

$$S_{\text{eik}}(y, \xi) = \exp \left\{ -\frac{1}{2}\bar{\alpha}_s \int_{0^+}^y \frac{dy'}{y'} \int_{0^+}^{\xi} \frac{d\xi'}{\xi'} \right\}. \quad (5.37)$$

The two form factors  $S_{\text{eik}}(y_1, \bar{\xi})$  and  $S_{\text{eik}}(y_1, \xi_1)$  in eq. (5.36) are the Sudakov form factors for the incoming and outgoing gluons  $p$  and  $q_1$  respectively. The Sudakov form factor for gluon  $q_1$  is integrated with  $\xi < \xi_1 \equiv \xi_{pq_1}$ . This constraint is due to coherence of QCD radiation and corresponds to the fact that the emission from gluon  $q_1$  is bounded into a cone centered around  $q_1$  with aperture given by  $\xi < \xi_1$ .

## 6. The initial state radiation distribution

In this section, extending the calculation of sect. 4, we solve the recursive relations for  $|M_n|^2$  given in eqs. (5.2) and (5.5). The main new complication is that the eikonal form factors  $\mathbf{S}_{\text{eik}}^{(n)}$  are nondiagonal in colour. However, the colour algebra of virtual corrections can be performed by the same technique used for the real emission. We focus our attention on the initial state radiation distributions which are obtained when one inclusively sums over final state emission. In this way the singularities for  $\theta_{q_i q_j} \rightarrow 0$  and  $\theta_{p' q_j} \rightarrow 0$  cancel with the corresponding Sudakov form factors. Therefore we are left only with the singular contributions for  $\theta_{p q_i} \rightarrow 0$  together with the corresponding Sudakov and non-Sudakov form factors.

The Sudakov form factors are obtained by recurrent diagonalization of the various colour matrix eikonal form factors  $\mathbf{S}_{\text{eik}}^{(k)}$ ,  $k = 1, 2, \dots, n$ . We will show that

their contribution to the initial state radiation distribution is very simple and given by

$$S_{\text{eik}}^2(1, \bar{\xi}) = \exp \left[ -\bar{\alpha}_s \int_{0^+}^1 \frac{dy}{y} \int_{0^+}^{\bar{\xi}} \frac{d\xi}{\xi} \right], \quad \bar{\alpha}_s = \frac{C_A \alpha_s}{\pi}, \quad (6.1)$$

where  $\bar{\xi}$  corresponds to the maximum available phase space ( $\bar{\xi} \sim 1$ ). In the next section we will show that this form factor regularizes the infrared singularities of the various emitted gluons.

The non-Sudakov form factors  $S_{\text{ne}}$  are already diagonal in colour. They depend on the particular energy ordered region. In the energy ordered region

$$x \ll y_n \ll y_{n-1} \ll \dots \ll y_1 \sim 1, \quad (6.2)$$

the full non-eikonal form factor is

$$\tilde{S}_{\text{ne}}^2(12 \dots n) = \prod_{i=1}^n S_{\text{ne}}^2(y_i, y_{i+1}, Q_{it}), \quad y_{n+1} = x, \quad (6.3)$$

with  $Q_{it}$  the transverse momentum of  $Q_i = p - q_1 - \dots - q_i$ .

The complete result for the initial state radiation distribution in the phase space (6.2), is presented in eq. (6.25). Integrating these distributions, we obtain the structure function (see eq. (6.26)).

In contrast with the tree level case, the distribution in eq. (6.25) is not symmetric under the exchange of emitted gluons. The analysis of coherence of radiation, i.e. the angular ordering structure, is then more complex than in the tree approximation. This analysis is performed in the next section.

We refer to appendix B for the case of a quark in the initial state.

## 6.1. THE SOLUTION OF THE RECURRENCE RELATION FOR THE AMPLITUDE

As for the tree amplitude in sect. 4 we introduce the following ansatz for the colour decomposition of the partial subamplitude  $\tilde{h}_n$  defined in eq. (5.2)

$$\langle acb_1 \dots b_n | \tilde{h}_n \rangle = \sum_{\pi_{n+1}} \tilde{h}_n(p, l_0 \dots l_n) 2 \text{Tr}(\lambda^a \lambda^{b_{l_0}} \dots \lambda^{b_{l_n}}), \quad (6.4)$$

with the notation of sect. 4 ( $q_0 = p'$ ,  $b_0 = c$ ). This ansatz can be proved by induction.

We want to show that, to leading collinear order, this decomposition diagonalizes the colour matrix eikonal form factors. The key feature is that, to leading collinear

and  $1/N_c^2$  order, one has ( $\sigma_0 = N_c^2 - 1$ ,  $C_A = N_c$ )

$$\langle \tilde{\mathbf{h}}_n | (\mathbf{J}_{\text{eik}}^{(n)}(q))^2 | \tilde{\mathbf{h}}_n \rangle \simeq \sigma_0 \left( \frac{C_A}{2} \right)^n \sum_{\pi_{n+1}} |\tilde{\mathbf{h}}_n(p, l_0 \dots l_n)|^2 I_n(p, l_0 \dots l_n), \quad (6.5)$$

where

$$I_n(p, l_0 \dots l_n) = \frac{1}{2} C_A \left\{ (j_p(q) - j_{l_0}(q))^2 + \dots + (j_{l_n}(q) - j_p(q))^2 \right\}, \quad (6.6)$$

$$j_p(q) = \frac{p}{pq}, \quad j_l(q) = \frac{q_l}{q_l q}, \quad j_{p'} = \frac{p'}{p'q}. \quad (6.7)$$

The proof of eq. (6.5) is just the same as that of eq. (4.14) in sect. 4 and corresponds to the fact (see ref. [13]) that nonplanar corrections are also nonleading collinear.

From eq. (5.2) we then obtain

$$\begin{aligned} \langle \mathbf{h}_n | \mathbf{h}_n \rangle &\simeq \sigma_0 \left( \frac{1}{2} C_A \right)^n \sum_{\pi_{n+1}} |\tilde{\mathbf{h}}_n(p, l_0 \dots l_n)|^2 S_{\text{nc}}^2(y_n, x_n, Q_{nt}) \\ &\times \left[ \tilde{S}_{\text{eik}}^{(n)}(y_n, 0; p, l_0 \dots l_n) \right]^2, \end{aligned} \quad (6.8)$$

where  $S_{\text{nc}}$  is the non-eikonal form factor already diagonal in colour and  $\tilde{S}_{\text{eik}}^{(n)}$  is the projection of the colour matrix eikonal form factor and is given by

$$\tilde{S}_{\text{eik}}^{(n)}(y_n, 0; p, l_0 \dots l_n) = \exp \left[ \frac{1}{2} g_s^2 \int_0^{y_n} (dq) I_n(p, l_0 \dots l_n) \right]. \quad (6.9)$$

From eq. (6.8) and from the recurrence relation for  $\tilde{\mathbf{h}}_n$  in eq. (5.5), we obtain now the corresponding relation for the colour components  $\tilde{\mathbf{h}}_n(p, l_0 \dots l_n)$ . From eq. (5.5) we have

$$\begin{aligned} \langle \tilde{\mathbf{h}}_n | \tilde{\mathbf{h}}_n \rangle &\simeq g_s^2 S_{\text{nc}}^2(y_{n-1}, y_n, Q_{(n-1)t}) \langle \tilde{\mathbf{h}}_{n-1} | [\mathbf{S}_{\text{eik}}^{(n-1)}(y_{n-1}, y_n)]^\dagger \mathbf{J}_{\text{tot}}^{(n-1)}(q_n) \\ &\times \mathbf{J}_{\text{tot}}^{(n-1)}(q_n) [\mathbf{S}_{\text{eik}}^{(n-1)}(y_{n-1}, y_n)] | \tilde{\mathbf{h}}_{n-1} \rangle. \end{aligned} \quad (6.10)$$

To evaluate this we recall that, in eq. (6.2), the total emission current  $\mathbf{J}_{\text{tot}}^{(n-1)}(q_n)$  is proportional to  $\mathbf{J}_{\text{eik}}^{(n-1)}(q_n)$  (cf. eq. (4.2)). The colour matrix in eq. (6.10) is then a functional only of  $\mathbf{J}_{\text{eik}}^{(n-1)}(q_n)$ . We can repeatedly use eq. (6.5) to obtain the final

recurrence relation for the colour components (cf. eq. (4.14) to tree level)

$$|\tilde{h}_n(\dots lnl' \dots)|^2 \simeq -\frac{Q_n^2}{Q_{n-1}^2} g_s^2 |\tilde{h}_{n-1}(\dots ll' \dots)|^2 (j_l(q_n) - j_{l'}(q_n))^2 \\ \times S_{\text{nc}}^2(y_{n-1}, y_n, Q_{(n-1)t}) [S_{\text{eik}}^{(n-1)}(y_{n-1}, y_n; \dots ll' \dots)]^2, \quad (6.11)$$

where

$$S_{\text{eik}}^{(n-1)}(y_{n-1}, y_n; \dots ll' \dots) = \exp \left[ \frac{1}{2} g_s^2 \int_{y_n}^{y_{n-1}} (dq) I_{n-1}(\dots ll' \dots) \right]. \quad (6.12)$$

By  $(\dots ll' \dots)$  we represent the ordered set of momenta obtained from the original set  $(\dots lnl' \dots)$  by removing the softest momentum  $q_n$ . The function  $I_{n-1}(\dots ll' \dots)$  is obtained from  $I_n(\dots lnl' \dots)$  in eq. (6.6) by the replacement

$$(j_l(q) - j_n(q))^2 + (j_n(q) - j_{l'}(q))^2 \rightarrow (j_l(q) - j_{l'}(q))^2. \quad (6.13)$$

The rescaling factor  $Q_n^2/Q_{n-1}^2$  in eq. (6.11) is due to the replacement of  $\mathbf{J}_{\text{tot}}^{(n-1)}$  with  $\mathbf{J}_{\text{eik}}^{(n-1)}$  (cf. eq. (4.2)).

By using the solution of the recurrence relation at tree level in sect. 4 we can solve (6.11) and obtain the full amplitude ( $y_{n+1} \equiv x$ )

$$h_n(p, l_0 \dots l_n) \simeq h_n^{(\text{tree})}(p, l_0 \dots l_n) \prod_1^n S_{\text{nc}}(y_l, y_{l+1}, Q_{l'}) \tilde{S}_{\text{eik}}^{(\text{tot})}(y_n, \dots, y_1; p, l_0 \dots l_n). \quad (6.14)$$

The total eikonal form factor is given by

$$\tilde{S}_{\text{eik}}^{(\text{tot})}(y_n, \dots, y_1; p, l_0 \dots l_n) \\ = \prod_1^n \tilde{S}_{\text{eik}}^{(k)} = \exp \frac{1}{2} g_s^2 \left[ \int_0^{y_n} (dq) I_n + \int_{y_n}^{y_{n-1}} (dq) I_{n-1} + \dots + \int_{y_2}^{y_1} (dq) I_1 \right], \quad (6.15)$$

where  $I_k$  is a function of the hardest  $k+2$  momenta  $p, p', q_1, \dots, q_k$  which is obtained from  $I_n$  in eq. (6.6) by successively removing the softest gluons  $q_n, q_{n-1}, \dots, q_{k+1}$  according to eq. (6.13).

The total eikonal form factor can be further simplified by using the identity

$$\int_0^{y_n} (dq) I_n(p, l_0 \dots l_n) + \dots + \int_{y_2}^{y_1} (dq) I_1(pq_1 p') = \sum_{k=1}^n \int_0^{y_k} (dq) I'_k, \quad (6.16)$$

where  $I'_0 = 0$  and  $I'_k = I_k - I_{k-1}$ . We have then that  $I'_k$  involves only the soft emission currents of the three gluons  $q_k$ ,  $q_{l_k}$  and  $q_{l'_k}$ , where  $q_{l_k}$  ( $q_{l'_k}$ ) is the next gluon harder than  $q_k$  to the right (left) of  $q_k$  in the considered permutation. We have then  $I'_1 = I_1$  and for  $k \geq 2$

$$I'_k = \frac{C_A}{2} \left\{ (j_{l_k} - j_k)^2 + (j_k - j_{l'_k})^2 - (j_{l_k} - j_{l'_k})^2 \right\}. \quad (6.17)$$

Introducing the angular variable  $\xi$  of sect. 4 we have

$$\frac{1}{2} g_s^2 \int_0^{y_k} (d\mathbf{q}) I'_k = -\frac{1}{2} \bar{\alpha}_s \int_{0^+}^{y_k} \frac{dy}{y} \int_{0^+}^{\bar{\xi}} \frac{d\xi}{\xi} \left\{ \Theta(\xi_{kl_k} - \xi) + \Theta(\xi_{kl'_k} - \xi) - \Theta(\xi_{l_k l'_k} - \xi) \right\}, \quad (6.18)$$

where  $\xi_{kl_k} = 1 - \cos \theta_{q_k q_{l_k}}$ , etc. For the case  $k = 1$  we have instead

$$I'_1 = I_1 = \frac{C_A}{2} \left\{ (j_p - j_1)^2 + (j_1 - j_{p'})^2 + (j_{p'} - j_p)^2 \right\}. \quad (6.19)$$

By integration we obtain

$$\frac{1}{2} g_s^2 \int_0^{y_1} (d\mathbf{q}) I_1 = -\frac{1}{2} \bar{\alpha}_s \int_{0^+}^{y_1} \frac{dy}{y} \int_{0^+}^{\bar{\xi}} \frac{d\xi}{\xi} \left\{ \Theta(\xi_1 - \xi) + 1 \right\}, \quad (6.20)$$

and we recover the result of subsect. 5.4.

## 6.2. DISTRIBUTIONS

The calculation at tree level in sect. 4 can now be extended to obtain the complete distributions. From eq. (6.14), in the energy ordered region (6.2), we obtain

$$\begin{aligned} |M_n|^2 &\simeq \frac{\sigma_0 (g_s^2 C_A)^n}{x_n^2} \sum_{\pi_{n+1}} W_n(p, l_0 \dots l_n) \\ &\times \prod_1^n S_{\text{nc}}^2(y_k, y_{k+1}, Q_{kt}) \left[ \tilde{S}_{\text{eik}}^{(\text{tot})}(y_n, \dots, y_1; p, l_0 \dots l_n) \right]^2, \quad (6.21) \end{aligned}$$

where  $W_n(p, l_0 \dots l_n)$  is the multi-eikonal distribution in eq. (4.17).

To analyze the initial state branching and to compute the structure function we integrate over the final state evolution and we are left only with the singularities for  $\theta_{p q_k} \rightarrow 0$ ,  $k = 1, 2, \dots, n$ .

Recall that in each multi-eikonal distribution  $W_n(p, l_0 \dots l_n)$  in eq. (4.17) the initial branching angular variables  $\theta_{p q_k}$  are ordered (cf. eq. (4.3)). In each one of

these ordered regions the generic term in eq. (6.16) becomes ( $k > 2$ )

$$\frac{1}{2}g_s^2 \int_0^{y_k} (dq) I'_k \simeq -\frac{1}{2}\bar{\alpha}_s \int_{0^+}^{y_k} \frac{dy}{y} \int_{0^+}^{\xi_k} \frac{d\xi}{\xi}, \quad \xi_k = 1 - \cos \theta_{pq_k}. \quad (6.22)$$

This is due to the fact that since  $q_{l_k}(q_{l'_k})$  are to the right (left) of  $q_k$  in the permutation one has either the ordering  $\theta_{pq_{l_k}} \ll \theta_{pq_k} \ll \theta_{pq_{l'_k}}$  or the opposite one. In the first case one has  $\xi_{kl_k} \simeq \xi_{l_k l'_k} \simeq \bar{\xi} \sim 1$ . Similarly for the other case.

From eqs. (6.20) and (6.22) we have that in each angular ordered region the total eikonal form factor assumes the symmetric form

$$\tilde{S}_{\text{eik}}^{(\text{tot})}(y_n, \dots, y_1; p, l_0 \dots l_n) \simeq S_{\text{eik}}(y_1, \bar{\xi}) \prod_1^n S_{\text{eik}}(y_k, \xi_k), \quad (6.23)$$

where  $S_{\text{eik}}(y, \xi)$  is given by

$$S_{\text{eik}}(y, \xi) = \exp \left[ -\frac{1}{2}\bar{\alpha}_s \int_{0^+}^y \frac{dy'}{y'} \int_{0^+}^{\xi} \frac{d\xi'}{\xi'} \right]. \quad (6.24)$$

The various eikonal form factor in eq. (6.23) have a simple interpretation: the first one is the Sudakov form factor which will regularize the infrared singularities for the soft gluon emission of the incoming gluon  $p$  ( $y_1 \sim 1$ ). The form factor  $S_{\text{eik}}(y_k, \xi_k)$  instead regularizes the final state soft emission from gluon  $q_k$ . Because of coherence this emission takes place within a cone centered around  $q_k$  with aperture  $\xi < \xi_k$ . In the study of initial state branching, we integrate over the successive branching of emitted gluons  $k = 1, \dots, n$ . In this way all the Sudakov form factors  $S_{\text{eik}}(y_k, \xi_k)$  are cancelled by the final state singularities for  $\xi_{k_j} = 0$ . In the energy ordered phase space region (6.2) the distribution of initial state radiation is given by

$$|M_n|^2 \simeq \frac{\sigma_0 (2g_s^2 C_A)^n}{x_n^2} \sum_{\pi_n} \Theta_{l_n \dots l_1}^{\xi} \prod_1^n \frac{1}{\omega_k^2 \xi_k} \tilde{S}_{\text{nc}}^2(12 \dots n) S_{\text{eik}}^2(1, \bar{\xi}) + \dots \quad (6.25)$$

Finally the gluon structure function is

$$F(Q^2, x) = \sum_{n=1}^{\infty} \bar{\alpha}_s^n \int \prod_1^n \left( \frac{dy_i}{y_i} \frac{d\xi_i}{\xi_i} \right) \Theta_{12 \dots n}^y \sum_{\pi_n} \Theta_{l_n \dots l_2 l_1}^{\xi} \prod_1^n \Theta(Q - q_{i_l}) \frac{1}{x} \delta(x_n - x) \\ \times S_{\text{eik}}^2(1, \bar{\xi}) \tilde{S}_{\text{nc}}^2(12 \dots n), \quad (6.26)$$

where  $\Theta_{12 \dots n}^y$  is the energy ordering theta-function corresponding to the region (6.2) and  $\Theta^{\xi}$  is the angular ordering theta-function in the region

$$\bar{\xi} \gg \xi_{l_n} \gg \dots \gg \xi_{l_1}, \quad (6.27)$$

where  $\bar{\xi}$  is the maximum available phase space value  $\bar{\xi} \sim 1$ . As discussed in the introduction we define the structure function by integrating  $q_{it}$  up to  $Q$ , where  $q_{it}$  is the transverse momentum of gluon  $i$  and is given by

$$q_{it}^2 = 2(Ey_i)^2 \xi_i. \quad (6.28)$$

Recall that in the total cross section of deep inelastic process, the kinematical boundary for  $q_{it}$  is given by  $q_{it}^2 < Q^2/x$ . In defining the structure function we do not include the region of  $q_{it}$  in the range  $(Q^2, Q^2/x)$ , which corresponds to a Drell–Yan emission of hard jets with transverse momentum larger than the probe  $Q$ . Such processes with two different hard scales have to be analyzed in an independent way. Notice that, from the factorization theorem, the structure function here defined, i.e. with the transverse momenta restricted to  $q_{it} < E_T$ , provides a complete description of high  $E_T$  jet emission in  $p\bar{p}$  collisions.

## 7. The structure function and initial state branching

In this section we analyze the initial state radiation distribution (6.25) given in sect. 6 by stressing the following points.

(i) *The coherence structure of the initial state emission.* We generalize the analysis done in sect. 4 at tree level and find that the soft gluon emission takes place within an angular ordered region. As we shall discuss, although the distributions in eq. (6.25) have been computed in the semi-hard region  $x \rightarrow 0$ , they can be assumed to be valid in any region of  $x$ . This is due to the fact that extrapolating (6.25) into the region  $x \rightarrow 1$ , the resulting distributions match the ones in this latter region (see ref. [2]). By assuming the distributions in eq. (6.25) to be valid in any region of  $x$ , we have under control all the singular terms for  $z \rightarrow 0, 1$  in the Altarelli–Parisi distribution.

(ii) *The spacelike gluon anomalous dimension for  $N \rightarrow 1$ .* This is obtained by following the method of refs. [2, 6], i.e. from the multi-gluon distribution for  $x \rightarrow 0$  we deduce an equation for the structure function with fixed total transverse momentum of emitted gluons. By diagonalizing such equation we obtain an anomalous dimension which for  $N \rightarrow 1$  coincides with the Lipatov ansatz discussed in the sect. 1. As suggested in refs. [2, 6], this is a consequence of a cancellation of collinear singularities due to coherence.

(iii) *The initial state branching structure.* From the multi-gluon distributions in eq. (6.25) we find the probability for the emission of soft and fast gluons. At inclusive level, the infrared singularities in the soft gluon emission are properly regularized by the appropriate Sudakov form factor. In the case of a fast emitted gluon we identify a non-Sudakov form factor to be responsible for the cancellation of too singular contributions in the anomalous dimension.

## 7.1. ANGULAR ORDERED DISTRIBUTION AND COHERENCE

In order to see more clearly and exploit the structure of coherence of initial state radiation we consider the integral structure function in eq. (6.26) and we exchange the sum over  $\xi$ -ordering permutation with the sum over  $y$ -ordering permutation. In the integrand of eq. (6.26), we make the substitution

$$\Theta_{12\dots n}^y \sum_{\pi_n} \Theta_{l_n\dots l_2 l_1}^\xi \tilde{S}_{\text{ne}}^2(12\dots n) \rightarrow \Theta_{n\dots 21}^\xi \sum_{\pi_n} \Theta_{l_1 l_2 \dots l_n}^y \tilde{S}_{\text{ne}}^2(l_1 l_2 \dots l_n), \quad (7.1)$$

so that  $n$  gluons are now emitted in the  $\xi$ -ordered phase space

$$\bar{\xi} \gg \xi_n \gg \xi_{n-1} \gg \dots \gg \xi_2 \gg \xi_1, \quad (7.2)$$

where  $\bar{\xi}$  is the maximum available value fixed by coherence ( $\bar{\xi} \sim 1$ ). The non-eikonal form factor in eq. (6.3) is not symmetric under permutation and this exchange is quite laborious. Given the permutation corresponding to the energy ordered region

$$y_{l_n} \ll y_{l_{n-1}} \ll \dots \ll y_{l_2} \ll y_{l_1} \sim 1, \quad (7.3)$$

we want now to obtain a simple expression for  $\tilde{S}_{\text{ne}}^2(l_1 l_2 \dots l_n)$ . We first identify the set of  $m$  harder gluons  $q_{h_1}, q_{h_2}, \dots, q_{h_m}$  and  $(m+1)$  clusters  $C_1, C_2, \dots, C_{m+1}$  of relatively softer gluons as indicated in fig. 11. In this kinematical configuration, all emitted gluons are ordered according to increasing angles moving from right to left. We have then  $h_1 < h_2 < \dots < h_m$  corresponding to

$$\bar{\xi} \gg \xi_{h_m} \gg \dots \gg \xi_{h_2} \gg \xi_{h_1}. \quad (7.4)$$

Each gluon  $h_k$  is harder than the gluons within the cluster  $C_k$ . A gluon  $l$  belongs to cluster  $C_k$  when the following property is satisfied

$$\begin{aligned} l \in C_k & \quad \text{if } y_l < y_{h_k}, & \xi_{h_{k-1}} < \xi_l < \xi_{h_k}, \\ l \in C_{m+1} & \quad \text{if } y_l < x, & \xi_{h_m} < \xi_l < \bar{\xi}, \end{aligned} \quad (7.5)$$

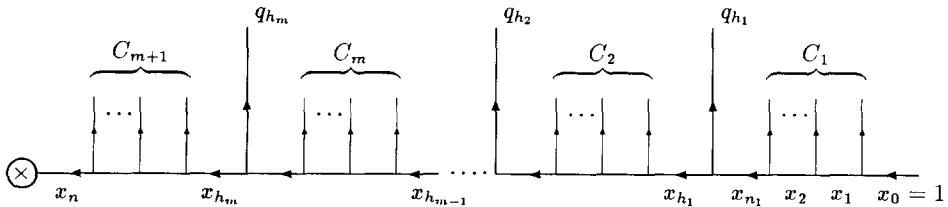


Fig. 11. Kinematical configurations for initial state emission. The angles between the emitted gluons and the incoming one increase from right to left. The energy of emitted gluons are specified in eqs. (7.3) and (7.5). Note that this is not a Feynman diagram.

where  $\xi_{h_0} = 0$ . We have then  $h_{k-1} < l < h_k$ , for  $l \in C_k$ , and the  $m$  harder gluons are ordered also in energies

$$y_{h_m} \ll y_{h_{m-1}} \ll \dots \ll y_{h_2} \ll y_{h_1} \sim 1. \quad (7.6)$$

Notice that in the phase space (7.5) we have

$$\begin{aligned} l \in C_k & \quad q_{lt} \ll q_{h_k t}, \\ l \in C_{m+1} & \quad q_{lt} \ll Q. \end{aligned} \quad (7.7)$$

In the kinematical configuration of fig. 11 we can greatly simplify the non-eikonal form factor  $\tilde{S}_{\text{ne}}^2(l_1 l_2 \dots l_n)$ . Due to the fact that  $S_{\text{ne}}^2(y_l, y_{l+1}, Q_{lt}) \simeq 1$  when gluon  $l$  is soft, we have that only fast gluons  $h_1, h_2, \dots, h_m$  contribute significantly to  $\tilde{S}_{\text{ne}}^2(l_1 l_2 \dots l_n)$

$$\tilde{S}_{\text{ne}}^2(l_1 l_2 \dots l_n) \simeq \prod_1^m S_{\text{ne}}^2(y_{h_k}, y_{h_{k+1}}, Q_{h_k t}). \quad (7.8)$$

The total transverse momentum  $Q_{h_k t}$  is given by the sum of the transverse momenta of all gluons which are harder than  $h_k$  (see sect. 5). However, due to eq. (7.7), we can neglect the contributions of all gluons within the soft clusters. Hence we can approximate

$$-Q_{h_k t} \simeq q_{h_k t} + q_{h_2 t} + \dots + q_{h_1 t}. \quad (7.9)$$

We are now ready to express the structure function in eq. (6.26) as an integral over the angular ordered region in (7.2) as follows

$$\begin{aligned} F(Q^2, x) &= \sum_{m=1}^{\infty} \bar{\alpha}_s^m \int \prod_1^m \left[ \frac{d y_{h_k}}{y_{h_k}} \frac{d \xi_{h_k}}{\xi_{h_k}} S_{\text{ne}}^2(y_{h_k}, y_{h_{k+1}}, Q_{h_k t}) \Theta(Q - q_{h_k t}) \right] \Theta_{h_m \dots h_2 h_1}^{\xi} \\ &\times S_{\text{cik}}^2(1, \bar{\xi}) \prod_{k=1}^{m+1} \left\{ \sum_{n_k=0}^{\infty} \bar{\alpha}_s^{n_k} \int_{C_k} \prod_1^{n_k} \left( \frac{d y_i}{y_i} \frac{d \xi_i}{\xi_i} \right) \Theta_{n_k \dots 21}^{\xi} \right\} \frac{1}{x_n} \delta(x - x_n). \end{aligned} \quad (7.10)$$

The transverse momentum  $q_{j t}$  of the emitted gluon  $j$  is given by eq. (6.28) and the phase space integration over the cluster  $C_k$  is defined in eq. (7.5)

$$\int_{C_k} \prod_1^{n_k} \left( \frac{d y_i}{y_i} \frac{d \xi_i}{\xi_i} \right) \Theta_{n_k \dots 21}^{\xi} = \int_{\xi_{h_{k-1}}}^{\xi_{h_k}} \prod_1^{n_k} \frac{d \xi_j}{\xi_j} \Theta_{n_k \dots 21}^{\xi} \int_{0^+}^{y_{h_k}} \prod_1^{n_k} \frac{d y_j}{y_j}. \quad (7.11)$$

Notice that, since gluons within the soft clusters have transverse momenta smaller than the ones of fast gluons (see eq. (7.7)), in the phase space we have included the transverse momentum limitation only for the  $m$  fast gluons.

From the integrand of eq. (7.10) we obtain the structure of initial state radiation. Before discussing in details the structure of this emission, we first perform all integrations in eq. (7.10) and compute the behaviour of  $F(Q^2, x)$  for  $x \rightarrow 0$ .

## 7.2. THE STRUCTURE FUNCTION FOR $x \rightarrow 0$

For  $x \rightarrow 0$ , essentially all the energy is taken by emitted hard gluons  $h_1, \dots, h_k$  so that we can approximate  $x_n \simeq 1 - y_{h_1} - \dots - y_{h_k}$ . In this case there are no energy constraints in the range of integration within the soft clusters and we can perform the corresponding integrals. Summing over any number of gluons in  $C_k$ , we have

$$\sum_{n_k=0}^{\infty} \bar{\alpha}_s^{n_k} \int_{C_k} \prod_1^{n_k} \left( \frac{dy_i}{y_i} \frac{d\xi_i}{\xi_i} \right) \Theta_{n_k, \dots, 21}^{\xi} = \exp \left[ \bar{\alpha}_s \int_{\xi_{h_{k-1}}}^{\xi_{h_k}} \frac{d\xi}{\xi} \int_{0^+}^{y_{h_k}} \frac{dy}{y} \right]. \quad (7.12)$$

In this real emission contributions, the infrared singularities for  $y \rightarrow 0$  are regularized by the Sudakov form factor  $S_{\text{eik}}^2(1, \bar{\xi})$ . Combining all soft cluster emission in eq. (7.12) with the Sudakov form factor, we have

$$S_{\text{eik}}^2(1, \bar{\xi}) \prod_1^{m+1} \exp \left[ \bar{\alpha}_s \int_{0^+}^{y_{h_k}} \frac{dy}{y} \int_{\xi_{h_{k-1}}}^{\xi_{h_k}} \frac{d\xi}{\xi} \right] = \prod_1^m \exp \left[ -\bar{\alpha}_s \int_{y_{h_{k+1}}}^{y_{h_k}} \frac{dy}{y} \int_{\xi_{h_k}}^{\bar{\xi}} \frac{d\xi}{\xi} \right], \quad (7.13)$$

which is infrared finite.

In the energy ordering (7.6) we introduce the energy fraction  $z_{h_k}$  related to the emission of the harder gluons

$$y_{h_{k-1}} = z_{h_k} y_{h_k}, \quad y_{h_1} \sim 1, \quad x \simeq z_{h_1} z_{h_2} \dots z_{h_m}. \quad (7.14)$$

We obtain the following result for  $x \rightarrow 0$

$$F(Q^2, x) = \delta(1-x) + \sum_{m=1}^{\infty} \int \prod_1^m \left[ dz_r \frac{\bar{\alpha}_s}{z_r} \frac{d\xi_r}{\xi_r} \Delta_{\text{ne}}(z_r, Q_{r_t}, q_{r_t}) \Theta(Q - q_{r_t}) \right] \\ \times \Theta_{m, \dots, 21}^{\xi} \delta(x - z_1 \dots z_m), \quad (7.15)$$

where the index  $r$  stands for  $h_k$ . We have introduced a new non-eikonal form factor  $\Delta_{\text{ne}}(z_r, Q_{r_t}, q_{r_t})$  which is obtained by combining  $S_{\text{ne}}^2$  with the part of the eikonal

form factor which remains after the soft cluster integration in (7.13)

$$\begin{aligned}
\Delta_{\text{ne}}(z_r, Q_{r_t}, q_{r_t}) &= S_{\text{ne}}^2(y_r, y_{r+1}, Q_{r_t}) \exp \left[ -\bar{\alpha}_s \int_{y_{r+1}}^{y_r} \frac{dy}{y} \int_{\xi_r}^{\bar{\xi}} \frac{d\xi}{\xi} \right] \\
&= \exp \left[ \bar{\alpha}_s \int_{y_{r+1}}^{y_r} \frac{dy}{y} \int \frac{dk_t^2}{k_t^2} \Theta(k_t - Q_{r_t}) \right] \\
&\quad \times \exp \left[ -\bar{\alpha}_s \int_{y_{r+1}}^{y_r} \frac{dy}{y} \int \frac{dk_t^2}{k_t^2} \Theta \left( k_t - q_{r_t} \frac{y}{y_r} \right) \right], \quad (7.16)
\end{aligned}$$

where we have introduced  $k_t^2 = 2E^2 y^2 \xi$  and  $q_{r_t}^2$  is defined in eq. (6.28). Notice the cancellation of the dependence on the phase space boundary  $\xi < \bar{\xi}$  and  $k_t^2 < 2(yE)^2 \bar{\xi}$ . By rescaling  $y_{r+1} = z_r y_r$  we obtain

$$\Delta_{\text{ne}}(z_r, Q_{r_t}, q_{r_t}) = \exp \left[ -\bar{\alpha}_s \int_{z_r}^1 \frac{dz}{z} \int_{(zq_{r_t})^2}^{Q_{r_t}^2} \frac{dq_t^2}{q_t^2} \right]. \quad (7.17)$$

This form factor is analogous to the one introduced in ref. [6].

Before performing the calculation of the anomalous dimension we consider some terms of the perturbative expansion in  $\alpha_s$  of the structure function in eq. (6.26) and its energy moments

$$F_N(Q^2) = \int_0^1 dx x^{N-1} F(Q^2, x) = [Q^2/\mu^2]^{\gamma_N}, \quad (7.18)$$

where  $\mu$  is the factorization scale and  $\gamma_N$  is the anomalous dimension. The term of order  $\alpha_s$  in the expansion of eq. (7.15), is given by

$$\begin{aligned}
F^{(1)}(Q^2, x) &= \frac{\bar{\alpha}_s}{x} \int_{\mu^2}^{Q^2} \frac{dq_t^2}{q_t^2} = \frac{\bar{\alpha}_s}{x} \ln \left( \frac{Q^2}{\mu^2} \right), \\
F_N^{(1)}(Q^2) &= \frac{\bar{\alpha}_s}{N-1} \ln \left( \frac{Q^2}{\mu^2} \right). \quad (7.19)
\end{aligned}$$

The order  $\alpha_s^2$  contribution is

$$\begin{aligned}
F^{(2)}(Q^2, x) &= \frac{\bar{\alpha}_s^2}{x} \int_x^1 \frac{dz_1}{z_1} \int_{\mu^2}^{Q^2} \frac{dq_{1t}^2}{q_{1t}^2} \left\{ \int_{(z_1 q_{1t})^2}^{Q^2} \frac{dq_{2t}^2}{q_{2t}^2} - \int_{(z_1 q_{1t})^2}^{q_{1t}^2} \frac{dq_{2t}^2}{q_{2t}^2} \right\} \\
&= -\frac{1}{2} \frac{\bar{\alpha}_s^2 \ln x}{x} \left[ \ln \left( \frac{Q^2}{\mu^2} \right) \right]^2, \quad F_N^{(2)}(Q^2) = \frac{1}{2} \left[ \frac{\bar{\alpha}_s}{N-1} \ln \left( \frac{Q^2}{\mu^2} \right) \right]^2, \quad (7.20)
\end{aligned}$$

which is just the exponentiation of  $F_N^{(1)}(Q^2)$ . Therefore the  $N \rightarrow 1$  anomalous dimension is

$$\gamma_N = \frac{\bar{\alpha}_s}{N-1} + \mathcal{O}(\bar{\alpha}_s^3), \quad (7.21)$$

which agrees with the exact result [14].

The first term in the integrand of eq. (7.20) is the contribution from two gluon emission. We have introduced the transverse momenta  $q_{1t}$  and  $q_{2t}$  defined by eq. (6.28). The angular ordering  $\xi_2 > \xi_1$  gives  $q_{2t} > z_1 q_{1t}$ . The negative term in the integrand comes from the order  $\alpha_s$  virtual correction to the emission of gluon  $q_1$ .

Notice that the real and virtual contributions in eq. (7.20) are individually more singular than the final expression. In the two contributions the  $q_{2t}$  integration diverges for  $z_1 \rightarrow 0$  and then give terms of order  $\alpha_s^2 \ln^2(x)/x$ . Summing the real emission and the virtual corrections, the  $q_{2t} \rightarrow 0$  singularities cancel and one obtains the less singular result in eq. (7.20). This cancellation has been already noticed [2, 6]. In the following we shall see its generalization to all orders.

We now explicitly evaluate the structure function and the anomalous dimension for  $N \rightarrow 1$ . This is obtained by transforming eq. (7.15) in the form of a recurrence relation. Following the method of ref. [2, 6], we introduce the total transverse momentum distribution  $\tilde{F}(\mathbf{Q}_t, x)$  and the unintegrated distribution  $\mathcal{F}(x, \mathbf{Q}_t, z, q_t)$  defined by

$$\begin{aligned} F(Q^2, x) &= \frac{1}{x} \int d^2 Q_t \tilde{F}(\mathbf{Q}_t, x) \\ &= \delta(1-x) + \frac{1}{x} \int d^2 Q_t \int_{\mu^2}^{Q^2} \frac{d^2 q_t}{\pi q_t^2} \int_x^1 \frac{dz}{z} \mathcal{F}(x, \mathbf{Q}_t, z, q_t). \end{aligned} \quad (7.22)$$

In these unintegrated distributions the dependence on  $\mu$  and  $Q$  is understood. The distribution  $\mathcal{F}(x, \mathbf{Q}_t, z, q_t)$  is obtained from eq. (7.15) by setting  $Q_t = Q_{mt}$ ,  $z = z_m$  and  $q_t = q_{mt}$ . Hence  $Q_t$  is the total transverse momentum of the emitted gluons,  $(1-z)$  and  $q_t$  are the energy fraction and transverse momentum of the last harder emitted gluon. Note that  $Q_t$  and  $q_t$  are constrained\* by the kinematical boundary  $Q_m^2 < z Q_{m-1}^2$ , which essentially gives

$$Q_t^2 > z q_t^2. \quad (7.23)$$

\* We are grateful to Marcello Ciafaloni for drawing our attention on this boundary.

From eq. (7.15) we deduce the following integral equation

$$\begin{aligned} \mathcal{F}(x, \mathbf{Q}_t, z, q_t) &= \Theta(Q_t^2 - zq_t^2) \left[ \bar{\alpha}_s \delta^2(\mathbf{Q}_t + \mathbf{q}_t) \delta\left(1 - \frac{x}{z}\right) \Delta_{\text{ne}}(x, \mathbf{Q}_t, q_t) \right. \\ &\left. + \bar{\alpha}_s \int_{x/z}^1 \frac{dz'}{z'} \int_{\mu^2}^{Q_t^2} \frac{d^2q_t'}{\pi q_t'^2} \Theta(q_t - z'q_t') \Delta_{\text{ne}}(z, \mathbf{Q}_t, q_t) \mathcal{F}\left(\frac{x}{z}, \mathbf{Q}_t + \mathbf{q}_t, z', q_t'\right) \right], \end{aligned} \quad (7.24)$$

where the transverse momentum constraint  $z'q_t' < q_t$  is obtained from angular ordering.

We now transform eq. (7.24) into a differential equation: first we integrate eq. (7.24) over  $z$  and  $q_t$  and then we differentiate over  $x$ . We can write

$$x \frac{\partial}{\partial x} [\tilde{F}(\mathbf{Q}_t, x) - \delta(1-x)\delta^2(\mathbf{Q}_t)] = \tilde{F}'_1(\mathbf{Q}_t, x) + \tilde{F}'_2(\mathbf{Q}_t, x), \quad (7.25)$$

where

$$\begin{aligned} \tilde{F}'_1(\mathbf{Q}_t, x) &= -\frac{\bar{\alpha}_s}{\pi Q_t^2} \delta(1-x) + \bar{\alpha}_s \int_x^1 \frac{dz}{z} \int_{\mu^2}^{Q_t^2} \frac{dq_t^2}{q_t^2} \\ &\times \left\{ \int_{\mu^2}^{Q_t^2} \frac{d^2q_t'}{\pi q_t'^2} \Theta(q_t' - zq_t) \mathcal{F}(x, \mathbf{Q}_t, z, q_t) \right. \\ &\left. - \int_{\mu^2}^{Q_t^2} \frac{d^2q_t'}{\pi q_t'^2} \Theta(q_t' - zq_t) \mathcal{F}(x, \mathbf{Q}_t + \mathbf{q}_t', z, q_t) \right\}, \end{aligned} \quad (7.26)$$

$$\tilde{F}'_2(\mathbf{Q}_t, x) = \bar{\alpha}_s \int_{Q_t^2}^{Q_t^2} \frac{dq_t^2}{q_t^2} \left\{ \tilde{F}(\mathbf{Q}_t + \mathbf{q}_t, x) - \tilde{F}\left(\mathbf{Q}_t + \mathbf{q}_t, \frac{x}{z_0}\right) \right\}, \quad z_0 = \frac{Q_t^2}{q_t^2}. \quad (7.27)$$

The contribution  $\tilde{F}'_2$  embodies the constraints from the kinematical boundaries  $z = 1$  and  $z = z_0$  in eq. (7.23). We shall show that  $\tilde{F}'_2$  gives a nonleading contribution to the structure function for  $N \rightarrow 1$ .

The two terms in  $\tilde{F}'_1$  come by differentiating the virtual and real emission contributions in eq. (7.24). We explicitly see that the singularity in  $q_t'^2$  for  $z \rightarrow 0$  is cancelled. This is the generalization to all order of the cancellation of collinear singularities in the two-loop case (see (7.20)). We can neglect in eq. (7.26) the bound from the angular ordering  $q_t' > zq_t$  which corresponds to neglect terms of order  $z$ . In

this way we can perform the integration over  $z$  and  $q_t$  and obtain

$$\tilde{F}'_1(\mathbf{Q}_t, x) = \bar{\alpha}_s \left\{ \int_{\mu^2}^{Q_t^2} \frac{d^2 q_t}{\pi q_t^2} \tilde{F}(\mathbf{Q}_t, z) - \int_{\mu^2}^{Q^2} \frac{d^2 q_t}{\pi q_t^2} \tilde{F}(\mathbf{Q}_t + \mathbf{q}_t, z) \right\}. \quad (7.28)$$

By integrating eq. (7.25) we obtain

$$\tilde{F}(\mathbf{Q}_t, x) = \delta(1-x) \delta^2(\mathbf{Q}_t) - \int_x^1 \frac{dz}{z} \{ \tilde{F}'_1(\mathbf{Q}_t, z) + \tilde{F}'_2(\mathbf{Q}_t, z) \}, \quad (7.29)$$

with  $\tilde{F}'_1$  and  $\tilde{F}'_2$  given in eqs. (7.27) and (7.28). This equation for the structure function at fixed  $\mathbf{Q}_t$  is equivalent, at the leading order level, to the equation obtained by Ciafaloni [6] from his analysis mainly done at the one-loop level.

We can now diagonalize (7.29) by introducing the energy moment distribution  $\tilde{F}_N$  defined by

$$F_N(Q^2, \mu^2) = \int d^2 Q_t \tilde{F}_N(\mathbf{Q}_t, \mu), \quad (7.30)$$

where the  $Q$ -dependence is understood. We obtain

$$\begin{aligned} \tilde{F}_N(\mathbf{Q}_t, \mu) = & \delta^2(\mathbf{Q}_t) + \frac{\bar{\alpha}_s}{N-1} \left\{ \int_{\mu^2}^{Q_t^2} \frac{d^2 q_t}{\pi q_t^2} \tilde{F}_N(\mathbf{Q}_t + \mathbf{q}_t, \mu) \right. \\ & \left. - \int_{\mu^2}^{Q_t^2} \frac{d^2 q_t}{\pi q_t^2} \tilde{F}_N(\mathbf{Q}_t, \mu) \Theta(Q_t - q_t) \right\} \\ & - \bar{\alpha}_s \int_{Q_t^2}^{Q^2} \frac{d^2 q_t}{\pi q_t^2} \tilde{F}_N(\mathbf{Q}_t + \mathbf{q}_t, \mu) \left( \frac{1 - z_0^{N-1}}{N-1} \right), \end{aligned} \quad (7.31)$$

where the last term, coming from eq. (7.27) can be neglected since it is less singular for  $N \rightarrow 1$  than the first term. In terms of anomalous dimension, we have

$$\tilde{F}_N(\mathbf{Q}_t, \mu) = \delta^2(\mathbf{Q}_t) + \frac{\gamma_N}{\pi Q_t^2} \left[ \frac{Q_t^2}{\mu^2} \right]^{\gamma_N}, \quad (7.32)$$

and eq. (7.31) becomes

$$1 = \frac{\bar{\alpha}_s}{N-1} \left\{ \frac{\epsilon_1^{\gamma_N}}{\gamma_N} + \int_{\epsilon_1}^1 d\eta \left[ \frac{\eta^{\gamma_N-1} - 1}{1-\eta} \right] + \int_{\epsilon_2}^1 d\eta \left[ \frac{\eta^{-\gamma_N} - 1}{1-\eta} \right] \right\} + \mathcal{O}(\bar{\alpha}_s), \quad (7.33)$$

with  $\epsilon_1 = \mu^2/Q_1^2$ ,  $\epsilon_2 = Q_1^2/Q^2$ . For  $0 < \gamma_N < 1$  we can take the asymptotic limit  $\epsilon_1 \rightarrow 0$  and  $\epsilon_2 \rightarrow 0$  and obtain a relation for the anomalous dimension. The  $O(\bar{\alpha}_s)$  contribution in eq. (7.33) comes from kinematical constraints in eq. (7.23) and gives a non-leading contribution for  $N \rightarrow 1$ . The anomalous dimension  $\gamma_N$  is given by the Lipatov ansatz discussed in the introduction

$$N - 1 = \bar{\alpha}_s [2\psi(1) - \psi(\gamma_N) - \psi(1 - \gamma_N)] = \bar{\alpha}_s f(\gamma_N), \quad (7.34)$$

which gives

$$\gamma_N = \frac{\bar{\alpha}_s}{N-1} \left\{ 1 + 2 \sum_{k=0}^{\infty} \zeta(3+2k) \gamma_N^{3+2k} \right\}, \quad (7.35)$$

where  $\zeta(j)$  are the Riemann zeta-functions. By expanding we have\*

$$\gamma_N(\alpha_s) = \sum_{j=1}^{\infty} g_j \left( \frac{\bar{\alpha}_s}{N-1} \right)^j, \quad \bar{\alpha}_s = \frac{\alpha_s C_A}{\pi}, \quad (7.36)$$

and the first few coefficients are

$$\begin{aligned} g_1 &= 1, & g_2 &= 0, & g_3 &= 0, \\ g_4 &= 2\zeta(3) = 2.401736\dots, & g_5 &= 0, & g_6 &= 2\zeta(5) = 2.073853\dots, \\ g_7 &= 12\zeta^2(3) = 17.305004\dots, & g_8 &= 2\zeta(7) = 2.016698\dots, \\ g_9 &= 32\zeta(5)\zeta(3) = 39.846771\dots, \\ g_{10} &= 2\{48\zeta^3(3) + \zeta(9)\} = 168.252213\dots, \\ g_{11} &= 2\{20\zeta(7)\zeta(3) + 10\zeta^2(5)\} = 69.940094\dots, \\ g_{12} &= 2\{220\zeta(5)\zeta^2(3) + \zeta(11)\} = 659.948242\dots, \\ g_{13} &= 2\{440\zeta^4(3) + 24\zeta(9)\zeta(3) + 24\zeta(7)\zeta(5)\} = 1937.998169\dots, \\ g_{14} &= 2\{312\zeta(7)\zeta^2(3) + 312\zeta^2(5)\zeta(3) + \zeta(13)\} = 1715.077881\dots \end{aligned} \quad (7.37)$$

As mentioned in the introduction, the fact that the two- and three-loop corrections gives zero contribution, does not imply that the one-loop result ( $\gamma_N^1 = \bar{\alpha}_s/(N-1)$ ) gives a good approximation to the structure function for  $x \rightarrow 0$ . As indicated by the

\* We are grateful to Enrico Onofri for discussing the most efficient way to obtain these coefficients.

growth of the coefficients in eq. (7.37),  $\gamma_N$  has a singularity for  $N$  above 1. To see this, notice [2, 3] that  $f(\gamma_N)$  in eq. (7.34) is symmetric for  $\gamma_N \rightarrow 1 - \gamma_N$  and has a minimum at  $\gamma_N = \frac{1}{2}$ . As a result  $\gamma_N$  has a square root singularity at  $N = N^*$  given by  $N^* = 1 + \bar{\alpha}_s f(\frac{1}{2})$ , and the structure function grows as  $F(Q, x) \sim x^{-N^*}$ .

### 7.3. INITIAL STATE BRANCHING

The initial state branching is described by the integrand of the structure function in eq. (7.10). We introduce the spacelike momenta  $Q_j$  with the relative energy fractions ( $x_j = (\bar{p}Q_j)/(p\bar{p})$ )

$$Q_j = p - q_1 - \dots - q_j, \quad x_j = 1 - y_1 - \dots - y_j, \quad (7.38)$$

and the energy fraction  $(1 - z_j)$  for the emitted gluons ( $x_0 = 1$ )

$$y_j = (1 - z_j)x_{j-1}, \quad x_j = x_0 z_1 z_2 \dots z_j. \quad (7.39)$$

In eq. (7.10) one sums over all possible ordering in the energy of the emitted gluons. This is obtained by considering all kinematical configurations of fig. 11. Here one identifies the fast gluons  $h_1, h_2, \dots, h_m$  corresponding to ( $r = h_k$ )

$$z_r \ll 1, \quad y_r = (1 - z_r)x_{r-1} \simeq x_{r-1}, \quad (7.40)$$

and the soft gluons emitted within clusters  $C_1, C_2, \dots, C_{m+1}$  corresponding to

$$1 - z_l \ll 1, \quad y_l = (1 - z_l)x_{l-1} \ll x_{l-1}. \quad (7.41)$$

In this kinematical configuration one has

$$x_n = z_1 z_2 \dots z_n \simeq z_{h_1} z_{h_2} \dots z_{h_m}. \quad (7.42)$$

From the analysis in the previous subsection we find useful to write the virtual contributions in eq. (7.10) in the form

$$\begin{aligned} & S_{\text{eik}}^2(1, \bar{\xi}) \prod_1^m S_{\text{ne}}^2(y_{h_k}, y_{h_{k+1}}, Q_{h_k t}) \\ &= \prod_1^m \Delta_{\text{ne}}(z_{h_k}, Q_{h_k t}, q_{h_k t}) \prod_1^m \exp \left[ -\bar{\alpha}_s \int_{\xi_{h_{k-1}}}^{\xi_{h_k}} \frac{d\xi}{\xi} \int_{0^+}^{x_{h_{k-1}}} \frac{dy}{y} \right], \end{aligned} \quad (7.43)$$

where we have introduced the non-Sudakov form factor  $\Delta_{\text{ne}}$  defined in eq. (7.17). The remaining form factors, as shown in the previous subsection, regularize the infrared divergences of soft gluons within  $C_1, \dots, C_{m+1}$ . By using eq. (7.43) and the

previous variables, the structure function in eq. (7.10) can be cast in the form

$$F(Q^2, x) = \sum_{m=1}^{\infty} \int \mathcal{B}_{\text{soft}}^{(m+1)} \prod_1^m \left\{ dz_{h_k} \frac{\bar{\alpha}_s}{z_{h_k}} \frac{d\xi_{h_k}}{\xi_{h_k}} \Delta_{\text{nc}}(z_{h_k}, Q_{h_k}, q_{h_k}) \mathcal{B}_{\text{soft}}^{(k)} \right\} \\ \times \Theta_{h_m, \dots, h_2, h_1}^{\xi} \prod_1^m \Theta(Q - q_{h_k}) \delta(x - z_1 z_2 \dots z_n), \quad (7.44)$$

where  $\mathcal{B}_{\text{soft}}^{(k)}$  corresponds to the emission of soft gluons in cluster  $C_k$  and is given by

$$\mathcal{B}_{\text{soft}}^{(k)} \equiv \exp \left[ -\bar{\alpha}_s \int_{\xi'}^{\xi} \frac{d\xi''}{\xi''} \int_{0^+}^{x'} \frac{dy}{y} \right] \sum_{n_k=0}^{\infty} \bar{\alpha}_s^{n_k} \int_{\xi'}^{\xi} \Theta_{n_k, \dots, 21}^{\xi} \prod_1^{n_k} \frac{d\xi_l}{\xi_l} \int_{0^+}^{x'} \prod_1^{n_k} \frac{dy_l}{y_l}, \quad (7.45)$$

where  $\xi_{h_k} = \xi$ ,  $\xi_{h_{k-1}} = \xi'$  and  $x_{h_{k-1}} = x'$ . This part of the branching includes the appropriate virtual corrections which cancel the infrared singularities for  $y \rightarrow 0^+$  (see previous subsection).

Since we want to study the initial state radiation at the (partially) exclusive level, we need to regularize these infrared divergences. As usual we assume a lower cutoff in the transverse momenta of the emitted gluons. From eqs. (6.28) and (7.39) we set

$$(1 - z_l) > \epsilon_l \equiv Q_0 / (Ex_{l-1} \sqrt{\xi_l}), \quad (7.46)$$

and the cluster emission  $\mathcal{B}_{\text{soft}}^{(k)}$  becomes

$$\mathcal{B}_{\text{soft}}^{(k)} = \Delta_{\text{eik}}(x', \xi, \xi') \sum_{n_k=0}^{\infty} \bar{\alpha}_s^{n_k} \int_{\xi'}^{\xi} \Theta_{n_k, \dots, 21}^{\xi} \prod_{l=1}^{n_k} \frac{d\xi_l}{\xi_l} \int_0^{1-\epsilon_l} \frac{dz_l}{1-z_l}, \quad (7.47)$$

where we have introduced the Sudakov form factor

$$\Delta_{\text{eik}}(x, \xi, \xi') = \exp \left[ -\bar{\alpha}_s \int_{\xi'}^{\xi} \frac{d\xi''}{\xi''} \int_0^{1-\epsilon''} \frac{dz}{1-z} \right], \quad \epsilon'' = Q_0 / (Ex \sqrt{\xi''}). \quad (7.48)$$

The cluster  $\mathcal{B}_{\text{soft}}^{(k)}$  contribution can be written as a branching process for the soft gluon emission. Taking into account that for the soft emission within the cluster  $C_k$  we have  $x_l \simeq x' \equiv x_{h_{k-1}}$ , we obtain ( $\xi_0 = \xi'$ )

$$\Delta_{\text{eik}}(x', \xi, \xi') = \Delta_{\text{eik}}(x', \xi, \xi_{n_k}) \left[ \prod_1^{n_k} \Delta_{\text{eik}}(x', \xi_l, \xi_{l-1}) \right] \\ \simeq \Delta_{\text{eik}}(x_{n_k}, \xi, \xi_{n_k}) \left[ \prod_1^{n_k} \Delta_{\text{eik}}(x_{l-1}, \xi_l, \xi_{l-1}) \right]. \quad (7.49)$$

The cluster emission can be written as

$$\mathcal{P}_{\text{soft}}^{(k)} = \sum_{n_k=0}^{\infty} \int \Delta_{\text{eik}}(x_{n_k}, \xi, \xi_{n_k}) \times \prod_{l=1}^{n_k} \left\{ \frac{d\xi_l}{\xi_l} \Theta(\xi_l - \xi_{l-1}) dz_l \frac{\bar{\alpha}_s}{1-z_l} \Theta(1 - \epsilon_l - z_l) \Delta_{\text{eik}}(x_{l-1}, \xi_l, \xi_{l-1}) \right\}. \quad (7.50)$$

The quantity in the braces can be interpreted as probability distribution [7] for the soft gluon emission. Note that  $\Delta_{\text{eik}}(x_{l-1}, \xi_l, \xi_{l-1})$  has the correct relation with the real emission distribution function and the phase space in eq. (7.50).

If we insert eq. (7.50) in (7.44) we obtain the general branching process with two types of probabilities: the fast and the soft one given respectively by  $\mathcal{P}_{\text{fast}}$  and  $\mathcal{P}_{\text{soft}}$ .

The soft one is obtained from eq. (7.50)

$$d\mathcal{P}_{\text{soft}}(l) = \frac{d\xi_l}{\xi_l} \Theta(\xi_l - \xi_{l-1}) dz_l \frac{\bar{\alpha}_s}{1-z_l} \Theta(1 - \epsilon_l - z_l) \Delta_{\text{eik}}(x_{l-1}, \xi_l, \xi_{l-1}). \quad (7.51)$$

The branching distribution for fast gluons  $h_k$  is given by ( $h_k = r$ )

$$d\mathcal{P}_{\text{fast}}(r) = \frac{d\xi_r}{\xi_r} \Theta(Q - q_{rt}) \Theta(\xi_r - \xi_{r-1}) dz_r \frac{\bar{\alpha}_s}{z_r} \Delta_{\text{ne}}(z_r, Q_{rt}, q_{rt}) \times \Delta_{\text{eik}}(x_{r-1}, \xi_r, \xi_{r-1}). \quad (7.52)$$

It corresponds to the contributions of gluon  $h_k$  in the integrand of eq. (7.44) and includes the form factor  $\Delta_{\text{eik}}$  in the left-hand side of eq. (7.50).

In terms of these two quantities, the structure function has the simple form

$$F(Q^2, x) = \sum_{n=1}^{\infty} \int \Delta_{\text{eik}}(x_n, \bar{\xi}, \xi_n) \prod_1^n d\mathcal{P}(i) \delta(x - z_1 z_2 \dots z_n), \quad (7.53)$$

$$\text{with} \quad d\mathcal{P}(i) = d\mathcal{P}_{\text{fast}}(i) + d\mathcal{P}_{\text{soft}}(i). \quad (7.54)$$

The two distributions in eq. (7.54) can be combined more systematically. Observe that the non-Sudakov form factor  $\Delta_{\text{ne}}(z, Q_t, q_t) \rightarrow 1$  for  $z \rightarrow 1$ . Therefore, to double logarithmic accuracy, we can multiply  $d\mathcal{P}_{\text{soft}}$  by the non-Sudakov form factor and we obtain

$$d\mathcal{P}(i) = \frac{d\xi_i}{\xi_i} \Theta(Q - q_{it}) \Theta(\xi_i - \xi_{i-1}) dz_i \frac{\alpha_s}{2\pi} P(z_i) \Theta(1 - \epsilon_i - z_i) \times \Delta_{\text{ne}}(z_i, Q_{it}, q_{it}) \Delta_{\text{eik}}(x_{i-1}, \xi_i, \xi_{i-1}), \quad (7.55)$$

where

$$P(z) = 2C_A \left( \frac{1}{z} + \frac{1}{1-z} \right), \quad (7.56)$$

is the singular part for  $z \rightarrow 1, 0$  of the Altarelli–Parisi gluon distribution  $P_g(z)$  in eq. (4.31). The finite terms  $-2 + z(1+z)$  in  $P_g$  are not obtained from our analysis at the leading infrared accuracy.

From eqs. (7.52) and (7.51) or (7.55) we can define a Markov process for the initial state branching. Due to the fact that the non-Sudakov form factor for the emission of gluon  $i$  depends on  $Q_{it}$ , we have that the Markov process involves the variables  $q_{it}$ ,  $z_i$ ,  $Q_{it}$  and  $x_i$ . From the distribution (7.54) or (7.55) one obtains  $q_{i+1t}$  and  $z_{i+1}$  while  $Q_{(i+1)t}$  and  $x_{i+1}$  are determined by momentum conservation.

It is a pleasure to acknowledge many helpful discussions over some years on the topics of this paper with Marcello Ciafaloni. Discussions with Al Mueller and Bryan Webber are also acknowledged.

## Appendix A

In this appendix we outline the calculation of the two-gluon emission amplitude in a general axial gauge. Our purpose is to explicitly check the gauge invariance of the results in subsect. 3.1. We consider the amplitude for the process

$$p + q \rightarrow p' + q_1 + q_2, \quad (A.1)$$

where  $q$  is the hard spacelike momentum carried by the gauge invariant current  $(F_{\mu\nu}^a)^2$  and  $p, p', q_1, q_2$ , are incoming and outgoing gluon momenta. The generalization to incoming quark, which is straightforward, will not be considered in the following. We refer to sect. 2 for our notational conventions.

We use a general axial gauge  $\eta \cdot A = 0$  and evaluate the amplitude (A.1) at tree level. By performing a graph by graph calculation, spurious gauge poles of type  $(\eta \cdot Q_1)^{-1}$  and  $(\eta \cdot Q_2)^{-1}$  will appear in intermediate results. We may introduce a relevant simplification by using Feynman polarization tensors  $g^{\mu\nu}$  for internal gluon lines. This follows from the fact that external gluons are on mass shell and have physical polarization; then Ward identities automatically guarantee that, at tree level, only transverse polarizations propagate in internal legs.

Since external gluons are physical ones, the use of the eikonal approximation for soft gluon emission by external lines is still allowed. Therefore, in the strongly ordered region

$$x = 1 - y_1 - y_2 \ll y_2 \ll y_1 \sim 1, \quad (A.2)$$

we limit ourselves to evaluate the leading  $x \rightarrow 0$  diagrams in fig. 12, with the incoming gluon helicity conserved along the line  $p, q_1$ .

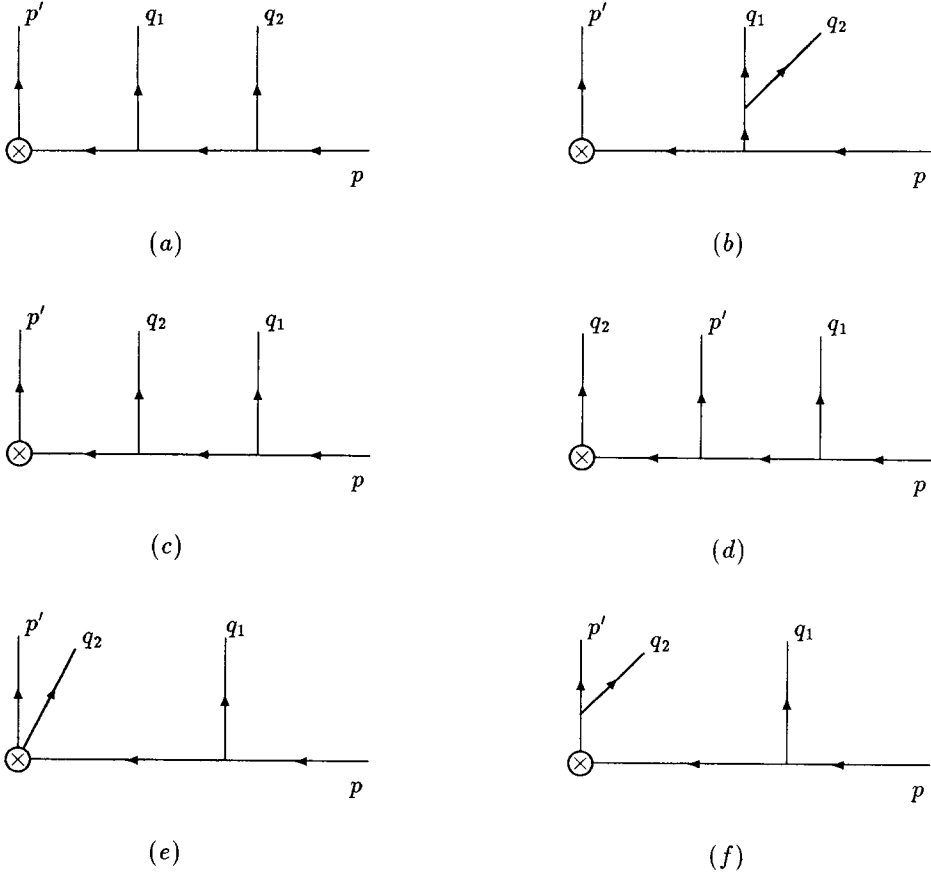


Fig. 12. Feynman diagrams for  $n = 2$  amplitude in a general axial gauge.

As usual, the first two diagrams figs. 12a, b can be evaluated in terms of eikonal emission of the softest gluon  $q_2$  from the harder external ones  $p$  and  $q_1$ . The amplitude  $M_2^{(a+b)}$  has the factorized form

$$M_2^{(a+b)} \simeq \frac{2(Q_2 - x_2 p) \cdot \epsilon^{(\lambda')}(p')}{x_2 Q_2^2} \langle acb_1 b_2 | \mathbf{h}_2^{(a+b)} \rangle, \quad (\text{A.3})$$

where

$$\langle acb_1 b_2 | \mathbf{h}_2^{(a+b)} \rangle = g_s \langle acb_1 | -\mathbf{T}_p \frac{p}{pq_2} + \mathbf{T}_1 \frac{q_1}{q_1 q_2} | \mathbf{h}_1 \rangle. \quad (\text{A.4})$$

Eq. (A.4) is normalized according to eq. (3.3) and  $\mathbf{h}_1$  is the analogue of eq. (3.2) with  $\epsilon^{(\lambda)}(p)$ ,  $\epsilon^{(\lambda_1)}(q_1)$  replaced by the polarization vectors in our axial gauge.

We come now to the diagram in fig. 12f. The corresponding amplitude  $M_2^{(f)}$  is given by

$$M_2^{(f)} \simeq \frac{2p}{x(pp')Q_1^2} \cdot V(Q_1, p') \cdot \epsilon^{(\lambda)}(p') g_s \langle acb_1 | \mathbf{T}_{p'} \frac{p'}{p'q_2} | \mathbf{h}_1 \rangle, \quad (\text{A.5})$$

where  $V^{\mu\nu}(Q_1, p')$  denotes the hard vertex in eq. (2.4).

Since we have introduced eikonal vertices for the emission of  $Q_1$  and  $q_2$ , eq. (A.5) is valid up to terms of relative order  $x_1, y_2$ . Expression (A.5) can be simplified with the following approximations. Firstly we replace  $p'$  by  $\bar{p}$  and secondly, by using the conservation property

$$Q_1^\mu V_{\mu\nu}(Q_1, \bar{p}) = 0, \quad (\text{A.6})$$

we have

$$\begin{aligned} 2p \cdot V(Q_1, \bar{p}) \cdot \epsilon^{(\lambda)}(p') &= -\frac{2(Q_1 - x_1 p)}{1 - y_1} \cdot V(Q_1, \bar{p}) \cdot \epsilon^{(\lambda)}(p') \\ &= -2p\bar{p}(Q_1 - x_1 p) \cdot \epsilon^{(\lambda)}(p'). \end{aligned} \quad (\text{A.7})$$

By inserting eq. (A.7) into eq. (A.5) we get

$$M_2^{(f)} \simeq -\frac{2(Q_1 - x_1 p) \cdot \epsilon^{(\lambda)}(p')}{xQ_1^2} g_s \langle acb_1 | \mathbf{T}_{p'} \frac{\bar{p}}{\bar{p}q_2} | \mathbf{h}_1 \rangle. \quad (\text{A.8})$$

Let us consider now the diagrams in figs. 12c–e. It is simple to check that, for the subprocess  $Q_1 + q \rightarrow p' + q_2$  in these graphs, the current  $Q_1$  is conserved apart from contributions of relative order  $y_2$ . Therefore, analogously to eqs. (A.6) and (A.7) we can approximate the eikonal vertex  $2p^\mu$  for the  $Q_1$  emission with

$$\frac{2(x_1 p - Q_1)^\mu}{1 - y_1}. \quad (\text{A.9})$$

By introducing this approximation in individual diagrams and using eikonal vertices for soft gluon emission, we see that the diagram in fig. 12d vanishes in the leading infrared order whilst that of fig. 12e gives a contribution

$$M_2^{(e)} \simeq \frac{2(Q_1 - x_1 p) \cdot \epsilon^{(\lambda)}(p')}{xQ_1^2} g_s \langle acb_1 | \mathbf{T}_{p'} \frac{\bar{p}}{(1 - y_1)p\bar{p}} | \mathbf{h}_1 \rangle. \quad (\text{A.10})$$

Since for  $x \rightarrow 0$  we have  $\bar{p}q_2 = y_2 p\bar{p} \simeq (1 - y_1)p\bar{p}$ , the contribution in eq. (A.10) completely cancels the contribution in eq. (A.8).

The evaluation of the diagram in fig. 12c is less simple because in the vertex  $Q_1 \rightarrow q_2 + Q_2$  the gluon  $q_2$  is not the softest one and we cannot use the eikonal approximation. In particular we can check that the eikonal contribution is infrared subleading and the dominant terms are the remaining ones. We get

$$\begin{aligned}
M_2^{(c)\mu_2} &\simeq -\frac{2(Q_1 - x_1 p)^\mu}{xp\bar{p}(1-y_1)Q_1^2 Q_2^2} \left[ g_\mu^{\mu_2} (p - q_1 + q_2)_\rho + (p - q_1 - 2q_2)_\mu g_\rho^{\mu_2} \right] \\
&\quad \times V^{\nu\rho}(Q_2, \bar{p}) \epsilon_\nu^{(\lambda')} (p') g_s \langle acb_1 | (\mathbf{T}_p - \mathbf{T}_1) | \mathbf{h}_1 \rangle \\
&\simeq \frac{2(Q_1 - x_1 p)^\mu}{xp\bar{p}(1-y_1)Q_1^2 Q_2^2} \left[ g_\mu^{\mu_2} 2(1-y_1)p\bar{p} + (p - q_1 - 2q_2)_\mu \bar{p}^{\mu_2} \right] \\
&\quad \times (Q_2 - x_2 p) \cdot \epsilon^{(\lambda')} (p') g_s \langle acb_1 | (\mathbf{T}_p - \mathbf{T}_1) | \mathbf{h}_1 \rangle, \tag{A.11}
\end{aligned}$$

where the two contributions in the square brackets come respectively from the terms with helicity conservation along the lines  $(Q_1, q_2)$  and  $(Q_2, q_2)$ . Performing the Lorentz algebra in eq. (A.11) we obtain

$$M_2^{(c)} \simeq \frac{2(Q_2 - x_2 p) \cdot \epsilon^{(\lambda')} (p')}{xQ_2^2} \langle acb_1 b_2 | \mathbf{h}_2^{(c)} \rangle, \tag{A.12}$$

where

$$\begin{aligned}
\langle acb_1 b_2 | \mathbf{h}_2^{(c)} \rangle &= \left[ \frac{2(Q_1 - x_1 p)}{Q_1^2} - \frac{2(Q_1 - x_1 p) \cdot q_2}{Q_1^2} \frac{\bar{p}}{(1-y_1)p\bar{p}} + \frac{1+y_1}{2(1-y_1)} \frac{\bar{p}}{p\bar{p}} \right] \\
&\quad \times g_s \langle acb_1 | \mathbf{T}_{p'} | \mathbf{h}_1 \rangle. \tag{A.13}
\end{aligned}$$

Here we have used the colour conservation (see eq. (3.10)). Recalling the approximations

$$1 + y_1 \simeq 2, \quad (1 - y_1)p\bar{p} \simeq y_2 p\bar{p}, \quad p' \sim \bar{p},$$

we can identify eq. (A.13) with

$$\langle acb_1 b_2 | \mathbf{h}_2^{(c)} \rangle \simeq g_s \langle acb_1 | \mathbf{J}_{\text{nc}}(Q_2, q_2) + \mathbf{T}_{p'} \frac{p'}{p'q_2} | \mathbf{h}_1 \rangle, \tag{A.14}$$

where  $\mathbf{J}_{\text{nc}}$  is given in eq. (3.5). The sum of eqs. (A.3) and (A.14) reproduces the factorized result in eq. (3.1) and (3.3) thus showing explicitly its gauge independence.

The gauge invariant analysis we have performed in this appendix for the  $n = 2$  emission amplitude is quite complicated and makes clear the difficulties one meets in trying to generalize to higher values of  $n$ . In particular, the computation of the diagram in fig. 12c shows the complication related to the evaluation of the contributions with gluon emission by soft internal lines. In this case the usual eikonal coupling is infrared subleading and both the other two helicity flows have to take into account. Let us stress once more the important simplification due to the choice of the axial gauge with  $\eta = \bar{p}$ . In this latter case, as discussed in subsect. 2.1, the introduction of the effective hard vertex (2.11) automatically selects a single leading helicity flow.

## Appendix B

The deep inelastic scattering process involving the hard current  $(F_{\mu\nu}^a)^2$  is examined in this appendix by including quark contributions. Since, as discussed in the introduction, only exchanged and radiated gluons give the leading behaviour for  $x \rightarrow 0$ , we limit ourselves in considering the case with a quark in the initial state. By referring to the notations in eq. (1.7) (see fig. 1),  $p$  and  $q_1$  will denote respectively the momenta of the incoming and outgoing quarks and  $p', q_2, \dots, q_n$  are gluon momenta.

We introduce an amplitude  $\mathbf{M}_n^{(q)}(pp'q_1q_2\dots q_n; s\lambda's_1\lambda_2\dots\lambda_n)$  and a space of colour vectors  $\{|\alpha c\alpha_1 b_2 \dots b_n\rangle\}$ . Here  $s$  and  $s_1$  are the helicity indices for the quarks  $p$  and  $q_1$  with colours  $\alpha, \alpha_1$  and  $\lambda', \lambda_i$  denote the polarizations of the gluons  $p', q_i$  with colours  $c, b_i$ . The analogous of eq. (2.18) is now

$$M_n^{(q)} = \langle \alpha c\alpha_1 b_2 \dots b_n | \mathbf{M}_n^{(q)}(pp'q_1q_2\dots q_n; s\lambda's_1\lambda_2\dots\lambda_n) \rangle. \quad (\text{B.1})$$

The gluons charges  $\mathbf{T}_i$  ( $i \geq 2$ ) act on the colour space as in eq. (2.19), whilst for the quark charges  $\mathbf{t}_1$  and  $\mathbf{t}_p$  we have

$$\mathbf{t}_1^b |\alpha c\alpha_1 b_2 \dots b_n\rangle = t_{\beta_1\alpha_1}^b |\alpha c\beta_1 b_2 \dots b_n\rangle, \quad (\text{B.2a})$$

$$\mathbf{t}_p^b |\alpha c\alpha_1 b_2 \dots b_n\rangle = t_{\alpha\beta}^b |\beta c\beta_1 b_2 \dots b_n\rangle, \quad (\text{B.2b})$$

where  $t_{\alpha\beta}^b$  are  $SU(N)$  generators in the fundamental representation ( $\mathbf{t}^a \mathbf{t}^a = C_F$ ). Note the transposition of the colour indices in eqs. (B.2a) and (B.2b) due to the fact that  $q_1$  and  $p$  are outgoing and incoming quarks respectively.

The analysis of the  $x \rightarrow 0$  leading diagrams contributing in the energy ordered region

$$x \ll y_n \ll y_{n-1} \ll \dots \ll y_2 \ll y_1 \sim 1, \quad (\text{B.3})$$

goes along the same lines of sects. 2–4. The reason for this fact is that soft gluon emission by the fast quarks  $p$  and  $q_1$  can be again evaluated by using the eikonal

approximation. Therefore the soft gluon factorization theorems in sects. 3 and 4 are still valid. The only differences arise from the underlying spin and colour index space on which soft gluon factorization takes place. For the present case we have to introduce the subamplitude  $\mathbf{h}_1^{(q)(\text{tree})}$  given by

$$\langle \alpha c \alpha_1 | \mathbf{h}_1^{(q)(\text{tree})}(pp'q_1) \rangle = \bar{u}^{(s_1)}(q_1) u^{(s)}(p) g_s t_{\alpha_1 c}^c, \quad (\text{B.4})$$

where  $\bar{u}, u$  are quark spinors. The amplitude  $M_n^{(q)}$  for the emission of  $n-1$  gluons including virtual corrections is given by the recurrence relations (3.1), (5.2), (5.5) which we rewrite for sake of completeness

$$M_n^{(q)} \simeq \frac{2(Q_n - x_n p) \cdot \epsilon^{(\lambda)}(p')}{x Q_n^2} \langle \alpha c \alpha_1 b_2 \dots b_n | \mathbf{h}_n^{(q)}(pp'q_1 q_2 \dots q_n) \rangle, \quad (\text{B.5})$$

$$|\mathbf{h}_n^{(q)}\rangle \simeq \mathbf{S}_{\text{eik}}^{(n)}(y_n, 0) S_{\text{nc}}(y_n, x_n, Q_{n1}) |\tilde{\mathbf{h}}_n^{(q)}\rangle, \quad (\text{B.6})$$

$$\begin{aligned} & \langle \alpha c \alpha_1 \dots b_n | \tilde{\mathbf{h}}_n^{(q)} \rangle \\ & \simeq g_s \langle \alpha c \alpha_1 \dots b_{n-1} | \mathbf{J}_{\text{tot}}^{(n-1)b_n}(q_n) \mathbf{S}_{\text{eik}}^{(n-1)}(y_{n-1}, y_n) S_{\text{nc}}(y_{n-1}, y_n, Q_{n-1t}) | \tilde{\mathbf{h}}_{n-1}^{(q)} \rangle. \end{aligned} \quad (\text{B.7})$$

In eq. (B.7), the current  $\mathbf{J}_{\text{tot}}$  and the form factors  $\mathbf{S}_{\text{eik}}, S_{\text{nc}}$  are given respectively by eqs. (3.4), (5.3) and (5.4) and the initial condition is  $\tilde{\mathbf{h}}_1^{(q)} = \mathbf{h}_1^{(q)(\text{tree})}$  as given in eq. (B.4).

As in the pure Yang–Mills case, the coherence property (4.2) for the square of the total soft insertion current  $\mathbf{J}_{\text{tot}}$  allows us to express  $|M_n^{(q)}|^2$  in terms of eikonal currents. Starting from eqs. (B.5), (B.6) and (B.7) we get

$$|M_n^{(q)}|^2 = \frac{4g_s^{2(n-1)}}{x^2 Q_1^2} \left[ \prod_{i=1}^n S_{\text{nc}}(y_i, y_{i+1}, Q_{it}) \right]^2 \langle \mathbf{h}_n^{(q)\text{R}} | \mathbf{h}_n^{(q)\text{R}} \rangle, \quad (\text{B.8})$$

where we have defined the reduced subamplitude  $\mathbf{h}_n^{(q)\text{R}}$  as follows (note that colour indices are understood)

$$|\mathbf{h}_n^{(q)\text{R}}\rangle = \mathbf{S}_{\text{eik}}^{(n)}(y_n, 0) \mathbf{J}_{\text{tot}}^{(n-1)}(q_n) \mathbf{S}_{\text{eik}}^{(n-1)}(y_{n-1}, y_n) \dots \mathbf{J}_{\text{tot}}^{(1)}(q_2) \mathbf{S}_{\text{eik}}^{(1)}(y_1, y_2) | \mathbf{h}_1^{(q)(\text{tree})} \rangle. \quad (\text{B.9})$$

Eqs. (B.8) and (B.9) are formally equivalent to those for the pure Yang–Mills case. With respect to this latter case the only differences arise in computing the colour algebra for  $\langle \mathbf{h}_n^{(q)\text{R}} | \mathbf{h}_n^{(q)\text{R}} \rangle$  since in eq. (B.9) colour charges in both the adjoint and fundamental representations are present. This fact prevents us in using the techniques of ref. [13] to evaluate the multi-gluon squared amplitudes  $|M_n^{(q)}|^2$ .

In order to explain more clearly colour charge effects, let us consider the case with  $n = 1, 2$  at tree level. For  $n = 1$  we get ( $\sigma'_0 = N_c$ )

$$|M_1^{(q)(\text{tree})}|^2 = \sigma'_0 \frac{g_s^2 C_F}{x^2} W_{pp'}(q_1), \quad (\text{B.10})$$

where the eikonal distribution  $W_{pp'}(q_1)$  is defined in eq. (4.19).

Eq. (B.10) coincides with (4.16) for the pure Yang–Mills case apart for the obvious replacements  $\sigma_0 \rightarrow \sigma'_0$  and  $C_A \rightarrow C_F$  respectively due to the sum over the final state colours and to the different colour charge of the incoming parton. However it is important to note that eq. (B.10) cannot be extrapolated in the  $x \rightarrow 1$  region. All the amplitudes  $M_n^{(q)(\text{tree})}$  vanish in the leading order for this latter region since soft quark radiation is not infrared singular. It follows that the constraint  $x \ll y_1 \sim 1$  cannot be released for the incoming quark case.

Performing the azimuthal integration of eq. (B.10) as in eq. (4.21) and by taking into account only the initial state collinear singularity we obtain the quark structure function contribution

$$\begin{aligned} F_q^{(1)(\text{tree})}(Q^2, x) &\simeq \int \frac{d\xi_1}{\xi_1} dy_1 \frac{C_F \alpha_s}{\pi} \frac{1}{x^2} \delta\left(1 - \frac{x}{x_1}\right) \Theta(Q - q_{1t}) \\ &= \int \frac{d\xi_1}{\xi_1} dz_1 \frac{C_F \alpha_s}{\pi} \frac{1}{z_1} \delta(x - z_1) \Theta(Q - q_{1t}). \end{aligned} \quad (\text{B.11})$$

Eq. (B.11) differs from eq. (4.27) for the absence of the factor  $1/y_1$ . This is due to the constraint  $y_1 \sim 1$  which, by introducing the energy fraction  $z_1 = x_1 = 1 - y_1$  leads to the appearance in eq. (B.11) of the Altarelli–Parisi probability splitting function  $P_{gq}$  for the process quark  $\rightarrow$  gluon

$$P_{gq}(z) = 2C_F/z. \quad (\text{B.12})$$

For  $n = 2$  we have

$$\begin{aligned} |M_2^{(q)(\text{tree})}|^2 &= \sigma'_0 \frac{g_s^4 C_F}{x^2} W_{pp'}(q_1) \\ &\times \left\{ 2C_F W_{pq_1}(q_2) + C_A [W_{p'q_1}(q_2) + W_{p'p}(q_2) - W_{pq_1}(q_2)] \right\}, \end{aligned} \quad (\text{B.13})$$

which correctly reduces itself to (4.16) for  $\sigma'_0 \rightarrow \sigma_0$  and  $C_F \rightarrow C_A$ . Performing azimuthal averages of the eikonal distributions [13] or equivalently by introducing

strong ordering in angles [11], eq. (B.13) gives

$$|M_2^{(q)(\text{tree})}|^2 = \sigma_0' \frac{(2g_s^2)^2 C_F}{x^2} \prod_{i=1}^2 \frac{1}{\omega_i^2 \xi_i} [C_F \Theta_{12}^\xi + C_A \Theta_{21}^\xi] + \dots, \quad (\text{B.14})$$

where the ellipses stands for contributions with final state or subleading initial state collinear singularities.

We stress the presence in eq. (B.14) of the colour factor  $C_A$  associated with the angular ordering  $\xi_2 > \xi_1$ . When  $\xi_2 > \xi_1$  the  $q_2$  gluon is radiated coherently by the incoming and outgoing quarks  $p$  and  $q_1$  so that its radiation pattern measures their total colour charge  $(-\mathbf{t}_p + \mathbf{t}_1)^2 = C_A$ . This coherent effect is similar [8–10] to the celebrated string effect for final state radiation.

It is important to note that expression (B.14) is a leading collinear one. For the incoming quark case this statement is very different from “leading in the number of colours  $N_c$ ”. In this latter approximation eq. (B.13) should lead to a different radiation pattern.

In recovering from eq. (B.14) the structure function we must remember the constraint  $\omega_1 \approx E$  (e.g.  $y_1 \sim 1$ ). Moreover we can release the constraint  $x \ll y_2$  since eq. (B.14) coincides with  $|M_2^{(q)(\text{tree})}|^2$  evaluated in the complementary region  $y_2 \ll x$  [11, 12]. We obtain the result

$$F_q^{(2)(\text{tree})}(Q^2, x) \approx \int \prod_{i=1}^2 \left[ \frac{d\xi_i}{\xi_i} dy_i \Theta(Q - q_{it}) \right] \left( \frac{\alpha_s}{\pi} \right)^2 \times \frac{C_F}{y_2} (C_F \Theta_{12}^\xi + C_A \Theta_{21}^\xi) \frac{1}{x^2} \delta\left(1 - \frac{x}{x_2}\right), \quad (\text{B.15})$$

which, by referring to a single overall angular ordering  $\Theta_{21}^\xi$  and introducing the corresponding energy fractions (4.28), gives

$$F_q^{(2)(\text{tree})}(Q^2, x) \approx \int \prod_{i=1}^2 \left[ \frac{d\xi_i}{\xi_i} \frac{dz_i}{z_i} \Theta(Q - q_{it}) \right] \left( \frac{\alpha_s}{\pi} \right)^2 \mathcal{P}_2(x, z_1, z_2) \Theta_{21}^\xi, \quad (\text{B.16})$$

where

$$\begin{aligned} \mathcal{P}_2(x, z_1, z_2) &= \left( \frac{C_F^2}{(1-z_1)z_2} + \frac{C_F C_A}{z_1 z_2 (1-z_2)} \right) \delta\left(1 - \frac{x}{z_1 z_2}\right) \\ &= [P_q(z_1) P_{gq}(z_2) + P_{gq}(z_1) P(z_2)] \delta\left(1 - \frac{x}{z_1 z_2}\right), \end{aligned} \quad (\text{B.17})$$

and we have introduced the  $z \rightarrow 1$  Altarelli–Parisi probability splitting function  $P_q(z)$  for the process quark  $\rightarrow$  quark

$$P_q(z) = 2C_F/(1-z). \quad (\text{B.18})$$

Eq. (B.16) admits a simple interpretation in terms of an angular ordered branching process with probabilities given by the Altarelli–Parisi splitting functions.

Obviously, in the leading infrared order we are working, the quark splitting probabilities (B.12) and (B.18) we obtain, contain only the  $z \rightarrow 1, 0$  singular part of the full Altarelli–Parisi distributions.

After this detailed discussion of the  $n = 1, 2$  cases at tree level, we come back to the general multi-gluon distribution (B.8). The colour algebra complications encountered in performing the evaluation of eq. (B.8) for  $n = 1, 2$  can be overcome by noting the close resemblance between eq. (B.9) and matrix elements obtained within the QCD coherent state framework [11, 12]. Actually, eq. (B.9) can be expressed in the following way

$$g_s^{n-1} \langle b_2 \dots b_n | \mathbf{h}_n^{(q)\text{R}} \rangle = \Theta_{12\dots n}^y \langle q_2 \dots q_n; b_2 \dots b_n | \prod_{p_i} U^{(p_i)}(E; \xi_2, \xi_0) | \mathbf{h}_1^{(q)(\text{tree})} \rangle, \quad (\text{B.19})$$

where  $p_i = p, q_1, p'$ , and  $U^{(p)}$  is the QCD coherent state operator defined by the recurrence relation

$$U^{(p)}(E; \xi, \xi_0) = \bar{P}_y \exp \left\{ g_s \int (dq) \Theta(E - \omega_q) \Theta(\xi - \xi_{pq}) \Theta(\xi_{pq} - \xi_0) \right. \\ \left. \times (A_\mu^a(\mathbf{q}) + A_\mu^{a\dagger}(\mathbf{q})) \left[ \mathcal{U}^{(q)}(\omega_q; \xi, \xi_0) \right]_{ab} \mathbf{t}_p^b \frac{p^\mu}{pq} \right\}, \quad (\text{B.20})$$

where  $\mathcal{U}$  is the analogue of  $U$ , but in the adjoint representation of the colour group  $A_\mu^a, A_\mu^{a\dagger}$  are annihilation and creation operators for the gluon free field and  $|q_2 \dots q_n; b_2 \dots b_n\rangle$  is a vector in the colour and Fock space of the gluon field.

By substituting eq. (B.19) into eq. (B.8), the multi-gluon distribution  $|M_n^{(q)}|^2$  turns out to be equivalent to that for the region  $x \sim 1$  [11] apart from the factors  $S_{nc}$  which however are infrared subleading in this latter region. As for the pure Yang–Mills case, we can therefore assume eq. (B.8) to be valid for any  $x$  value. We shall see that this approximation is equivalent to neglect nonsingular terms for  $z \rightarrow 0, 1$  in the Altarelli–Parisi splitting functions.

Eq. (B.19) allows to evaluate the reduced subamplitude  $|\mathbf{h}_n^{(q)\text{R}}\rangle$  in the leading infrared and collinear order by using the techniques presented in ref. [11] to which we refer for further details.

We start by introducing two angular cones with maximum aperture  $\xi_{\max} \sim \bar{\xi}$  around the directions of the incoming and outgoing parton  $p$  and  $p'$ . Gluon radiation takes place in the leading collinear order within such cones. Then in the leading collinear approximation, the energy ordered coherent state (B.20) can be replaced by an angular ordered coherent state [11]. The recurrence relation satisfied by this latter is similar to eq. (B.20) with  $\bar{P}_y$  replaced by  $\bar{P}_\xi$ . At this point angular ordering is implemented.

The coherent state operator  $\mathcal{U}^{(p')}(E; \bar{\xi}, \xi_0)$ , takes into account collinear singularities for  $\xi_{p'i} \rightarrow 0$  and gives rise to the contributions known [2, 13] from the analysis of final state soft radiation. As done for the pure Yang–Mills case in sects. 4, 6 and 7, we neglect these standard contributions and analyze the initial state collinear singularities.

Large and small angle initial state radiation with respect to  $\xi_1$  can be factorized in operator form by using  $(p_i = p, q_1)$

$$U^{(p_i)}(E; \bar{\xi}, \xi_0) = U^{(p_i)}(E; \bar{\xi}, \xi_1) U^{(p_i)}(E; \xi_1, \xi_0). \quad (\text{B.21})$$

By inserting eq. (B.21) into (B.19) and collecting large angle coherent state operators on the right (we recall that the coherent state operators (B.21) commute each other in the Fock space), we get

$$\begin{aligned} g_s^{n-1} \langle b_2 \dots b_n | \mathbf{h}_n^{(q)\text{R}} \rangle &= \Theta_{12 \dots n}^y \langle q_2 \dots q_n; b_2 \dots b_n | \left[ \prod_{p_i} U^{(p_i)}(E; \xi_1, \xi_0) \right] \\ &\quad \times \left[ \prod_{p_i} U^{(p_i)}(E; \bar{\xi}, \xi_1) \right] | \mathbf{h}_1^{(q)\text{(tree)}} \rangle + \dots, \end{aligned} \quad (\text{B.22})$$

where the dots correspond to terms with collinear singularities for  $\xi_{p'i} \rightarrow 0$ . Eq. (B.22) shows that large angle radiation is described by the coherent state operator

$$\begin{aligned} \prod_{p_i = p, q_1} U^{(p_i)}(E; \bar{\xi}, \xi_1) &= \bar{P}_\xi \exp \left\{ g_s \int (dq) \Theta(E - \omega_q) \Theta(\bar{\xi} - \xi) \Theta(\xi - \xi_1) \right. \\ &\quad \left. \times (A_\mu^a(\mathbf{q}) + A_\mu^{a\dagger}(\mathbf{q})) \left[ \mathcal{U}^{(q)}(\omega_q; \bar{\xi}, \xi_0) \right]_{ab} \mathbf{J}^{b\mu}(q) \right\}, \end{aligned} \quad (\text{B.23})$$

driven by the eikonal current

$$\mathbf{J}^\mu(q) = -\mathbf{t}_p \frac{p^\mu}{pq} + \mathbf{t}_1 \frac{q_1^\mu}{q_1 q}. \quad (\text{B.24})$$

Since in the large angle region  $\xi \gg \xi_1$ ,  $p$  and  $q_1$  can be considered essentially parallel, we can replace  $q_1$  by  $p$  in eq. (B.24) and then use the colour charge

conservation  $(-\mathbf{t}_p + \mathbf{t}_1 + \mathbf{T}_{p'})|\mathbf{h}_1^{(q)(\text{tree})}\rangle = 0$  in eq. (B.22) to obtain

$$\prod_{p_i} U^{(p_i)}(E; \bar{\xi}, \xi_1)|\mathbf{h}_1^{(q)(\text{tree})}\rangle = \mathcal{U}^{(p)}(E; \bar{\xi}, \xi_1)|\mathbf{h}_1^{(q)(\text{tree})}\rangle. \quad (\text{B.25})$$

The appearance of the coherent state operator  $\mathcal{U}$  in the adjoint representation clearly shows the coherent effect of the large angle gluon emission: the combined radiating action of the incoming and outgoing quarks simulates radiation by a gluon.

Inserting eq. (B.25) into eq. (B.22) one obtains

$$g_s^{n-1}\langle b_2 \dots b_n | \mathbf{h}_n^{(q)\text{R}} \rangle \simeq \Theta_{12\dots n}^y \langle q_2 \dots q_n; b_2 \dots b_n | \times U^{(p)}(E; \xi_1, \xi_0) \mathcal{U}^{(p)}(E; \bar{\xi}, \xi_1) |\mathbf{h}_1^{(q)(\text{tree})}\rangle, \quad (\text{B.26})$$

where we have again neglected the terms with final state collinear singularities  $\xi_{1i} \rightarrow 0$ , due to the coherent state operator  $U^{(q_1)}(E; \xi_1, \xi_0)$ .

We are now ready to compute the multi-gluon distribution (B.8). Let us start for notational simplicity from the tree level distribution. In this case the form factors  $S_{\text{ne}}$  in eq. (B.8) reduce themselves to unity and the matrix element on the right-hand side in eq. (B.26) is completely symmetric with respect to  $q_2, \dots, q_n$ . It follows that by summing over all permutations  $\{2, \dots, n\}$ , the constraint  $\Theta_{12\dots n}^y$  can be released. The square of the matrix element in eq. (B.26) can be simply evaluated as in ref. [11] because, due to the angular ordering, interference terms are automatically suppressed. The initial state contribution to the multi-gluon distribution which we obtain, is the following

$$|M_n^{(q)(\text{tree})}|^2 \simeq \sigma_0' \frac{(2g_s^2)^n}{x_n^2} \sum_{k=1}^n \Theta_{n,\dots,k+1}^\xi \Theta_{k+1,1,k}^\xi \Theta_{k,\dots,2}^\xi \times \left[ \prod_{i=k+1}^n \frac{C_A}{\omega_i^2 \xi_i} \right] \frac{C_F}{\omega_1^2 \xi_1} \left[ \prod_{j=2}^k \frac{C_F}{\omega_j^2 \xi_j} \right] + \dots, \quad (\text{B.27})$$

to be compared with eq. (4.22) after summing over all permutations. We recall that the constraint  $\omega_1 \simeq E$  is understood into (B.27). The two terms  $i \geq k+1$  and  $j \leq k$  in (B.27) are due respectively to coherent large angle emission and incoherent small angle radiation.

Eq. (B.27) gives the following contribution to the structure function

$$F_q^{(\text{tree})}(Q^2, x) \simeq \sum_{n=2}^{\infty} \sum_{k=1}^n \int_{Q > q_{in}} \left[ \prod_{i=k+1}^n \frac{C_A \alpha_s}{\pi} \frac{d\xi_i}{\xi_i} \frac{dy_i}{y_i} \right] \frac{C_F \alpha_s}{\pi} \frac{d\xi_1}{\xi_1} dy_1 \times \left[ \prod_{j=2}^k \frac{C_F \alpha_s}{\pi} \frac{d\xi_j}{\xi_j} \frac{dy_j}{y_j} \right] \Theta_{n,\dots,k+1}^\xi \Theta_{k+1,1,k}^\xi \Theta_{k,\dots,1}^\xi \frac{1}{x_n^2} \delta\left(1 - \frac{x}{x_n}\right), \quad (\text{B.28})$$

where the absence of the  $1/y_1$  factor is due to the constraint  $y_1 \sim 1$  for  $|M_n^{(q)}|^2$ . Introducing into eq. (B.28) energy fractions defined with respect to the angular ordering as follows

$$\begin{aligned} x_i &= z_1 z_2 \dots z_i, & (i \geq k+1), \\ x_j + y_1 &= z_2 z_3 \dots z_j, & (j \leq k), \end{aligned} \quad (\text{B.29})$$

we obtain

$$\begin{aligned} F_q^{(\text{tree})}(Q^2, x) &\simeq \sum_{n=2}^{\infty} \sum_{k=2}^n \int \left[ \prod_{l=1}^k \frac{\alpha_s}{2\pi} \frac{d\xi_l}{\xi_l} dz_l \Theta(Q - q_{l1}) \right] \Theta_{n, \dots, k+1}^{\xi} \Theta_{k+1, 1, k}^{\xi} \Theta_{k, \dots, 1}^{\xi} \\ &\times \left[ \prod_{i=k+1}^n P(z_i) \right] P_{gq}(z_1) \left[ \prod_{j=2}^k P_q(z_j) \right] \delta(x - z_1 \dots z_n), \end{aligned} \quad (\text{B.30})$$

where the splitting functions  $P(z)$ ,  $P_{gq}(z)$  and  $P_q(z)$  are defined in eqs. (4.30), (B.12) and (B.18) and turn out to coincide with the  $z \rightarrow 0, 1$  limit of the Altarelli–Parisi splitting probabilities. Note that the absence of the singular factor  $1/y_1$  in eq. (B.28) has led to the appearance of  $P_{gq}$  and  $P_q$  into eq. (B.30).

We now come back to include virtual corrections. For this case the nonsymmetric non-eikonal form factor

$$\tilde{S}_{\text{ne}}(1, 2, \dots, n) = \prod_{i=1}^n S_{\text{ne}}(y_i, y_{i+1}, Q_{it}), \quad y_{n+1} = x, \quad (\text{B.31})$$

appearing in eq. (B.8) does not allow to eliminate the energy ordering  $\Theta_{1, 2, \dots, n}^y$  by summing over the permutations. In order to proceed, we divide the gluons  $q_2, q_3, \dots, q_n$  in two subsets according to whether their emission angle  $\xi_i$  is larger or smaller than  $\xi_1$ . In this configuration we have  $q_{it} \ll q_{1t}$  for every gluon  $q_i$  such that  $\xi_i < \xi_1$ . It follows that the non-eikonal form factor (B.31) which turns out, does not depend on the kinematical variables of the gluons  $q_i$  emitted at small angles. The sum over the permutations allows therefore to eliminate the energy ordering between the gluons emitted at large and small angles. We obtain

$$\begin{aligned} |M_n^{(q)}|^2 &\simeq \frac{4}{x^2 Q_1^2} \sum_{k=1}^n \tilde{S}_{\text{ne}}^2(1, k+1, \dots, n) \Theta_{1, k+1, \dots, n}^y \Theta_{1, 2, \dots, k}^y \\ &\times \left| \langle q_{k+1} \dots q_n | \mathcal{Q}^{(p)}(E; \bar{\xi}, \xi_1) \right. \\ &\left. \otimes \langle q_2 \dots q_k | U^{(p)}(E; \xi_1, \xi_0) \right| \mathbf{h}_1^{(q)(\text{tree})} \Big|^2 + \dots \end{aligned} \quad (\text{B.32})$$

At this point the virtual corrections in eq. (B.32) can be evaluated in the leading order as in ref. [11]. The small angle coherent state  $U_{(p)}$  gives rise to a form factor

$S_{\text{eik}}^{(q)}(1, \xi_1)$  similar to  $S_{\text{eik}}$  in eq. (6.24) apart from the replacement  $\bar{\alpha}_s = (C_A \alpha_s)/\pi \rightarrow (C_F \alpha_s)/\pi$ . The large angle coherent state  $\mathcal{U}_{(p)}$  yields the form factor  $S_{\text{eik}}^{-1}(1, \xi_1) S_{\text{eik}}(1, \bar{\xi})$ . In order to replace energy ordering with angular ordering we proceed as in subsect. 7.1 and we arrive to the final result

$$|M_n^{(q)}|^2 = \frac{\sigma'_0}{\sigma_0} \sum_{k=1}^n |M_{n-k}^{(\xi > \xi_1)}|^2 \frac{(2g_s^2)^k C_F}{\omega_1^2 \xi_1} \Theta_{1,k}^{\xi} \times \left[ \prod_{j=2}^k \frac{C_F}{\omega_j^2 \xi_j} \right] \Theta_{k,\dots,2}^{\xi} [S_{\text{eik}}^{(q)}(1, \xi_1)]^2. \quad (\text{B.33})$$

In eq. (B.33)  $|M_{n-k}^{(\xi > \xi_1)}|^2$  is the multi-gluon amplitude we have computed in sect. 7 for the pure Yang–Mills case. The superscript  $(\xi > \xi_1)$  mean that the angular variables  $\xi$  for both real and virtual emission in  $M_{n-k}$  are constrained by  $\xi > \xi_1$ .

Starting from eq. (B.33), the evaluation of the quark structure function for  $x \rightarrow 0$  is straightforward. It amounts to note that the integration over the soft gluon radiation incoherently emitted at small angles  $\xi < \xi_1$  completely cancels the eikonal form factor  $S_{\text{eik}}^{(q)}(1, \xi_1)$  in eq. (B.33). As a result of this cancellation, only coherent soft gluon radiation for angles larger than  $\xi_1$  is left. This contribution is exactly the same computed in subsect. 7.2 for the pure Yang–Mills case and we obtain

$$F_{qN}(Q^2) = \frac{C_F}{C_A} [F_N(Q^2) - 1], \quad (\text{B.34})$$

where  $F_N$  is the gluon structure function whose anomalous dimension are given by the Lipatov ansatz.

We conclude this appendix by discussing the structure of the initial state branching with incoming quark. A simple analysis of the multi-gluon distribution (B.33) along the lines of subsect. 7.3 yields the following branching distributions

$$d\mathcal{P}_{gq}(i) = \frac{d\xi_i}{\xi_i} \Theta(Q - q_{it}) \Theta(\xi_i - \xi_{i-1}) \frac{dz_i}{z_i} \frac{\alpha_s}{2\pi} \times P_{gq}(z_i) \Delta_{\text{ne}}(z_i, Q_{it}, q_{it}) \Delta_{\text{eik}}^{(q)}(x_{i-1}, \xi_i, \xi_{i-1}), \quad (\text{B.35})$$

$$d\mathcal{P}_q(i) = \frac{d\xi_i}{\xi_i} \Theta(Q - q_{it}) \Theta(\xi_i - \xi_{i-1}) \frac{dz_i}{z_i} \frac{\alpha_s}{2\pi} \times P_q(z_i) \Delta_{\text{ne}}(z_i, Q_{it}, q_{it}) \Delta_{\text{eik}}^{(q)}(x_{i-1}, \xi_i, \xi_{i-1}) \Theta(1 - \epsilon_i - z_i), \quad (\text{B.36})$$

respectively for the quark  $\rightarrow$  gluon and quark  $\rightarrow$  quark splitting. In eqs. (B.35) and

(B.36) we have used the same notations as for (7.55) and

$$\Delta_{\text{cik}}^{(q)}(x, \xi, \xi') = \exp \left[ -\frac{\alpha_s C_F}{\pi} \int_{\xi'}^{\xi} \frac{d\xi''}{\xi''} \int_0^{1-\epsilon''} \frac{dz}{1-z} \right], \quad \epsilon'' = Q_0 / (Ex\sqrt{\xi''}), \quad (\text{B.37})$$

is the Sudakov form factor for the quark.

## References

- [1] For a review see: L.A. Gribov, E.M. Levin and M.G. Ryskin, Phys. Rep. 100 (1983) 1
- [2] For a review see: A. Bassetto, M. Ciafaloni and G. Marchesini, Phys. Rep. 100 (1983) 201
- [3] L.N. Lipatov, Yad. Fiz. 23 (1976) 642 [Sov. J. Phys. 23 (1976) 338];  
E.A. Kuraev, L.N. Lipatov and V.S. Fadin, Zh. Eksp. Teor. Fiz. 72 (1977) 373 [Sov. Phys. JETP 45 (1977) 199];  
Ya. Balitskii and L.N. Lipatov, Sov. J. Nucl. Phys. 28 (1978) 6;  
T. Jaroszewicz, Acta Phys. Pol. B11 (1980) 965; Phys. Lett. B116 (1982) 291;  
A.V. Kisselev, Phys. Lett. B214 (1988) 434
- [4] N. Mitra, Nucl. Phys. B218 (1983) 145
- [5] A.H. Mueller and J. Qiu, Nucl. Phys. B268 (1986) 427;  
A.H. Mueller and H. Navelet, Nucl. Phys. B282 (1987) 727;  
A.H. Mueller, Self-consistent small- $x$  behaviour in QED, Columbia preprint CU-TP-409
- [6] M. Ciafaloni, Nucl. Phys. B296 (1987) 249
- [7] G. Marchesini and B.R. Webber, Nucl. Phys. B310 (1988) 461
- [8] A.H. Mueller, Phys. Lett. B104 (1981) 161;  
A. Bassetto, M. Ciafaloni, G. Marchesini and A.H. Mueller, Nucl. Phys. B207 (1982) 189;  
B.I. Ermolaev and V.S. Fadin, JETP Lett. 33 (1981) 285;  
Yu.I. Dokshitzer, V.S. Fadin and V.A. Khoze, Z. Phys. C15 (1983) 325; C18 (1983) 37
- [9] Yu.I. Dokshitzer, V.A. Khoze and S.I. Troyan, *in* Perturbative QCD, ed. A.H. Mueller (World Scientific, Singapore, 1989), to be published;  
L.V. Gribov, Yu.I. Dokshitzer, S.I. Troyan and V.A. Khoze, Sov. Phys. JETP 68 (1988) 1;  
R.K. Ellis, G. Marchesini and B.R. Webber, Nucl. Phys. B286 (1987) 643
- [10] Yu.I. Dokshitzer, V.A. Khoze, S.L. Troyan and A.H. Mueller, Rev. Mod. Phys. 60 (1988) 373
- [11] S. Catani and M. Ciafaloni, Nucl. Phys. B236 (1984) 61; B249 (1985) 301
- [12] S. Catani, M. Ciafaloni and G. Marchesini, Nucl. Phys. B264 (1986) 588
- [13] F. Fiorani, G. Marchesini and L. Reina, Nucl. Phys. B309 (1988) 439
- [14] G. Curci, W. Furmanski and R. Petronzio, Nucl. Phys. B175 (1980) 27;  
W. Furmanski and R. Petronzio, Z. Phys. C11 (1982) 293;  
J. Kalinowski, K. Konishi, P.N. Scharbach and T.R. Taylor, Nucl. Phys. B181 (1981) 253;  
E.G. Floratos, C. Kounnas and R. Lacaze, Phys. Lett. B98 (1981) 89;  
I. Antoniadis and E.G. Floratos, Nucl. Phys. B191 (1981) 217
- [15] S. Parke and T. Taylor, Phys. Lett. B157 (1985) 81;  
M. Mangano, S. Parke and Z. Xu, *in* Proc. Les Rencontres de Physique de la Vallée d'Aoste, La Thuile, Italy, 1987, ed. M. Greco (Editions Frontières, Gif-sur-Yvette) p. 513;  
M. Mangano, S. Parke and Z. Xu, Nucl. Phys. B298 (1988) 653;  
M. Mangano, Nucl. Phys. B309 (1988) 461